Extraction of K, Al and Ti containing compounds from ash produced by low temperature combustion

AC Collins

orcid.org 0000-0002-5134-9638

Thesis accepted in fulfilment of the requirements for the degree *Doctor of Philosophy in Chemistry* at the North-West University

Promoter:	Prof CA Strydom
Co-promoter:	Prof JR Bunt
Assistant Promoter:	Dr JC van Dyk

Graduation October 2019

20271387

“I never saw a wild thing sorry for itself.

A small bird will drop frozen dead from a bough

without ever having felt sorry for itself.”

- *D. H. Lawrence*

PREFACE

Format of thesis

The format of this thesis is in accordance with the academic rules of the North-West University (approved on November 22nd, 2013), where rule **A.5.4.2.7** states: "Where a candidate is permitted to submit a thesis in the form of a published research article or articles, or as an unpublished manuscript or manuscripts in article format and more than one such article or manuscript is used, the thesis must still be presented as a unit, supplemented with an inclusive problem statement, a focused literature analysis and integration and with a synoptic conclusion, and the guidelines of the journal concerned must also be included."

Rule **A.5.4.2.8** states: "Where any research article or manuscript and/or internationally examined patent is used for the purpose of a thesis in article format to which other authors and/or inventors than the candidate contributed, the candidate must obtain a written statement from each co-author and/or co-inventor in which it is stated that such co-author and/or co-inventor grants permission that the research article or manuscript and/or patent may be used for the stated purpose and in which it is further indicated what each co-author's and/or co-inventors share in the relevant research article or manuscript and/or patent was."

Rule **A.5.4.2.9** states: "Where co-authors or co-inventors as referred to in A 5.4.2.8 above were involved, the candidate must mention that fact in the preface and must include the statement of each co-author or co-inventor in the thesis immediately following the preface."

Format of numbering and referencing

It should be noted that the formatting, referencing style, the numbering of tables and figures, and general outline of the manuscripts were adapted to ensure uniformity throughout the thesis. The format of manuscripts which have been submitted and/or published adheres to the author guidelines as stipulated by the editor of each journal and may appear in a different format to what is presented in this thesis. The headings and original technical content of the manuscripts were not modified from the submitted and/or published versions, and only minor spelling and typographical errors were corrected.

STATEMENT FROM CO-AUTHORS

To whom it may concern,

The listed co-authors hereby give consent that A.C. Collins may submit the following manuscript(s) as part of her thesis entitled: Extraction of K, AI and Ti containing compounds from ash produced by low temperature combustion, for the degree Philosophiae Doctor in Chemistry, at the North-West University:

FACTSAGE™ thermo-equilibrium simulations of mineral transformations in coal combustion ash.
A.C. Collins, C.A. Strydom, J.C. van Dyk, J.R. Bunt.
The Journal of the Southern African Institute of Mining and Metallurgy 2018, 118, 1-8.

Sulphuric acid leaching of South African combustion ash – dissolution of Al, K, and Ti from laboratory coal ash
A.C. Collins, C.A. Strydom, R.H. Matjie, J.R. Bunt, and J.C. van Dyk.

Ammonium sulphate sintering of South African combustion ash – the recovery of Al, K, and Ti from laboratory prepared ash
A.C. Collins, C.A. Strydom, R.H. Matjie, J.R. Bunt, and J.C. van Dyk.

Alkaline dissolution of laboratory-produced South African coal ash containing potassium species
A.C. Collins, C.A. Strydom, R.H. Matjie, J.R. Bunt, and J.C. van Dyk.

(This letter of consent complies with rules ***A5.4.2.8 and A.5.4.2.9*** of the academic rules, as specified by the North-West University)

Signed at Potchefstroom

Prof Christien Strydom

3 June 2019

Christien A. Strydom

Date

John Reginald Bunt

3/6/2019

John R. Bunt

Date

3/6/2019

Johannes C. van Dyk

Date

Prof Christien Strydom for Dr Matjie

3 June 2019

Ratale H. Matjie

Date

ACKNOWLEDGEMENTS

The author would like to acknowledge a few people/ institutions who contributed to the completion of this study.

- First and foremost, my heavenly Father for His unchanging love, guidance, strength and the opportunities throughout the course of this study;
- The North-West University, Sasol Technology (Pty) Ltd, the South African Research Chairs Initiative of the Department of Science and Technology, and National Research Foundation of South Africa for financially supporting the research done during this study;
- My supervisors Prof Christien Strydom Prof John Bunt for all their patience, guidance, encouragement, and insight throughout this study;
- Dr Johan van Dyk for acquiring of the coal samples, training on the FACTSAGE™ modelling software and his advice whenever needed;
- Dr RH Matjie for his invaluable advice and always making time to help with difficulties as they appeared throughout this study;
- Belinda Venter for the XRF and XRD analyses done on all the samples generated throughout this study;
- My colleagues from the Coal Research Group for their suggestions and assistance;
- To my friends for all their support, encouragement, and prayers when things got difficult;
- And lastly, my family for their prayers, love, support, and always believing in me.

ABSTRACT

South African coal samples can contain up to 30% aluminium oxide which is constituted in the mullite and insoluble aluminium silicate mineral phases. This suggests that coal ash, produced in power plants or thermal processing of coal fines, has the potential to be a good source material for the recovery of aluminium. The aim of this investigation was to use modelling software to predict mineral transformation during thermal processing of the coal samples; after which the dissolution potential of aluminium from the amorphous material (metakaolinite ($Al_2O_3.2SiO_2$)); and aluminium, potassium, and titanium in the amorphous aluminosilicate glass phases were determined. The starting material used in the recovery procedures was produced by low-temperature combustion (<1100°C) of South African coal samples. One of the coal samples was spiked with a 10 wt.% K_2CO_3 additive, which is used as a catalyst; to determine the influence this potassium compound had on the dissolution of aluminium, and subsequently potassium and titanium from the ash. FACTSAGE™ modelling software was used for the prediction runs; while three different recovery methods were used for the dissolution of the inorganic elements; i.e. H_2SO_4 leaching, $(NH_4)_2SO_4$ sintering and NaOH leaching.

FACTSAGE™ modelling software and accompanying databases were used to investigate the influence of operating conditions on the slagging behaviour of South African coal samples; along with the role that additives, such as potassium carbonate when added as a catalyst, have on the slagging behaviour. The results obtained through the prediction models indicated that the addition of potassium carbonate to the pulverized coal before thermal processing, lead to a decrease in melt formation temperature and a decrease in melt percentage. The extent of influence the potassium had on the coal behaviour during thermal processing, depended largely on the percentage of potassium present in the sample along with the composition of the coal. The basic components present in the coal will also influence the mineral transformation and slagging behaviour, due to their fluxing behaviour.

Sulphuric acid leaching, with conditions similar to procedures used for the recovery of aluminium from clay sources, showed that coal ash prepared at 700°C yielded higher dissolution efficiencies of aluminium and potassium than the ash prepared at 1050°C. This is due to stable mineral phases present in the ash samples produced at higher temperatures. The addition of potassium carbonate to the coal sample resulted in higher dissolution efficiencies for aluminium from the ash. The highest dissolution efficiencies achieved were 87% Al and 89% K with the following experimental conditions: 700°C ash leached with a 6.12 M H_2SO_4 solution, using a solid to liquid ratio of 1:5 at a temperature of 80°C for 8 hours. The high dissolution efficiencies were due to the formation of acid-soluble amorphous phases, such as metakaolinite, K_2CO_3 melt, K_2CO_3, potassium-alum ($KAl(SO_4)_2$, and potassium aluminosilicate (gls).

Subjecting the SA1 and SA2 blend ash samples prepared at 700°C to the ammonium sulphate sintering method, yielded maximum dissolution efficiency of 43% Al and 56% K for the SA1 ash sample (without K_2CO_3). These efficiencies were reached due to the formation of soluble ammonium aluminium sulphate and potassium sulphate. The addition of K_2CO_3 to the SA2 coal sample resulted in a lower Al dissolution efficiency due to the formation of insoluble potassium-alum. The dissolution of this mineral phase would require an added dissolution procedure.

Alkaline leaching of the SA1 and SA2 blend ash samples yielded low dissolution efficiencies for Al and K when leached with the 1 M NaOH solution. Dissolution of the inorganic elements did not increase when an 8 M NaOH solution was used, however; the increase in alkaline solution concentration promoted the growth of sodalite (zeolite A) crystals within the ash. High K dissolution efficiencies of 59% and 89% were observed for the SA1 and SA2 blend ash respectively. The highest dissolution efficiencies were obtained by sequential leaching of either ash sample; with leaching conditions as follows: 4 hours leaching time, at a temperature of 80°C, using a 1:5 solid to liquid ratio.

The overall conclusions made from this investigation is sulphuric acid leaching remains the most successful recovery method for aluminium. The addition of K_2CO_3 increased the dissolution efficiency of aluminium, even when low sulphuric acid concentration solutions were used. Ammonium sulphate sintering is another viable method for the recovery of aluminium from coal ash, but a different dissolution procedure is needed to solubilize the formed potassium-alum. Alkaline leaching of the ash samples did not yield good dissolution results, but the formation of zeolite crystals may be another viable utilization method for coal ash.

Keywords: Coal ash, low-temperature combustion, extraction, potassium, aluminium, titanium

TABLE OF CONTENT

LIST OF FIGURES

LIST OF TABLES

LIST OF MINERAL PHASES

Anhydrite	$CaSO_4$
Anatase	TiO_2
Anorthite	$CaAl_2Si_2O_8$
Calcite	$CaCO_3$
Cordierite	$Mg_2Al_4Si_5O_{18}$
Cristobalite	SiO_2
Diopside	$MgCaSi_2O_6$
Dolomite	$CaMg(CO_3)_2$
Fluorapatite	$Ca_5(PO_4)_3$
Gypsum	$CaSO_4{\cdot}2H_2O$
Hatrurite	Ca_3SiO_5
Hematite	Fe_2O_3
Illite	$(K, H_2O)(Al, Mg, Fe)_2(Si, Al)_4O_{10}{\cdot}(OH)_2(H_2O)$
K/Na/Ca-feldspar	$K/Na/Ca\text{-}AlSi_3O_8$
Kalisilite	$KAlSiO_4$
Kaolinite	$Al_2Si_2O_5(OH)_4$
Leucite	$KalSi_2O_6$
Lime	CaO
Maghemite	Fe_2O_3
Magnetite	Fe_3O_4
Mascagnite	$Al_2O_3{\cdot}2SiO_2$
Metakaolinite	$Al_2(Si_2O_7)$
Microcline	$KAlSi_3O_8$
Mullite	$3Al_2O_3{\cdot}2SiO_2$
Muscovite	$K(Al_2)(Si_3AlO_{10})(OH)_2$
Periclase	MgO
Potassium-alum	$KAl(SO_4)_2{\cdot}12H_2O$
Portlandite	$Ca(OH)_2$
Pyrite	Fe_2S
Pyrrhotite	$Fe_{(x-1)}S_x$
Quartz	SiO_2
Rutile	TiO_2
Sillimanite	Al_2SiO_5
Sodalite	$Na_8Al_6Si_6O_{24}(OH)_2(H_2O)_2$

Chapter 1

Introduction

In this chapter, a brief overview on the nature of this investigation will be given based on available data and literature. The reasoning of this investigation will be stated in a basic hypothesis, method of investigation pursued, and specific aims and objectives.

1.1 Problem statement and substantiation

Coal ash is a solid residue that is formed during the combustion/gasification of coal (Cheng-you *et al.*, 2012; Seidel, 1999). This by-product of thermal processing, if not used as a material of resource in other industrial processes, is considered a pollutant and waste material (Blissett & Rowson, 2012; Nayak & Panda, 2010). Bricks, cement, concrete, ceramic products, building materials and composite manufacturing are just some applications for which ash can be utilized (Dutta *et al.*, 2009; Izquierdo & Querol, 2012; Nayak & Panda, 2010). Due to the higher energy demand, the production of ash keeps increasing since coal power generation plants are still one of the most important electricity suppliers throughout developing countries (Izquierdo & Querol, 2012; Nayak & Panda, 2010). The excess ash produced during these processes that are not utilized are then stored in stockpiles or disposed of in landfills or lagoons (Dutta *et al.*, 2009; Izquierdo & Querol, 2012; Neupane & Donahoe, 2013). Disposal of ash without the proper precautions may lead to pollution of groundwater, air and soil (Cheng-you *et al.*, 2012; Izquierdo & Querol, 2012; Medina *et al.*, 2010; Norris *et al.*, 2010). Thus, new ways to utilize this by-product of combustion/gasification could reduce its environmental impact (Medina *et al.*, 2010).

The ash formed during combustion/gasification is a heterogeneous material as a result of unevenly distribution of elements within the ash (Izquierdo & Querol, 2012), and is composed primarily of aluminium, silica, ferrous oxide and varying amounts of organic and inorganic oxides (Blissett & Rowson, 2012; Seidel, 1999). The overall composition of the ash will, however, depend on the geological setting where the parent coal was mined, the rank of the coal, and the thermal processing conditions under which the ash was created (Blissett & Rowson, 2012; Neupane & Donahoe, 2013; Seferinoglu, 2003; Seidel, 1999). Different thermal processing conditions will produce ash with different properties (Medina *et al.*, 2010). These minerals within the coal will undergo complete or partial thermal transformation during heat treatment (Neupane & Donahoe, 2013). Some of these transformations may include decomposition of the minerals, volatilization, fusion and agglomeration of particles or condensation. Some of these mineral transformations may render them susceptible to leaching (Izquierdo & Querol, 2012).

Since coal ash is rich in aluminium compounds and contains a variety of metals, it may be considered as a good source for the recovery of these elements (Matjie *et al.*, 2005b; Seidel, 1999). Recovery and recycling of elemental compounds from the coal ash have been accomplished through various leaching methods. Some of these methods differed in the lixiviant used for leaching and has succeeded in the leaching the elements with varying degrees of success (Bai *et al.*, 2011; Kai *et al.*, 2011). Factors such as the chemical and mineral composition of the ash may have an influence on the leachability of the elements from the ash (Seidel, 1999). Another factor that has a large influence on the leaching of an element from the ash is the pH of the lixiviant and hence the pH of the slurry (Izquierdo & Querol, 2012). Impurities within the ash may also influence the leaching of the elements

from the ash, since they may react with the lixiviant. By first removing water-soluble compounds from the ash, lixiviant consumption may be reduced (Kai *et al.*, 2011).

The more readily leached potassium compounds are those that are absorbed onto the surface of the glassy particles; while the rest of the potassium present in the ash is tightly bound to the structure of the glassy particles (Izquierdo & Querol, 2012). The leaching of aluminium from ash is a more difficult task to accomplish since mullite spheres are formed through chemical reactions of silica and alumina during high-temperature thermal processing of the coal (Cheng-you *et al.*, 2012). Most of the free aluminium and some other elements can be found within these spheres. These spheres are strongly resistant to acid digestion during the leaching process, and will thus influence the leachability of aluminium. During the leaching experiments, the formation of $CaSO_4$ may also inhibit the leachability of aluminium (Bai *et al.*, 2011; Nayak & Panda, 2010). As with the aluminium, titanium compounds are found within the glassy particles that had formed during thermal processing (Izquierdo & Querol, 2012).

The extraction of elemental compounds from coal ash has thus far only been done on ash samples that were prepared at veritably high temperatures (> 1000°C) or relatively low temperatures (± 500°C). Very little research has been done on ash that has been prepared at the temperatures 850°C < T < 1050°C. Since the thermal conditions have an influence on the mineral transformations and thus ultimately the leachability of the elements from the ash, further investigation is needed on the recovery of elements from ash prepared at temperatures below 1000°C. Potassium salts are known compounds added to coal during the catalytic gasification process. The addition of a potassium compound to the coal may lead to an increase in the reaction rate of the coal, accompanied by a decrease in the gasification process temperature. The decrease in gasification temperature will result in the formation of low-temperature ash. Recycling of potassium compounds from the coal ash after catalytic gasification of coal will lead to the reduction of processing costs. A method to recover the potassium from the coal ash needs to be investigated. Simultaneous extraction of aluminium and titanium will be economically favourable and beneficial for other industrial processes. Applying chemical thermo-equilibrium modelling to the coal, and using the mineral compositions obtained for the ash samples, insight into the ash composition and leachability of specific elements present in the ash might be gained and used to determine a recovery method. FACTSAGE™ modelling supplies insight into specific mineral interactions, slag formation and slag-liquid temperatures of mineral compositions. The value of the modelling in this study will be that these thermochemistry models can be used to analyse equilibrium conditions for reactions occurring between inorganic and/or organic materials, and also provide insight into the mineral transformation and slag formation processes. The database will assist in understanding, also predicting, what might happen to the specific coal and mineral sources during gasification or combustion processes.

1.2 Basic Hypothesis

Ash produced during combustion/gasification of coal and coal fines is a good source material to be used for the recovery of aluminium- and other valuable inorganic metallic compounds, such as potassium and titanium. Instead of discarding the produced coal ash, recovery of inorganic elements can be achieved by submitting the coal ash to suitable recovery methods. The percentage of element recovered from the coal ash will depend on the recovery method, conditions, and the coal ash properties (composition/ mineral phases).

1.3 Aims and Objectives

1.3.1 FACTSAGE™ thermo-equilibrium modelling

- Physical and chemical assessment of the coal ash produced from different coal samples, varying in ash- and mineral composition;
- Chemical thermo-equilibrium modelling of the coal samples using the FACTSAGE™ modelling software;
- To predict the slagging tendencies and mineral transformations of the coal samples during thermal processing;
- To investigate the influence of potassium on slagging tendencies and mineral transformations during thermal processing.

1.3.2 Recovery of Al, K, and Ti through acid leaching, ammonium sulphate sintering, and alkaline leaching processes

- To determine the dissolution of aluminium, potassium, and titanium from the amorphous- and glassy mineral phases present in the coal ash samples;
- To use different analytical procedures for determining the dissolution efficiencies of the inorganic elements investigated;
- To compare the dissolution efficiencies obtained from the different analytical procedures;
- To determine the most effective procedure for the recovery of the inorganic elements from the coal ash;
- To determine zeolite A formation during alkaline leaching of the coal ash samples.

1.3.3 Potassium Addition

- To determine the influence of added potassium on the slagging temperature and mineral transformations; as observed during the FACTSAGE™ modelling;
- To determine the recoverability of potassium from the coal ash after thermal processing;
- To determine the influence added potassium had on the recoverability of the inorganic elements (Al and Ti) investigated.

1.4 Material and Methods

1.4.1 Coal, Ash, and Characterization

Four coal samples were selected according to their aluminium and potassium content, as determined by XRF analysis of the coal samples. Air drying of the coal samples for 2 days reduced excess moisture not associated with the coal structure. The coal was crushed with a crusher followed by a ball mill to obtain a particle size of <1 mm using standard methods (ISO 1988:1975 and ISO 139094:2016). One of the coal samples was taken and a blend prepared by adding a potassium compound (10 wt.% K_2CO_3) to the coal sample during the milling step. This was done to ensure thorough mixing, and to obtain a homogeneous sample.

The ash samples used in this investigation was prepared by first splitting each coal sample into four 5 kg sub-samples. Each sub-sample was placed into the hot zone of a rotary kiln, where the temperature was increased to 700°C at a heating rate of 10°C/min. A residence time of 3 hours at 700°C was set for all sub-samples. Experiments were conducted under airflow to facilitate combustion of the organic compounds and evolution of the volatile matter. The furnace was switched off after 3 hours so that the cooling rate was generally the natural cooling of the furnace. The four ash sub-samples were blended to form one homogenous ash sample. The bulk ash sample was again split into 4 sub-samples, from which one was kept to represent the ash sample prepared at 700°C. The other three sub-samples were placed in a muffle furnace, where the temperature was increased at a heating rate of 10°C/min, to 850°C, 950°C, and 1050°C. The residence time, for each of these temperatures, was set to be 3 hours. All the coal ash samples were submitted for XRF and XRD analyses.

1.4.2 FACTSAGE™ Modelling

FACTSAGE™ 7.2 modelling software was used and a two-zone gasification simulation model (van Dyk *et al.*, 2008c), was used. The simulation of a real gasification process was done by using similar operating conditions, i.e. similar flows and conditions such as the temperature, pressure, and mass flow, as input data (van Dyk *et al.*, 2006). The organic and inorganic components were divided into four components; moisture, fixed carbon, volatile matter, and minerals. Assuming that coal is composed of these components, the input data for the FACTSAGE™ software is done in elemental form, i.e. carbon, hydrogen, nitrogen, sulphur, and oxygen, as well as for the inorganic components. Input data can also be in mineral/ compound form. In this investigation, the input data was derived from ultimate-, proximate-, and ash composition analyses. The mass flow data for the volatile matter and fixed carbon are normalized to an elemental composition, similar to that of ultimate analysis. Since the ash flow (melt) is composed of a variety of mineral species, it is normalized to a mass flow for the different mineral species (van Dyk *et al.*, 2006).

Simulation Model

The simulation model used was developed on the principle that coal flows from the top, into the gasifier, as gas flows upwards from the zone below into the zone that is being modelled. Thus, as the coal flows downwards into the drying, devolatilization, and gasification (reduction) zone, it comes into contact with and reacts with the gas that flows upwards from the combustion (oxidising) zone. This approach was followed during the modelling of the combustion (oxidation) zone. The modelling zones differ from one another in two main areas: the input data used during the simulations and the temperature range at which the simulations are run. The temperature range used for the drying, devolatilization, and gasification (reduction) zone started at 25°C when the coal enters the gasifier and reacts with the gas that flows up from the combustion (oxidation) zone at a maximum temperature of 1400°C (van Dyk & Keyser, 2014; van Dyk *et al.*, 2009a). The databases used during the FACTSAGE™ modelling simulation calculations were FactFS, FToxid, and FTmisc. The FactPS database was used for all pure- and gaseous components during simulation, while the FTmisc database was used for the pure sulphur compound. The melt phase was imitated using the 'B-Slag-liq with SO_4' phase, which forms part of the FToxid database. During the simulations, only pure compounds from these databases were considered.

1.4.3 Sulphuric Acid Leaching

Low sulphuric acid concentration leaching

The coal ash (10 g) was weighed placed into the leaching vessel to which a 100 ml of sulphuric acid was added; this was done to maintain a 1:10 solid to liquid ratio. The sulphuric acid concentration used was varied between 1.02 M and 4.08 M. The coal ash – acid mixture was stirred (200 rpm) with an automatic overhead stirrer, at a reaction temperature of 45°C; while the leaching time varied from 30 min to 180 min with 30 min intervals. The hot mixture was filtered and washed with deionized water after the specific leaching time had been reached. The filtrate and leach liquor samples were combined to form the final liquid sample, which was submitted for ICP-OES digestion analysis and complexometric titration. XRF and XRD analyses were done on the dried ash residue samples.

High sulphuric acid concentration leaching

The coal ash (10 g) was weighed and placed into the leaching vessel to which a specific volume of a 6.12 M H_2SO_4 solution was added. The volume of H_2SO_4 added to the coal ash was determined so a solid to liquid ratio of 1:5 or 1:10 was maintained. Constant conditions used during leaching included a leaching time of 8 hours, at a reaction temperature of 80°C, and the solution concentration. An overhead automatic stirrer (200 rpm) was used during the leaching process. The hot mixture was filtered and washed with deionized water after the leaching time had been reached. The leach liquor and filtrate samples were combined to form the final liquid sample and which was subjected to ICP-OES digestion analysis and complexometric titration; while the dried ash residues were characterized through XRF and XRD analyses.

1.4.4 Ammonium Sulphate Sintering

Sintering Procedure

The coal ash and ammonium sulphate were weighed separately to obtain a ratio of 2:6 of ash: $(NH_4)_2SO_4$. The two solid components were mixed manually until a homogenous mixture was obtained. The mixture was poured into deep crucibles and placed in the middle of a muffle furnace. The temperature of the furnace was increased to 500°C at a heating rate of 10°C/ min, and the residence time for the mixture in the muffle furnace was 6 hours. The furnace was left to cool to ambient temperature after the residence time was reached. The ash residue was collected and subjected to the dissolution procedure.

Dissolution Procedure

The ash residue collected from the sintering procedure was weighed and placed into the leaching vessel. Using the mass of the ash residue, deionized water was added to the leaching vessel in a solid to liquid ratio of 1 g: 50 ml (ash residue: H_2O). The mixture was stirred for 18 hours using an automatic overhead stirrer (200rpm), and filtered after the leaching time was reached. The leach liquor was subjected to complexometric titration and the dried ash residue to XRF and XRD analyses.

1.4.5 Sodium Hydroxide Leaching

Leaching of the coal ash samples with alkaline solutions of different concentrations was done through the use of two types of leaching experiments, direct- and sequential leaching.

Direct leaching of the coal ash:

The coal ash (20 g) was weighed and placed into the leaching vessel; to which 100 ml of lixiviant was added. This was done to maintain a 1:5 solid to liquid ratio. Lixiviants used during the leaching experiments were H_2O, 1 M NaOH, and 8 M NaOH solutions. The mixture was stirred with an automatic overhead stirrer (200 rpm), for 4 hours, at a temperature of 80°C. After the leaching time had been reached, the hot mixture was filtered and washed with deionized water. The filtrate and leach liquor samples were combined and subjected for ICP-OES analysis, while the dried ash residues were subjected to XRF and XRD analyses.

Sequential leaching of the coal ash:

The coal ash (20 g) was weighed and placed into the leaching vessel; to which a 100 ml of the lixiviant, used during the first leaching step, was added. This was done to maintain a 1:5 solid to liquid ratio. The mixture was stirred with an automatic overhead stirrer (200 rpm) for 4 hours, at a temperature of 80°C. The hot mixture was filtered and washed with deionized water after the leaching time was reached. The ash residue obtained after filtration was placed back into the leaching vessel, to which a 100 ml of lixiviant used during the second leaching step, was added. The same experimental conditions and procedures were applied to the second leaching step, as was

done in the first leaching step. The leach liquor samples obtained from the first and second leaching steps were combined with both filtrates to form the final leach liquor sample. The final liquid sample was subjected to ICP-OES analysis, while the dried ash residue was subjected to XRF and XRD analyses. The lixiviants used during the first sequential leaching procedure were H_2O and an 8 M NaOH solution, in the first and second leaching step respectively; while 1 M NaOH and 8 M NaOH solutions were used in the first and second leaching steps of the second sequential leaching procedure.

1.5 Experimental Diagram

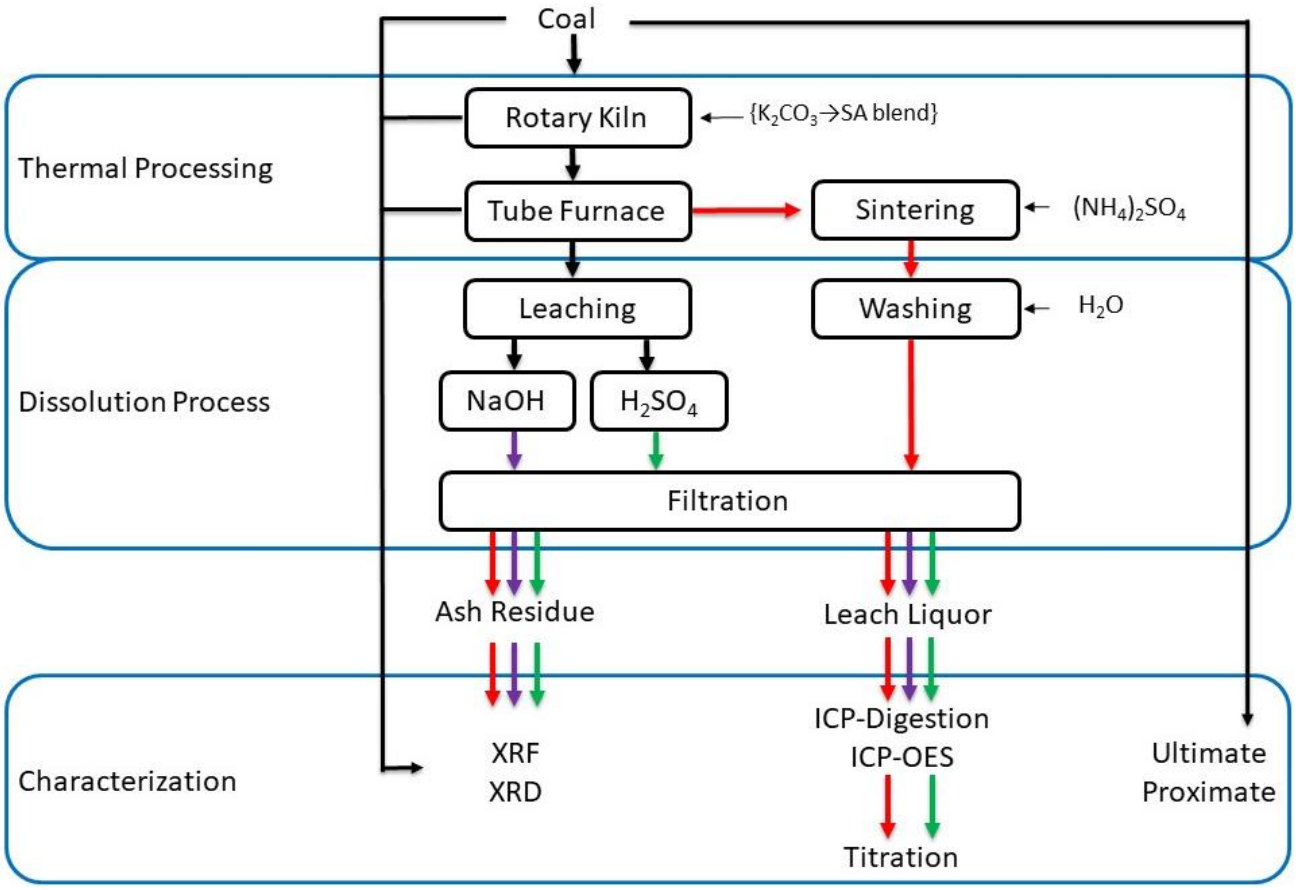

Figure 1-1: Schematic diagram of the experimental- and analytical procedures used throughout this investigation

1.6 Chapter Division

Chapter 1: Introduction

The introduction chapter gives the relevant literature concerning the topic of investigation. This information is framed in a basic hypothesis, a set of aims and objectives, and the methods used throughout the investigation.

Chapter 2: Literature review

This chapter states the relevant literature pertaining to the different topics presented in this investigation. The discussion topics include coal properties, the influence of catalysts during thermal processing, and the various recovery methods used during this investigation. The FACTSAGE™ modelling software and the application thereof is also discussed.

Chapter 3: Article 1: FACTSAGE™ thermo-equilibrium simulations on mineral transformations of combustion ash

In this chapter, FACTSAGE™ modelling software was utilized to simulate a gasification/ combustion process, using the characterization data as input information. The simulation runs for the different coal samples were done in an attempt to predict slagging tendencies of Al- and K- containing mineral transformations. The influence of an added potassium compound to the coal was also investigated with the simulations.

Chapter 4: Article 2: Sulphuric acid leaching of South African combustion ash – dissolution of Al, K, and Ti from laboratory coal ash

This chapter contains the information pertaining to sulphuric acid leaching of coal ash samples produced by low-temperature combustion of South African coals. Leaching experiments were done to determine the dissolution of Al, K, and Ti from the amorphous material and related soluble mineral phases present in the ash samples. The influence of a potassium compound, added to the coal prior to thermal processing, on the dissolution of these inorganic elements, was also investigated. The leaching conditions reflected those used for the recovery of aluminium from various clay sources.

Chapter 5: Article 3: Ammonium sulphate sintering of South African combustion ash: Recovery of Al, K, and Ti from laboratory prepared ash

In this chapter, the recovery of Al, K, and Ti from the coal ash was attempted through a solid phase ammonium sulphate sintering process. The sintered residue is subjected to a dissolution process, after which the dissolution of Al, K, and Ti from the ash were determined. The influence of added potassium on the formation of soluble phases during the sintering process was also investigated.

Chapter 6: Article 4: Alkaline dissolution of laboratory-produced South African ash containing potassium species

Alkaline leaching of coal ash produced during low-temperature combustion of South African coal samples, is discussed in this chapter. The leaching experiments were done to determine the dissolution of Al, K, and Ti from the ash, and the formation of zeolite structures when different concentrations of alkaline solution were used. The influence of leaching procedure, direct- or sequential leaching, was investigated; along with the influence of an added potassium compound on the dissolution of Al, K, and Ti, and the formation of zeolite structures.

Chapter 7: Conclusions and Recommendations

The conclusions reached after FACTSAGE™ modelling (chapter 3) of the coal samples and the conclusions made after submitting the coal ash samples to the various recovery methods for Al, K, and Ti (chapters 4-6), are stated in this chapter. Also stated in this chapter, are recommendations that could give insight into the questions derived from this investigation

Chapter 2

Literature Review

This chapter contains a brief review of the literature relevant to this investigation. The literature included coal properties, the influence of alkali catalysts on thermal processing, and recovery methods implemented for the recovery of the inorganic elements. The advantages and disadvantages of these methods will also be stated in the literature section. The use of FACTSAGE™ modelling software and its application is also mentioned. Literature relevant to the specific aspects of the investigation are included in those specified chapters.

2.1 Introduction

Coal is a heterogeneous material (fossil fuel), containing a variety of organic and inorganic material, which originated through the decomposition and metamorphoses of plant material. The geochemical process occurs over an extended period of time where these different materials are exposed to varying temperatures and pressures (Smoot & Smith, 1985). In young coal samples, such as peat and lignite, remains of plant material can still be found when examined under a microscope (Grainger & Gibson, 2012). The composition of a coal sample can be divided into two specific groups; the inorganic components also referred to as the mineral matter, and the organic components also referred to as maceral content (Ward, 2002). The maceral content for each coal type is dependent on the following factors:

i. the types of plant material that had collected;
ii. climate conditions;
iii. ecological conditions; and
iv. time (Falcon & Snyman, 1986).

Coal rank, or coalification stage, can be assigned to a coal sample by measuring the reflectance of the maceral (vitrinite) content of the sample (Grainger & Gibson, 2012). Factors that influence the coalification stages are:

i. time;
ii. temperature;
iii. pressure; and
iv. depth buried.

Coal can initially be classified into six ranks, depending on the maceral reflectance value and the measured carbon content (Ward, 2002). Figure 2-1 depicts a visual representation of the various coal ranks, accompanied by other factors that characterize each of the coalification stages.

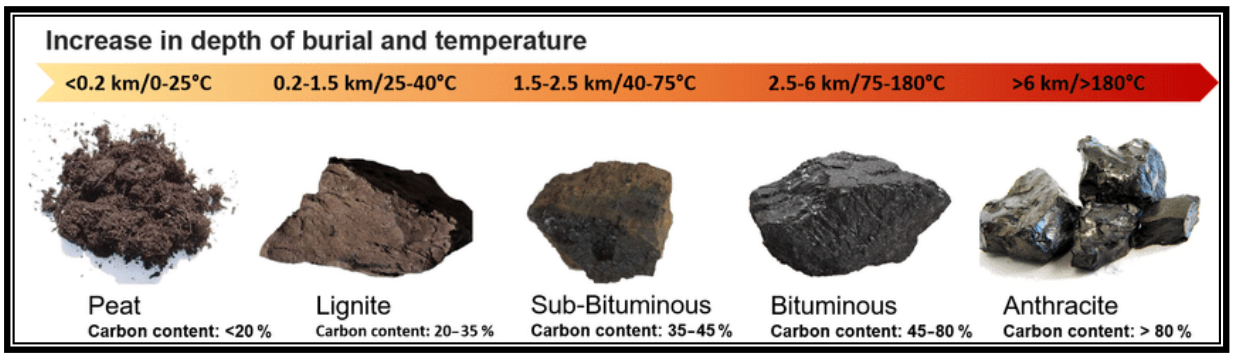

Figure 2-1: Visual representation of coal rank and coalification factors (Zazzeri *et al.*, 2016)

2.1.1 Macerals – Organic Components

Macerals are the organic constituents present in coal samples, which are derived from plant material deposition during the coalification process (Yu *et al.*, 2007). The maceral content of a coal sample will determine the rank of that coal, but will also determine how best to utilize the coal (Ward, 2002). The maceral content will also influence the chemical composition of the coal (Stach *et al.*, 1982). The benefits of coal processing technologies essentially originate from the maceral content of the coal (Green *et al.*, 1988); due to the energy output during coal combustion, methane adsorption and being a potential hydrocarbon source (Ward, 2002). Maceral groups exhibit different properties, chemically and physically, depending on the original plant material from which the maceral group is composed of, but also the environment in which coalification process took place (van Dyk *et al.*, 2006; Yu *et al.*, 2007). The maceral constituents in coal can be classified into three main groups according to their reflectance when viewed under a microscope. The maceral classification is presented in Table 2-1. These maceral groups are for sub-bituminous, bituminous, and anthracite coals.

- **Vitrinite** macerals are oxygen-rich and consist mainly of roots and wood (bark). They exhibit a medium reflectance and appear light grey during petrography analysis;
- **Liptinite** macerals are hydrogen-rich and consist of plant material and structures such as spores and resin. Liptinite has the lowest reflection and appears dark grey during petrography analysis; and
- **Inertinite** macerals are carbon-rich macerals and consists of oxidation products derived from the other maceral groups. Inertinite has the highest reflection and appears white during petrography analysis (Kentucky, 2018).

Table 2-1: Maceral group classification (Kentucky, 2018)

Macerals		Origin
Group	Maceral	
Vitrinite	Telinite	Plant cell walls (with visible structure)
	Collotelinite	Plant cell walls (gelified, structureless)
	Vitrodetrinite	Small particles of plant attritus (worn-down particles of plant humus)
	Collodetrinite	Mottled peat groundmass (originally attritus [worn-down particles])
	Corpogelinite	Primary and secondary cell infillings from humic gels
	Gelinite	Amorphous humic matter in crack fillings
Liptinite	Sporinite	Outer cell walls of plant spores and pollen
	Cutinite	Outer coatings (cuticles) of leaves, roots, stems
	Suberinite	Degraded (suberinized) cell walls of cork in bark and roots
	Resinite	Plant resins, balsams, latexes, fats, and waxes
	Alginite	Algae
	Bituminite	Amorphous fluorescent material of either algal or bacterial origin
	Exsudatinite	Secondary crack-filling material formed from maturation after oil generation
	Fluorinite	Secondary crack-filling material formed from maturation after oil generation
	Liptodetrinite	Fragments or degradation residues of liptinites
Inertinite	Fusinite	Carbonized (fusinized) plant cell walls (from fires and other processes)
	Semifusinite	Partly humified and dehydrated plant tissues
	Funginite	Fungal spores and other fungal tissues
	Secretinite	Possible oxidation product of resins
	Macrinite	Dehydrated small, clumped (flocculated) peat matrix substances
	Inertodetrinite	Tiny, carbonized (fusinized) inertinite precursors
	Micrinite	Secondary coalification residues of liptinitic substances

2.1.2 Mineral Matter – Inorganic Components

Mineral matter is the inorganic, non-combustible fraction that forms part of coal structure; which results in an ash component after gasification/ combustion of the coal. The ash is formed as the inorganic components decompose, melt, react, or oxidize during thermal processing. The formed ash is a concern during coal utilization processes, due to its propensity towards corrosion, abrasion, and fouling (Tomeczek & Palugniok, 2002; Ward, 2002).

The mineral matter in coal can be divided into two major mineral groups:

- **Extraneous minerals** are particles that contain over 90 wt.% of the mineral matter. These minerals can be separated from the coal through mechanical methods, such as crushing of the coal sample before combustion; and
- **Inherent minerals** are closely bonded to the organic coal particles. These minerals cannot be separated from the coal through mechanical means. These mineral make up less than 10 wt.% of particles present in the coal (Tomeczek & Palugniok, 2002).

The term “mineral matter” encompasses three types of constituents, namely:

- Inorganic salts and compounds that are dissolved in the water found within the coal pores;
- Inorganic compounds that form part of the organic (maceral) compound structures; and
- Inorganic particles, whether in crystalline or non-crystalline phase, which represents the true mineral constituents (Ward, 2002).

The most common (abundant) mineral components found in coal include:

- **Clay minerals,** which are the main mineral forms present in coals making up approximately 60% of the mineral matter. Kaolinite and illite are the two clay minerals most commonly found in coal. Clay minerals are mostly found as dispersed inclusion, or in cleats, fissures, or cavities;
- Calcite is the most common **carbonate** mineral found in coal, followed by siderite and then dolomite. Calcite minerals occur mostly in veins or cleat- and cavity fillings; while siderite and dolomite occur as nodules and crystals respectively;
- Quartz is an **oxide** mineral commonly found in coal, with concentrations varying greatly between coal sources. Small amounts of rutile, hematite, and magnetite are also found in the coal;
- Pyrite is the most common **sulphide** mineral found in coal, and is the main carrier of sulphur; while
- **Sulphate** minerals are not as abundant as the minerals described above but is present in some coal samples in the form of gypsum.

The mineral constituents in coal occur through a range of different processes. Mentioned below are only a few of these processes:

- Oxidation of the organic matter in the coal through low-temperature ash production;
- Minerals being washed or blown directly into the peat deposit; through floods, river water, airborne particles, or volcanic debris;
- Precipitation of mineral components in the pore water as the organic material accumulates;
- Relocating of water through the cracks and fissures;
- The formation of crystalline masses along with the original organic material; and
- Skeletal components of swamp organisms, plant tissue, or faecal material may contribute to the mineral matter in the coal (Ward, 1984).

2.2 Coal Ash

Coal is used throughout the world to satisfy the energy demands required, as the population growth increases. It is also considered to be one of the most abundant fossil fuels and is still a major commodity in the production of energy (Yu *et al.*, 2007). Power generation is accomplished through direct combustion of pulverized coal (Nayak & Panda, 2010; Smoot & Smith, 1985); by which large amounts of waste products are generated due to the increase in energy demand. Instead of discarding the formed ash, some percentage thereof is utilized in other industrial applications such as concrete manufacturing, building materials, road base, brick etc. (Izquierdo & Querol, 2012; Nayak & Panda, 2010). The ash not used in these industrial applications gets stored in landfills, stockpiles or waste lagoons (Izquierdo & Querol, 2012). The ash consists primarily of inorganic compounds, which are usually identified and classified as oxides (Nayak & Panda, 2010).

2.2.1 Coal Combustion

The most common method for power production is through pulverized coal combustion. Coal is pulverized to a fine powder consistency and injected into the furnace chamber with a stream of air. The majority of the ash produced travels as suspended particles with the combustion gasses. These particles are collected and is referred to as coal fly ash. During the combustion process, some ash particles fall to the bottom of the chamber, along with fragments that have been deposited on the walls of the chamber. This product is referred to as bottom ash (Robl *et al.*, 2017). The process of coal combustion and mineral transformation is presented in Figure 2-2.

Factors that influence mineral behaviour during the combustion process are as follow:

- Operating temperature;
- Particle size;
- Residence time;
- Mineral association; and
- Gas composition.

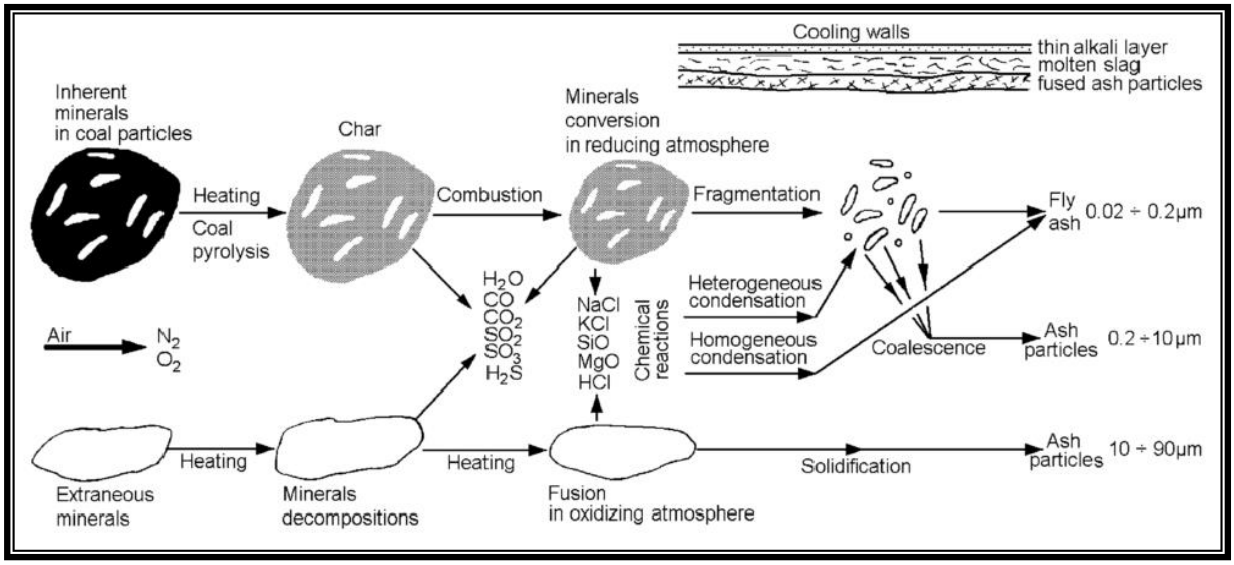

Figure 2-2: Mineral transformation of coal particles (Tomeczek & Palugniok, 2002)

2.2.2 Influence of Catalyst on the Ash Composition

Some minerals and inorganic compounds, mostly the basic compounds, found in coal may influence or change the properties of the coal during thermal processing. This is especially true for low ranking coals with high percentages of inorganic minerals. Alkali carbonates are known catalysts and are frequently used during gasification and combustion of coal (Tang & Wang, 2016).

Factors that influence the catalytic effectivity of alkali carbonates:

- The method used when mixing the alkali compound and coal;
- The alkalinity of the alkali carbonate;
- Dispersion of the alkali compound throughout the coal sample (Audley, 1987; Liu & Zhu, 1986);
- The chemical form in which these compounds are present; and
- The concentration of these compounds in the coal (Samaras *et al.*, 1996).

Known influences of alkali compounds are as follow:

- Some catalytic effect during thermal processing;
- May influence the range of products formed;
- Lower the operating temperature during gasification processes (Bexley *et al.*, 1986; Green *et al.*, 1988);
- Contribute to the conversion of carbonaceous material to the desired products; and
- Used to promote methane production (Nahas, 1983).

During thermal processing of coal containing K_2CO_3, redistribution of the potassium carbonate occurs and takes part in re-polymerization reactions (Jibril *et al.*, 2009). The potassium reacts with

the –COOH and –OH groups (Liu *et al.*, 2004) on the surface of the coal particle to form alkali-salt complexes (Yuh & Wolf, 1983).

Clay minerals like quartz, illite, and kaolinite will react with the potassium compounds to form insoluble and catalytically inactive mineral phases. These mineral phases formed when potassium and clay minerals react are mostly potassium aluminosilicates. The abundance of these potassium aluminosilicate minerals increases as thermal processing temperature increases (Bruno *et al.*, 1988; Formella *et al.*, 1986).

Possible reactions of potassium and clay minerals during thermal processing:

$K_2CO_{3(s)}$ + clay $minerals_{(s)} \rightarrow KAlSiO_{4(s)}$ (2-1)

$K_2CO_{3(s)}$ + clay, quartz, iron $minerals_{(s)} \rightarrow K(Al,Fe)SiO_{4(s)}$ (2-2)

2.3 Recovery Methods for Inorganic Compounds

Coal ash (a combination of bottom- and fly ash) presents a viable source material for the recovery of inorganic compounds (Su *et al.*, 2011). South African bituminous coal ash contains high percentages of Al_2O_3, ranging between 22-28% and SiO_2 percentages ranging between 40-60% (Hattingh *et al.*, 2011); whereas coal fly ash contains about 35% Al_2O_3 and 50% SiO_2 (Van der Merwe *et al.*, 2014). Izquierdo and Querol (2012) claims that even with the difference in coal samples i.e. physical properties and chemical composition, that leaching of the mineral compounds from the coal ash tends to follow the same trend. Following this statement, it would suggest that the leachability of mineral compounds from the ash may be determined by the following factors:

1. Decomposition of mineral phases followed by the formation of new solid mineral phase (with possible volatiles); and
2. The redistribution of mineral phases, which could present with different stabilities and leaching propensities (Seferinoglu, 2003).

Submitting coal ash or coal fly ash to acid leaching, alkali leaching, or any combination thereof, carries with it some advantages and disadvantages.

Advantages of chemical recovery methods

- Mineral matter in coal ash reacts/ dissolves in acidic and alkaline solutions (Rahman *et al.*, 2017);
- Most chemicals are readily available, and could be recycled;
- Selective recovery of inorganic elements from the coal ash is possible;
- Ash residue after certain acid leaching processes can be used in the industry; and
- Formation of zeolite structures that can be utilized in other applications (Fukasawa *et al.*, 2017).

Disadvantages of chemical recovery methods

- Corrosive effects of acidic and alkaline solutions on equipment;
- Extraction of the desired compounds from the leach liquors can be difficult, and might require specialized methods and chemicals;
- An acidic solid residue is left after acid leaching. If not used in other processes, specific waste disposal procedures are required;
- Alkaline sintering- and leaching procedures consume significant amounts of chemicals and energy, which makes industrial application expensive;
- When acidic and alkaline extraction methods are combined, significant quantities of chemicals are consumed during the process;
- Separation of the inorganic compounds from impurities in the leach liquor is difficult (Wu *et al.*, 2014).

2.3.1 Acid Leaching

The extraction of elements from coal ash through direct acid leaching is an effective and powerful method (Seferinoglu, 2003).

Proposed leaching mechanism

A proposed leaching mechanism by Seidel (1999), states that leaching of coal ash/ coal fly ash with sulphuric acid occurs when the reactant diffuses from the acid solution onto the ash particle. The formed products of sulphuric acid and inorganic compounds then diffuses back into the acid solution.

Paul *et al.* (2006) speculated that acid consumption during the leaching process takes place in two phases. Nayak and Panda (2010) made a similar statement concerning the two-phase acid consumption mechanism during the leaching process but added that the leach liquor obtained at the end would depend on these dissolution phases. These two phases are:

1. The first phase, where sulphuric acid reacts with the mineral phases on the surface of the ash particle, occurs quite rapidly;
2. The second and slower phase is during the interactions of the sulphuric acid with the bulk structure of the ash sample.

This means that the recovery of the elements associated with the surface of the ash particle is more effective, due to high susceptibility of these surface phase minerals to the leaching solution, than the elements bonded to the bulk structure of the ash particle (Izquierdo & Querol, 2012; Seferinoglu, 2003).

Factors that have the most influence on aluminium recovery

- Mineralogical and chemical composition of the sample is the most important factor to consider. This will differ between coal and ash samples;
- Carbonates show high dissolution efficiencies, due to the high solubility of the compounds in acid solution (Seferinoglu, 2003);
- Seferinoglu (2003) found that extraction is more effective when acid leaching is done at elevated temperatures (boiling point). Low extraction efficiencies were found when leaching was done at ambient temperature;
- Crushing of the sample before leaching will increase the ash particle surface area. This leads to an increase in surface reactions (phase 1), which would increase the dissolution of the inorganic compounds (Li *et al.*, 2012); and
- The leaching efficiency of specific elements, especially aluminium from coal ash can be promoted by increasing the acid concentration, reaction time and the solid to liquid ratio used during leaching (Nayak & Panda, 2010). However, when the acid concentration used is too high during the leaching process, it can act as a self-inhibitor. This is mainly due to the formation of gelatinous gypsum/ anhydrite mineral phases as the sulphate ion increases and bonds with calcium (Nayak & Panda, 2010; Seidel, 1999).

Possible reactions of Ca-bearing mineral phases with H_2SO_4 to produce gelatinous calcium sulphate and silicic precipitates:

$$CaO_{(s)} + H_2SO_{4(aq)} + H_2O_{(aq)} \rightarrow CaSO_4.2H_2O_{(s)} \quad (2\text{-}3)$$

$$CaCO_{3(s)} + H_2SO_{4(aq)} \rightarrow CaSO_{4(s)} + H_2O_{(aq)} + CO_{2(g)} \quad (2\text{-}4)$$

$$CaO.Al_2O_{3(s)} + 4H_2SO_{4(aq)} \rightarrow CaSO_{4(s)} + Al_2(SO_4)_{3(s)} + 4H_2O_{(aq)} \quad (2\text{-}5)$$

$$(CaO)_x.SiO_{2(s)} + XH_2SO_{4(aq)} \rightarrow xCaSO_{4(s)} + H_2SiO_{3(aq)} + (x\text{-}1)H_2O_{(aq)} \quad (2\text{-}6)$$

Advantages of sulphuric acid leaching method

- High solubility for most inorganic compounds in an acid medium; and
- Availability and affordability. Sulphuric acid is a by-product formed during smelting of precious metals (Paul *et al.*, 2006).

Disadvantages of sulphuric acid leaching method

- It is a corrosive leaching method, and specialized equipment is needed;
- Large quantities of acid are consumed during the leaching process;
- Specialized solid waste procedures are needed (acidic residue);
- Impurities are present in the final leach liquor (Xu *et al.*, 2016); and
- Extraction of aluminium from the leach liquor is difficult due to the presence of iron oxide (Li *et al.*, 2014).

2.3.2 Ammonium Sulphate (bisulphate) Sintering

The use of ammonium sulphate (ammonium bisulphate) sintering as an extraction method for aluminium from coal ash/ coal fly ash, is an attractive method due to the many advantages when compared to the other methods.

Advantages of using ammonium sulphate sintering recovery method

- Ammonium sulphate and the reaction products, ammonium aluminium sulphate and aluminium sulphate, are less corrosive than most acid leaching processes;
- Better utilization of coal ash and coal fly ash sources;
- Reduced waste residues when compared to other recovery methods (Li *et al.*, 2012);
- Ammonium sulphate can be recycled (Highfield *et al.*, 2012);
- Low-cost chemicals are used;
- The formed ammonium salts are water-soluble, and does not require complex extraction methods (Bayer *et al.*, 1982);
- Reduced energy consumption, no calcination process required (Wang *et al.*, 2014a); and
- The solid residue after aluminium extraction can be used for white carbon black production, or chemical production, due to its high silica content (Wu *et al.*, 2014).

Disadvantages of using ammonium sulphate sintering recovery method

- Non-selective reaction mechanism, which leads to the extraction of other major elements such as Ca, Ti, and Fe (Doucet *et al.*, 2016); and
- Extraction of impurities along with the aluminium during the dissolution step.

Proposed mechanism for ammonium sulphate and coal fly ash sintering

During the sintering process, ammonium sulphate reacts with the alumina within the porous glassy structure, by destroying the glassy phase structures, which were formed during high-temperature thermal processing of coal. This causes the glassy particles to aggregate and form large spherical structures (Wu *et al.*, 2014). The reaction between ammonium sulphate and coal ash is a solid-phase reaction, which means that ammonium sulphate has to be in excess during the sintering process. This is to ensure all possible reactions between the ammonium sulphate and coal ash. Ammonium aluminium sulphate and aluminium sulphate is generated during the sintering process (Li *et al.*, 2012).

A possible chemical reaction between ammonium sulphate and alumina (glassy phase) during the sintering process can be expressed, according to (Wu *et al.*, 2014) as follow:

$$4(NH_4)_2SO_{4(s)} + Al_2O_{3(s)} \rightarrow 2NH_4Al(SO_4)_{2(s)} + 6NH_{3(g)} + 3H_2O_{(g)} \quad (2.7)$$

Reactions between ammonium sulphate and glassy phase structure occur more readily than reactions with mullite, due to the stability of the mullite crystalline phase; which requires sufficient energy to break the Al-Si-O bonds (Wu *et al.*, 2014).

The ammonium aluminium sulphate can be recovered from the sintered solid, by means of a dissolution procedure (Li *et al.*, 2012) and can be converted into a number of desirable products, through specific dissolution procedures (Doucet *et al.*, 2016).

Decomposition of ammonium sulphate

Kiyoura and Urano (1970) studied the full thermal decomposition mechanism of ammonium sulphate. The mechanism consisted of at least two decomposition steps. This mechanism is schematically represented in Figure 2-3. From Figure 2-3, it can be seen that the first step in the decomposition mechanism was deamination of ammonium sulphate, to produced ammonium bisulphate. Reactions between ammonium bisulphate and ammonium sulphate during thermal processing produced triammonium hydrogen sulphate ($(NH_4)_3H(SO_4)_2$); which upon further heating releases ammonia to produce ammonium bisulphate. Dehydration of ammonium bisulphate leads to the formation of sulfamic acid (NH_2SO_3H), which decomposes into a variety of gas phases. The reaction of ammonium bisulphate and ammonium sulfamic acid produces ammonium pyrosulphate ($(NH_4)_2S_2O_7$).

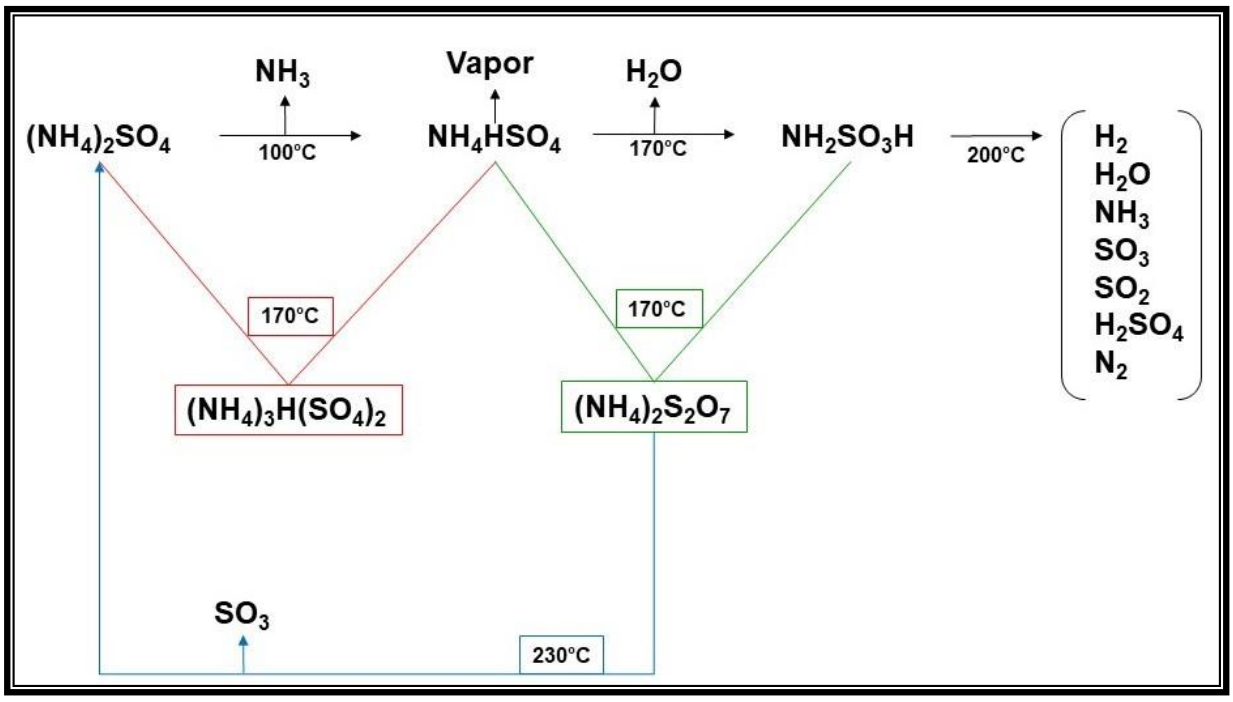

Figure 2-3: Schematic representation for the decomposition of ammonium sulphate (Kiyoura & Urano, 1970)

The decomposition of ammonium sulphate at low temperatures suggest that ammonium bisulphate might have reacted with the alumina present in the glassy phase structures.

Possible reactions for ammonium bisulphate and aluminium mineral phases (Wang *et al.*, 2014a) can be as follow:

$3Al_2O_3{\cdot}2SiO_{2(s)} + 12NH_4HSO_{4(s)} \rightarrow 6NH_4Al(SO_4)_{2(s)} + 6NH_{3(g)} + 9H_2O_{(g)} + 2SiO_{2(s)}$ (2-8)

$3Al_2O_3{\cdot}2SiO_{2(s)} + 9NH_4HSO_{4(s)} \rightarrow 3Al_2(SO_4)_{3(s)} + 9NH_{3(g)} + 9H_2O_{(g)} + 2SiO_{2(s)}$ (2-9)

Factors that influence the extraction of aluminium

- Sintering temperature;
- Sintering time;
- Particle size: with smaller sizes providing larger surface area for reactions; and
- The ammonium sulphate to coal ash/ coal fly ash ratio (Wang *et al.*, 2014a).

Recycling of ammonium sulphate

The spent ammonium sulphate can be recycled after the sintering and dissolution processes used for the extraction of aluminium. One recycling method is as follow:

i. Ammonia ($NH_{3\ (g)}$) is a by-product formed during the ammonium sulphate and coal ash/ coal fly ash sintering step. The ammonia gas evolved during this step is absorbed into water;
ii. The sintered residue is subjected to a hot H_2O dissolution procedure. Specific conditions are set for the dissolution step;
iii. The ammonium aluminium sulphate rich solution is separated from the solid residue through filtration;
iv. Aluminium hydroxide is precipitated from the solution by mixing the ammonium aluminium sulphate rich solution with the ammonia water (step i). Ammonia water encourages aluminium hydroxide precipitation (Bayer *et al.*, 1982; Li *et al.*, 2012); and
v. Ammonium sulphate salt is recycled after evaporation of the liquid Li *et al.* (2012).

2.3.3 Alkaline Leaching

Alkaline leaching of coal and coal fly ash is an alternative method for the recovery of inorganic elements, whilst also promoting the synthesis of zeolite structures (Fukasawa *et al.*, 2017). Zeolite synthesis provides another process for the utilization of coal ash and coal fly ash; which is more cost-effective than land disposal (Iqbal *et al.*, 2019). Using an alkali solution for the recovery of aluminium bearing compounds from coal ash is a promising method, by avoiding a calcination process, thus lowering the energy costs (Su *et al.*, 2011). van Jaarsveld and Van Deventer (1999) found that the type of alkali solution used during these hydrothermal processes plays an important role in zeolite formation, dissolution of alumina, and subsequently silica-bearing minerals. Sodium hydroxide was found to be a more effective alkali solution (van Jaarsveld & Van Deventer, 1999).

The dissolution of alumina and silica-bearing minerals from coal ash and coal fly ash, when using low NaOH concentration solutions, generate low percentages of sodium silicate and sodium aluminate. These compounds are then leached from the coal ash and coal fly ash samples.

Chemical reactions for the formation of sodium silicate and sodium aluminate are as follow:

$$2NaOH_{(aq)} + Al_2O_{3(s)} \rightarrow 2NaAlO_{2(aq)} + H_2O_{(aq)} \quad (2\text{-}10)$$

$$2NaOH_{(aq)} + SiO_{2(s)} \rightarrow Na_2SiO_{3(aq)} + H_2O_{(aq)} \quad (2\text{-}11)$$

When high sodium hydroxide solutions are used for the dissolution of alumina and silica bearing minerals (glass phase), the following reactions can occur:

$$SiO_{2(s)} + OH^-_{(aq)} \rightarrow H_2SiO_4^{2-}{}_{(aq)} \quad (2\text{-}12)$$

$$Al_2O_{3(s)} + OH^-_{(aq)} \rightarrow Al(OH)_4^-{}_{(aq)} \quad (2\text{-}13)$$

The presence of the ions formed in equation 2-12 and 2-13 in solution, will lead to the formation of sodium-aluminosilicate complexes. Possible chemical reactions for the formation of these complexes as proposed by Su *et al.* (2011) and Behera *et al.* (2017) respectively are as follow:

$$6H_2SiO_4^{2-}{}_{(aq)} + 6Al(OH)_4^-{}_{(aq)} + 6Na^+_{(aq)} \rightarrow Na_6(AlSiO_4)_6{\cdot}4H_2O_{(s)} + 12(OH^-)_{(aq)} + 8H_2O_{(aq)} \quad (2\text{-}14)$$

$$NaOH_{(aq)} + NaAlO_{2(aq)} + Na_2SiO_{3(aq)} \rightarrow Na_x(AlO_2)_y(SiO_2)_zNaOH{\cdot}H_2O_{(s)} \quad (2\text{-}15)$$

Possible reaction of sodium hydroxide with aluminium silicates may be represented by the following equation (Rahman *et al.*, 2017):

$$3Al_2SiO_2O_5(OH)_{4(s)} + 8NaOH_{(aq)} \rightarrow 2Na_4Si_3Al_3O_{12}(OH)_{(s)} + 9H_2O_{(aq)} \quad (2\text{-}16)$$

The formation of zeolite structures prevents the recovery of aluminium from the coal ash through direct alkali leaching methods; which can be remedied by a two-step alkali leaching method where the first alkali leaching step removes soluble silica from the solid sample. Removal of silica inhibits zeolite formation, which would then lead to high leaching values for aluminium (Su *et al.*, 2011). Addition of $Ca(OH)_2$ to the alkaline extraction process immobilizes the silica (Li *et al.*, 2014) through the formation of $NaCaHSiO_4$, which inhibits zeolite formation and promotes aluminium leaching (Yang *et al.*, 2014; Zhong *et al.*, 2009).

Zeolite structures can be dissolved through sulphuric acid leaching of the solid product containing these structures. Acid leaching of the solid sample containing the zeolite structures produces a solution containing sodium- and aluminium sulphates and silicic acid (Rahman *et al.*, 2017). This reaction can be presented as follow:

$$2Na_4Si_3Al_3O_{12}(OH)_{(s)} + 9H_2O_{(aq)} + 13H_2SO_{4(aq)} \rightarrow 4Na_2SO_{4(aq)} + 3Al_2(SO_4)_{3(aq)} + 6H_2SiO_{3(aq)} + 8H_2O_{(aq)} \quad (2\text{-}17)$$

Zeolites

Zeolites are multi-utility crystals, with a three-dimensional porous aluminosilicate framework; which occur naturally, or can be synthesized through crystallization of aluminosilicate gels in a basic environment (Bukhari *et al.*, 2015; Cheung & Hedin, 2014). The framework of the zeolite structure is negatively charged to facilitate ion exchange and sorption onto the structure (Cheung & Hedin, 2014). Zeolites are characterized by their physical properties such as porosity, cation exchange capacity and surface density (Belviso, 2018). Two common zeolite frameworks, SOD and LTA, are presented in Figure 2-4.

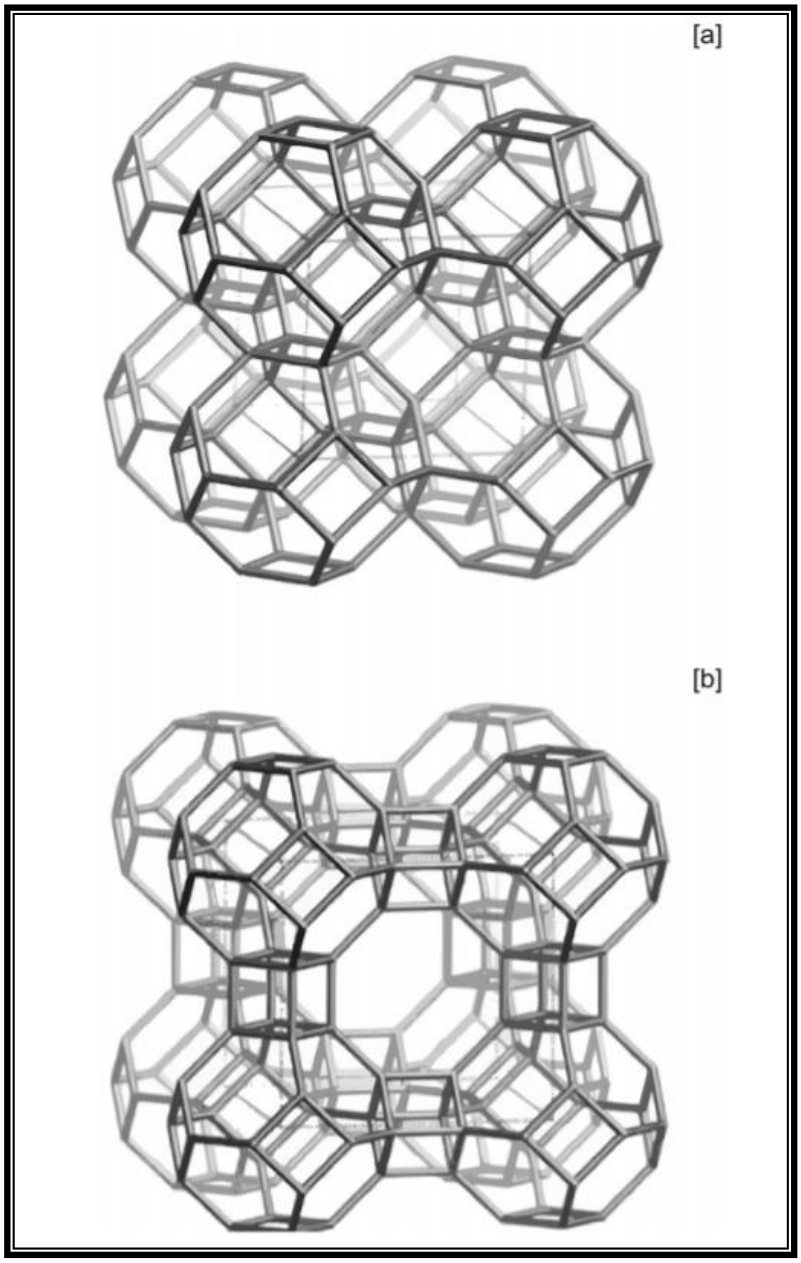

Figure 2-4: Structure of two common zeolite frameworks a) SOD and b) LTA (Belviso, 2018)

Zeolite synthesis

Zeolite structures can be precipitated from aluminosilicate solutions with the use of an alkaline media, but also through alkaline leaching of silica and alumina bearing material such as coal ash and coal fly ash (Bukhari et al., 2015). The formation of zeolite structures occurs on the surface of the ash particle during the leaching process (Jiang et al., 2015). Fukasawa et al. (2017) suggested that the silica and aluminium dissolution rate from the ash particle decreased in accordance with zeolite growth. This decrease in silica and alumina bearing mineral dissolution observed is due to the adsorption of zeolite on the reactive coal ash particle forming a film on the particle surface, which limits the diffusion of the lixiviant into the particle (Behera et al., 2017). Pulverization of the ash particles will thus improve zeolite growth as the larger surface area will promote silica and aluminium dissolution (Fukasawa et al., 2017).

Factors that may influence zeolite synthesis:

- Type of alkali solution used (van Jaarsveld & Van Deventer, 1999);
- Fukasawa et al. (2017) found that particle size is a significant factor. High percentages of sodalite were formed when the sample was pulverized before treatment;
- Leaching temperatures will influence reaction rates (Behera et al., 2017);
- The concentration of the alkali solution used (Fan *et al.*, 2008);
- The reaction time (Fan et al., 2008);
- Activation solution-to-coal fly ash ratio (liquid to solid ratio) (Belviso, 2018).

Utilization of Zeolites

The zeolites crystals, of which the basic structure consists of aluminosilicates which are formed during hydrothermal processing of coal ash and coal fly ash, can be utilized in various ways:

- Could be used as catalysts (Iqbal et al., 2019);
- CO_2 adsorbents (Fukasawa et al., 2017);
- Immobilization of radioactive waste material;
- Molecular sieves (Fan et al., 2008);
- Purification of water; and
- Purification gas components (Cheung & Hedin, 2014).

2.4 FACTSAGE™ Modelling

2.4.1 Introduction to FACTSAGE™

GTT Technologies are the developers and administrators of the FACTSAGE™ thermodynamic software and databases (van Dyk *et al.*, 2006). Thermodynamic modelling started as a research project between two universities in 1976 known as, "F*A*C*T- *Facility for the analysis of chemical thermodynamics".* (Bale *et al*., 2002). The FACTSAGE™ database was introduced in 2001, after merging of two computational software packages, F*A*C*T (FACT-win) and ChemSage (Bale *et al.*, 2009; Song *et al.*, 2009; van Dyk *et al.*, 2009a). The original software was designed to simulate the thermochemical processes during pyrometallurgical processing; which has since been expanded to include other fields such as geology, hydrometallurgy, combustion, etc. (Bale *et al.*, 2009).

The FACTSAGE™ modelling software and databases allow the user to perform the following actions:

- To manipulate the pure substance- and solution databases (Hanxu *et al.*, 2006; Song *et al.*, 2009);
- These databases were first created for complex chemical equilibrium reactions and process simulations but have been expanded to include chemical equilibrium calculations, phase diagram calculation and manipulation, and enthalpy changes (Gheribi *et al.*, 2012; van Dyk *et al.*, 2009a);
- The ability to simulate reactions containing carbon and minerals, while still being able to change process conditions (van Dyk *et al.*, 2009a).

The databases are put together through the evaluation and optimization of the models, using all available information (Hanxu *et al.*, 2006). Due to the complexity of thermodynamic models, the assembly of algorithms can be slow and sensitive (Song *et al.*, 2009).

2.4.2 FACTSAGE™ Modelling Software Applications

The FACTSAGE™ modelling software is a powerful tool, that can be used for predictions simulations and thermochemical calculations; which could be utilized for a number of different processes (Hanxu *et al.*, 2006). The ash fusion temperature of coal during thermal processing is one such thermochemical calculation that can with the modelling software. Ash fusion temperature is an important parameter used to access the quality of coal (Jak, 2002), and is one of the most accepted methods used to date (van Dyk *et al.*, 2009a). van Dyk *et al.* (2006) developed a prediction model based on a fixed-bed counter-current gasification process. The model consisted of three simulation zones, 1) drying and devolatilization zone, 2) gasification zone, and 3) the combustion and ash zone, as presented in Figure 2-5a. van Dyk and Waanders (2008) improved this model to a two-zone simulation model; 1) drying, devolatilization, and gasification zone and 2) combustion and ash zone, as shown in Figure 2-5b. The simulation predictions from this model, compared favourably with

experimental data obtained from HT-XRD analyses and supplies insight into specific mineral- and slag transformations.

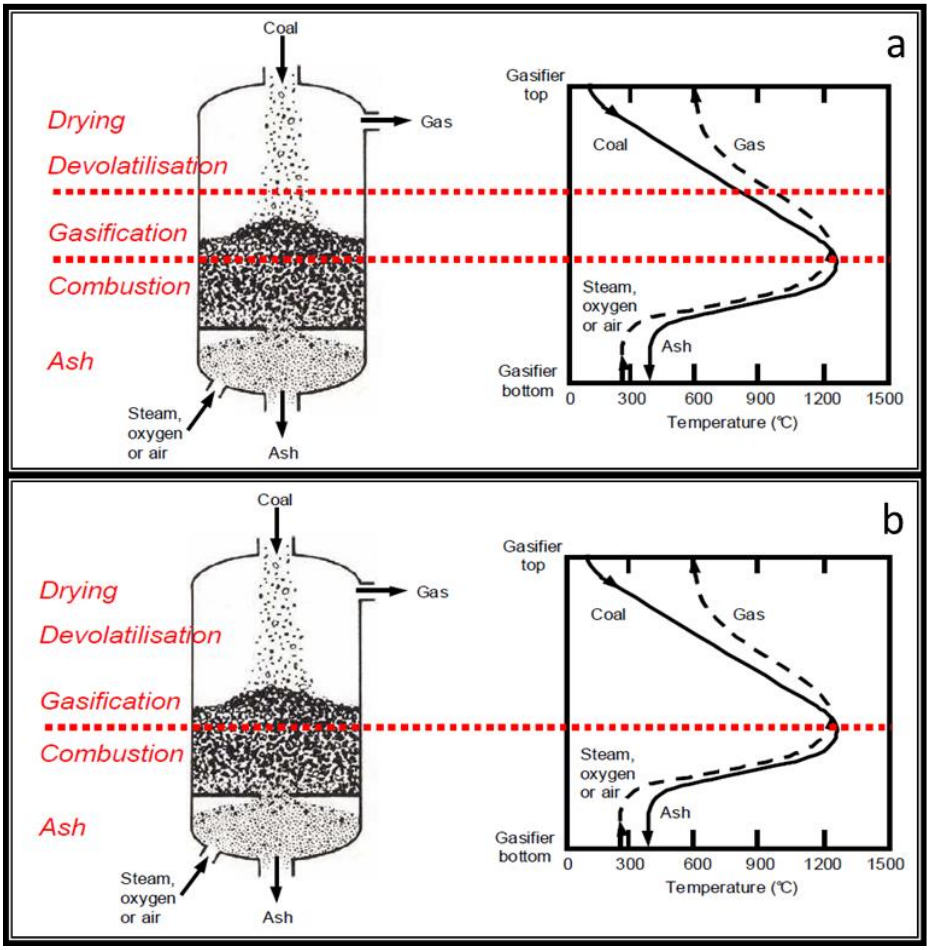

Figure 2-5: Processing zones in a Sasol-Lurgi gasifier (Slaghuis, 1993)

Viscosity modelling is another parameter that could be used in the prediction of slag behaviour of coal during the gasification process (van Dyk *et al.*, 2009a). Patterson and Hurst (2000) used the graphs obtained after viscosity modelling, to determine the flux requirements for coal samples used in slagging gasifiers.

The FACTSAGE™ modelling software has also been used for phase diagram predictions of complex minerals. Zhao *et al.* (2013) found that experimental mineral analysis compared favourably with the FACTSAGE™ phase diagram predictions. Suitable parameters such as chemical composition, temperature, pressure, atmosphere, etc. must be available to be used as input data into the software. This is to ensure that optimum results for any given simulation is obtained (Zhao *et al.*, 2013).

The main menu interface of the FACTSAGE™ modelling software is presented in Figure 2.6. In the figure, it can be seen that the different modules are grouped into four different categories, each with its own purpose. The four modules are as follow:

i. Info: This module contains all relevant information on the databases and modules. The FAQ is also stored in this module;

ii. Databases: Two types of databases are available, compound and solution database;

iii. Calculate: This module is used for calculation of thermochemical equilibria and phase diagrams;

iv. Manipulate: Contains a variety of modules that could be used to process tabular and graphical results.

Bale *et al.* (2016) offer a full description of the individual modules found in the four categories.

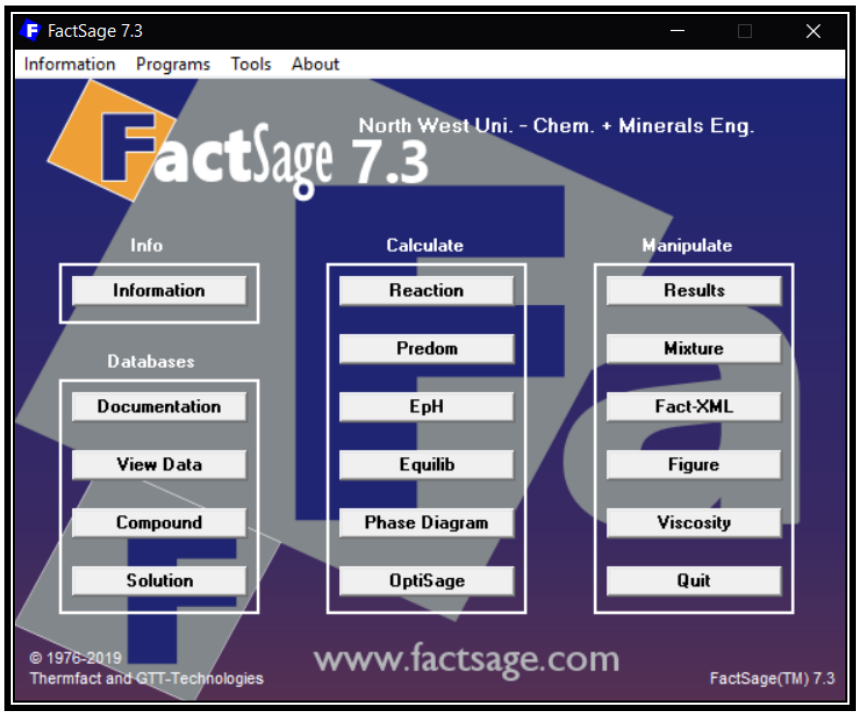

Figure 2-6: Main menu for the FACTSAGE™ software program

Chapter 3

FACTSAGE™ thermo-equilibrium simulations on mineral transformations of coal combustion ash

Anna C. Collins, Christien A. Strydom
Johannes C. van Dyk, and John R. Bunt

FACTSAGE™ thermo-equilibrium modelling was done on three South African coal samples and one American coal sample, to determine the influence of processing conditions on the slagging tendencies of the coal samples. The influence of K_2CO_3, when used as a catalyst during thermal processing, on the slagging behaviour of the coal, was also investigated.

The content of this paper was published in:

The Journal of the Southern African Institute of Mining and Metallurgy **2018**, 118, 1-8.

Abstract

Minerals in coal, their quantities, and thermal the conditions to which the coal is subjected to, will have an influence on mineral transformation and slag formation. More importantly, the type and estimated quantity of minerals that can be recovered after thermal processing. FACTSAGE™ Thermo-Equilibrium Software and associated databases supply the option to scientifically predict these mineral transformations during thermal processing. The aim of this investigation is to report on the influence of operating conditions on the slagging behaviour of South African coal, and the role that additives such as potassium carbonate have on the slagging behaviour. This was done by using the FACTSAGE™ modelling software and a model specifically developed to simulate the different reaction zones. The mineral transformations on K- and Al-containing inorganic compounds under certain thermal conditions were tracked to see whether these compounds remain in mineral form or form part of the slag. With the prediction results found in this investigation, the main contributors to slag formation were identified, and possible inorganic mineral transformations. The addition of potassium carbonate to the coal before thermal processing lead to a decrease in the melt formation temperature and decreased melt percentage. The influence of potassium on the coal behaviour during thermal processing depended on the percentage of potassium in the sample and coal composition. The basic components present in the coal also influenced the mineral transformation and slagging behaviour.

Keywords: FACTSAGE™, potassium, aluminium, Influence of K on slagging

3.1 Introduction

Coal is a heterogeneous material (sedimentary rock) composed of organic and inorganic components. The chemical and physical properties of coal vary depending on the source of the coal, i.e. the age and geological environment where the coal was mined (Oboirien *et al.*, 2011; Yu *et al.*, 2007). During the gasification of coal, the organic matter partially decomposes (Kong *et al.*, 2011); while mineral transformations occur (Song *et al.*, 2009). Coal ash is thus a collection of mineral and non-mineral inorganic elements that had undergone transformation as a result of thermal processing. The ash composition will depend on the organic and inorganic compounds present in the coal and/or any materials added to the coal prior to thermal processing (Kong *et al.*, 2014). This specific composition of the sample, the organic and inorganic components, determines the mineral matter transformation and, thus, the slag formation (van Dyk, 2006). Mineral behaviour during thermal processing depends on:

i. the different types of minerals (modes of occurrence) and quantities present within the coal sample (Benson *et al.*, 1995; Vassilev *et al.*, 1995);
ii. the operating temperatures; and
iii. the oxygen partial pressure thus, the atmosphere (Jak *et al.*, 1998).

When the coal is subjected to high(er) temperatures (>1100°C), melting and reactions of the component mineral matter occurs, thus slag formation occurs (Song *et al.*, 2009). It is assumed that slag formation is due to the mineral matter in the coal, coupled with the operating conditions (Guo *et al.*, 2014). In addition, the slagging tendency of coal ash depends on the ash composition, i.e. the different inorganic species present in the ash, as these minerals determine the ash fusion temperature (AFT) (van Dyk & Waanders, 2008). Consequently, the ash fusibility has generally been expressed as a function of the content of the principle oxides found within coal ash: i.e. SiO_2, Al_2O_3, TiO_2, Fe_2O_3, CaO, MgO, Na_2O, and K_2O (Seggiani, 1999). The ash fusion temperatures are determined by the modes (vapour, mineral grains) in which these elements occur in the ash. Although AFT is still widely used as a parameter for determining ash fusibility and melting characteristics of minerals (Jak *et al.*, 1998), accurate results are difficult to obtain due to the complex composition of coal ash. Because of the complex nature of coal and the associated minerals, prediction of the mineral behaviour/transformation during thermal processing is a difficult task (Jak *et al.*, 1998), when applying tradition methods (Hanxu *et al.*, 2006).

FACTSAGE™ simulation of the process provides a means by which mineral behaviour/transformation towards equilibrium conditions can be predicted. It is an important tool that can be used to describe equilibrium ash properties, mineral transformation, inorganic behaviour, and the slagging tendency of coal ash at specific temperatures (van Dyk & Waanders, 2008), which can then be compared to experimental results. The modelling software was mainly developed for

complex chemical equilibrium and process simulations, but can also be used to calculate and manipulate phase diagrams for minerals and mineral complexes (van Dyk *et al.*, 2009a). One of the advantages of using the FACTSAGE™ databases is that carbon reactions can be studied in conjunction with minerals, while still being able to change atmospheric conditions (van Dyk *et al.*, 2006). The FACTSAGE™ software can also provide information on the phases that have reached equilibrium during thermal processing, the composition and also the proportions in which these phases are present (Hanxu *et al.*, 2006). A wide range of thermochemical calculations can also be performed with the FACTSAGE™ software (Hanxu *et al.*, 2006; Zhao *et al.*, 2013).

A FACTSAGE™ model was developed by Van Dyk et al (van Dyk *et al.*, 2006) in order to understand the chemistry and mineral transformation during a fixed bed counter current gasification process. This model consisted of a three-zone simulation:

1. Drying and devolatilization zone;
2. Gasification zone; and
3. Combustion and ash zone.

van Dyk and Waanders (2008) later developed a new model which originated through modification of the original model. This model consisted of a two-zone simulation:

1. Drying, devolatilization, and gasification zone (reduction zone); and
2. Combustion and ash zone (oxidation zone).

Both the original and improved thermodynamic equilibrium models were validated with high-temperature X-ray diffraction (HT-XRD) (van Dyk & Waanders, 2008; van Dyk *et al.*, 2008c).

The recovery of inorganic compounds from coal ash produced during thermal processing may have economical value, instead of being discarded. Potassium salts are known to be used as gasification catalysts, i.e. they promote the production of methane during gasification (Nahas, 1983) and lower the operating temperatures of the gasification process (Green *et al.*, 1988). This then provides a good source material for possible recovery of spent potassium, for re-utilization in industrial processes (Ge *et al.*, 2014). Thus the main aim of this investigation is to not only evaluate the influence of operating temperatures on slagging behaviour of South African coal ash but also to determine if the addition of a potassium compound (to the coal) influenced the slagging behaviour. This influence of potassium on the coal behaviour was evaluated by adding different percentages of potassium to the system (modelling simulation) for each of the coal samples consisting of different compositions. The mineral transformations, especially Al- and K- containing minerals, during the simulation runs will also be tracked and discussed.

3.2 Material and Methods

3.2.1 Coal Samples

During this investigation, 3 South African (SA1, SA2, and SA3) samples and 1 American (US1) sample was used. The South African samples originated from mines located in the Mpumalanga region and the American coal from North Dakota. These samples were collected and sampled by the mine itself, and a representative sample of 50 kg was used during this study. The coal samples from various mines were selected so different ranks of coal would be represented, and by characterizing the ash content of the coal, a variation in potassium content and acidity would be represented. The coal rank was determined using the ASTM D388-12 classification standard. The acidity was determined from the XRF results (Table 3-3) using the following equation:

$$\text{Acidity} = (SiO_2+Al_2O_3)/(Fe_2O_3+CaO+MgO+Na_2O+K_2O) \text{ (van Dyk } et\ al.\text{, 2008d)} \quad (3\text{-}1)$$

The rank and acidity, as determined with the equation, for the four coal samples are presented in Table 3-1.

Table 3-1: Coal rank and acidity values for the four coal samples

COAL SAMPLE	COAL RANK	ACIDITY
SA1	Medium Volatile Bituminous	18.4
US1	Lignite	2.95
SA2	High Volatile Bituminous	2.91
SA3	Medium Volatile Bituminous	6.31

3.2.2 Sample Preparation

The coal was prepared by air drying the entire sample received from the mine, to reduce the excess moisture not associated with the coal structure. After drying, the coal samples were crushed using a crusher and ball mill to obtain a sample size of <1 mm. The SA2 blend sample was prepared by the addition of the potassium compound (5 wt%) to the coal during the milling step. This was done to ensure a heterogeneous mixture of additive and coal.

Predicting the influence of potassium percentage on the mineral transformation and slagging behaviour was investigated using FACTSAGE™ modelling. The percentage potassium added was calculated according to the ash yield of the coal, i.e. specific percentage potassium was loaded to the sample according to coal ash percentage.

3.2.3 Analytical Methods

The coal samples were subjected to ultimate, proximate, and XRF analyses. Sample preparation was done according to the ISO 13909-4: 2001 standard method. The ISO standard characterization methods used on the coal samples are summarized in Table 3-2. The ash composition of the coal ash samples was determined through XRF analysis, where the composition is presented as elemental oxides.

Table 3-2: Coal characterization methods

ANALYSES	STANDARD METHOD
Proximate analysis	
Moisture content	ISO 11722: 1999
Ash content	ISO 1171: 2010
Volatile content	ISO 562: 2010
Fixed carbon	By calculation
Ultimate analysis	ISO 29541: 2010
Ash composition (XRF)	ASTM D4326

3.2.4 FACTSAGE™ Modelling

3.2.4.1 Introduction

FACTSAGE™ 7.2 modelling software was used to investigate the mineral transformations and speciation of the four coal samples that were selected for this study. A two-zone gasification simulation model (van Dyk *et al.*, 2008c), described earlier, was used. In order to simulate a real gasification process, similar operating conditions had to be used and applied within the model, i.e. similar flows and conditions such as the temperature, pressure, and mass flow (van Dyk *et al.*, 2006). Although coal is a complex heterogeneous material that consists of both organic and inorganic components varying in percentages and mineral types, it is assumed that coal consists of four basic components to accommodate the model used for the simulations. These four components are moisture, fixed carbon, volatile matter, and minerals. Assuming that coal is composed of these components, the input data for the FACTSAGE™ software is done in elemental form, i.e. carbon, hydrogen, nitrogen, sulphur, and oxygen, as well as for the inorganic components. Input data can also be in mineral/ compound form. In this paper, the input data was derived from the results obtained from ultimate-, proximate-, and ash composition analyses. The mass flow data for the volatile matter and fixed carbon are normalized to an elemental composition, similar to that of ultimate analysis. Since the ash flow (melt) is composed of a variety of mineral species, it is normalized to a mass flow for the different mineral species (van Dyk *et al.*, 2006).

3.2.4.2 Simulation Model

The model used in this investigation was developed on the principle that coal flows from the top into the gasifier, as gas flows upwards from the zone below into the zone that is being modelled. Thus, as the coal flows downwards into the drying, devolatilization, and gasification (reduction) zone, it comes into contact with and reacts with the gas that flows upwards from the combustion (oxidising) zone. A similar approach was followed during the modelling of the combustion (oxidation) zone. As the organic and mineral matter in coal enters the combustion (oxidation) zone, they react with the reagent gas that flows into the gasifier at 340°C (van Dyk *et al.*, 2009a). The two modelling zones, as described in van Dyk *et al.* (2008c), differ from one another in two main areas: the input data used during the simulations and the temperature range at which the simulations are run. The temperature range used for the drying, devolatilization, and gasification (reduction) zone started at 25°C when the coal enters the gasifier and reacts with the gas that flows up from the combustion (oxidation) zone at a maximum temperature of 1400°C (van Dyk & Keyser, 2014; van Dyk *et al.*, 2009a). The databases used during the FACTSAGE™ modelling simulation calculations were FactFS, FToxid, and FTmisc. The FactPS database was used for all pure- and gaseous components during simulation, while the FTmisc database was used for the pure sulphur compound. The melt phase was imitated using the 'B-Slag-liq with SO_4' phase, which forms part of the FToxid database. During the simulations, only pure compounds from these databases were considered.

3.3 Results and Discussion

3.3.1 Characterization Results

The chemical characterization of the coal ash samples, that is the ultimate and proximate analyses results are presented in Table 3-3. From these results; the ash yield percentages varied between 20% and 30% for the different samples. High volatile content was also observed for the South African coal samples. This is similar to previous observations made for South African coals (Hattingh *et al.*, 2011).

The ash composition results for the coal ash samples are presented in Table 3-4. These results indicate that the coal ash samples consist primarily of alumina (Al_2O_3) and silica oxide (SiO_2), with K_2O percentages between 0.43% and 2.06%. The SA2 blend sample with the added potassium compound had a K_2O percentage of 16.1%, along with the Al_2O_3 and SiO_2. Other compounds present in the ash sample to be taken note of, are the CaO, Fe_2O_3, Na_2O, and MgO oxides. These compounds are known for their fluxing potential during thermal processing of coal. From Table3-4, it can be seen that moderate percentages of these compounds were present in the coal ash samples.

Table 3-3: Ultimate and Proximate analyses results for the coal samples

Sample	*SA1*	*US1*	*SA2*	*SA2 Blend*	*SA3*
Proximate Analysis (air-dried basis)					
Moisture content	3.3	18.0	3.7	4.6	4.0
Ash yield	28.3	20.5	28.5	26.8	22.4
Volatile content	18.2	30.5	21.2	21.5	21.9
Fixed carbon	50.2	31.0	46.5	47.1	51.7
Ultimate Analysis (air-dried-ash free basis)					
% Carbon content	56.4	43.3	53.7	54.6	59.1
% Hydrogen content	3.0	3.2	2.6	3.4	3.1
% Nitrogen Content	1.2	0.7	1.3	1.3	1.4
% Oxygen content	7.4	13.3	8.9	8.5	8.9
% Sulphur content	0.5	1.0	1.3	0.8	1.1

Table 3-4: XRF analysis results for the coal ash samples

Sample	*SA1*	*US1*	*SA2*	*SA2 Blend*	*SA3*
SiO_2	63.2	52.2	41.6	36.6	55.2
Al_2O_3	28.5	15.4	25.2	21.6	25.9
CaO	1.5	9.1	13.0	10.1	5.1
SO_3	1.5	8.1	7.6	5.1	4.3
Fe_2O_3	2.0	5.2	5.7	4.9	5.5
MgO	0.8	3.5	3.2	2.9	1.8
Na_2O	-	2.9	-	0.1	-
K_2O	0.7	2.1	1.1	16.1	0.4
TiO_2	1.5	0.8	1.8	1.6	1.3
BaO	-	0.6	0.2	0.5	0.1
SrO	-	0.3	0.3	0.3	0.1
MnO	-	0.1	0.1	0.1	0.1
P_2O_5	0.1	0.1	0.3	0.3	0.1
Cr_2O_3	0.1	-	-	-	-

3.3.2 FACTSAGE™ Modelling

Thermochemical calculations which form part of the FACTSAGE™ modelling software (applying the EQUILIB Tool), make it possible to predict the equilibrium behaviour of the inorganic compounds during thermal processing. Equilibrium mineral transformation and slag formation can, therefore, be predicted; under specific conditions. The influence of potassium, when used as an additive, was modelled using the following approach: Potassium addition was done according to the ash yield of the coal; i.e. a specific percentage (1, 5 or 10 mass %) of the ash yield is represented by the potassium oxide seen in Table 3-4. Figures 3-1 to 3-5 present the FACTSAGE™ simulation graphs for the feed coal and coal blend samples in the reduction zone. Figure 3-6 indicates the AFT versus the percentage of basic compound, and Figures 3-7 to 3-9 present the FACTSAGE™ simulation graphs for the feed coal and coal blend samples in the oxidizing zone.

As SA1 and SA3, containing the lowest percentages of K_2O and MgO, highest percentages SiO_2, and highest acidity, behave similarly according to the FACTSAGE™ simulation results, only the

results obtained for SA1 are shown and discussed. US1 and SA2 have similar acidity values as calculated from the XRF data, both containing high percentages of K_2O and MgO; hence the results from SA2 are shown and discussed. The FACTSAGE™ results for SA2 and the SA2 blend are shown and discussed.

3.3.3 Drying, Devolatilization and Gasification (reduction) Zone

3.3.3.1 Mineral transformation of the coal samples

The mineral transformation simulation for SA1 is presented in Figure 3-1. From the graph, it can be seen that the temperature at which melt stars to form was predicted to be 1175°C. The temperature at which the melt starts to form depends on the types of clays and fluxing minerals, their concentrations within the sample, and their melting temperatures, present in the coal (Liu *et al.*, 2013). The transformation of quartz (SiO_2 (S_2)) to quartz (SiO_2 (S_4)) took place as the temperature increased above 800°C. Even though quartz is inactive during thermal processing, the transformation of the mineral to a more stable will take place as the temperature increase. The SiO_2 (S_x) refers to a stable phase for the mineral at a specific temperature (van Dyk *et al.*, 2008d). Stable phases of the different minerals present in the sample will influence the ash fusion temperatures. As thermal processing temperature increases above 1175°C, a decrease in the percentage quartz was observed during the simulation. This decrease may result due to glass formation and partial melting of quartz (Zhou *et al.*, 2012). According to the simulation results, sillimanite (Al_2SiO_5), anorthite ($CaAl_2Si_2O_8$), cordierite ($Mg_2Al_4Si_5O_{18}$), and microcline ($KAlSi_3O_8$) contributed to the percentage melt as these minerals reached their melting temperatures or crystallization points. This same trend in mineral transformation was observed for SA3 during the simulation runs. However, the total percentage of slag formed at 1400°C for SA3 (80%) was higher than that of SA1 (50%). Higher percentages of anorthite and cordierite minerals present in SA3 may cause the higher slag percentage.

The mineral transformation for SA2 is presented in Figure 3-2. From the figure, high percentages of anorthite is predicted. Other minerals such as microcline, quartz (S_2), quartz (S_4), and enstatite ($MgSiO_3$) minerals types are also present but in percentages lower than 10%. The percentage melt increased with temperature as the minerals reach their melting temperatures or crystallization points. US1 exhibited similar mineral transformation trends as that of SA2 during the simulations. The melt starting temperature for US1 was lower (1025°C) than that of SA2 (1125°C). The total percentage of slag formed for US1 (86%) at 1400°C was higher than SA2 (55%). This may be due to high percentages of anorthite, diopside, and K/Na-feldspar minerals ($K/NaAlSi_3O_8$)) minerals present in US1.

Presented in Figure 3-3 is the mineral transformation simulation for SA2 blend, which is the coal sample with the added potassium compound prior to thermal processing. From these results, it can be seen that the temperature at which the melt starts to form was below 1000°C.

The influence of potassium addition to the coal prior to thermal processing can be seen when Figure 3-3 is compared with that of SA2 in Figure 3-2. A decrease in the melt formation temperature (1125°C to 975°C) and percentage melt formation (55% to 43%) was observed.

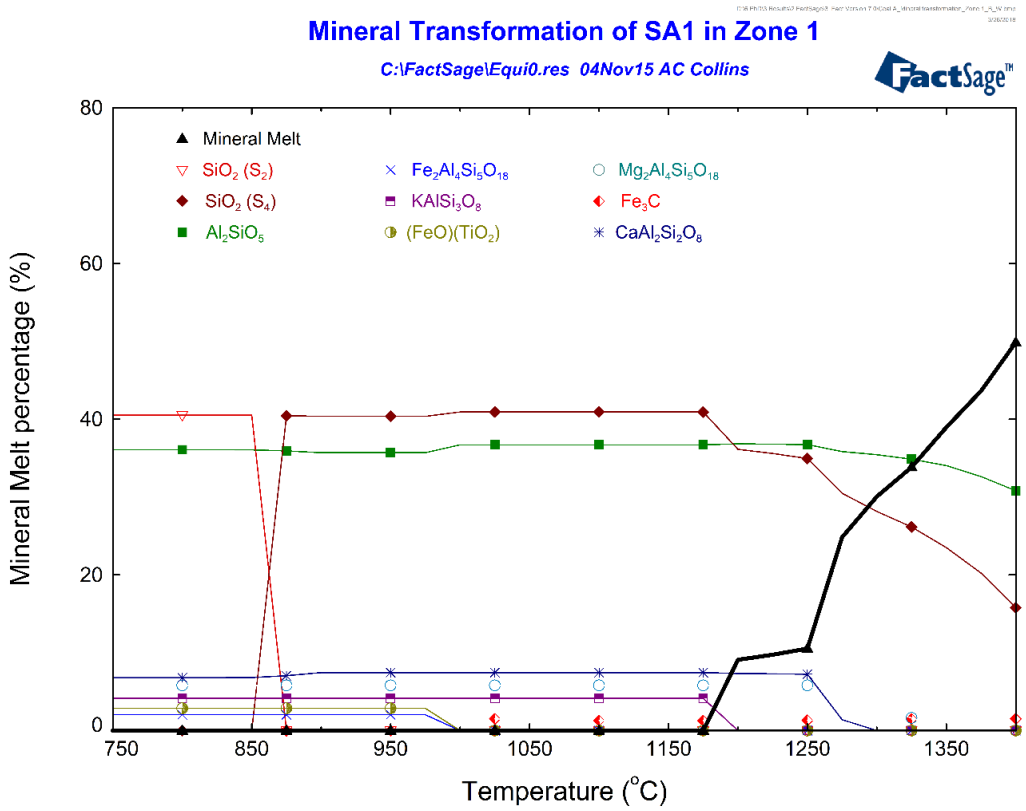

Figure 3-1: Calculated mineral transformations for SA1 in the reduction zone

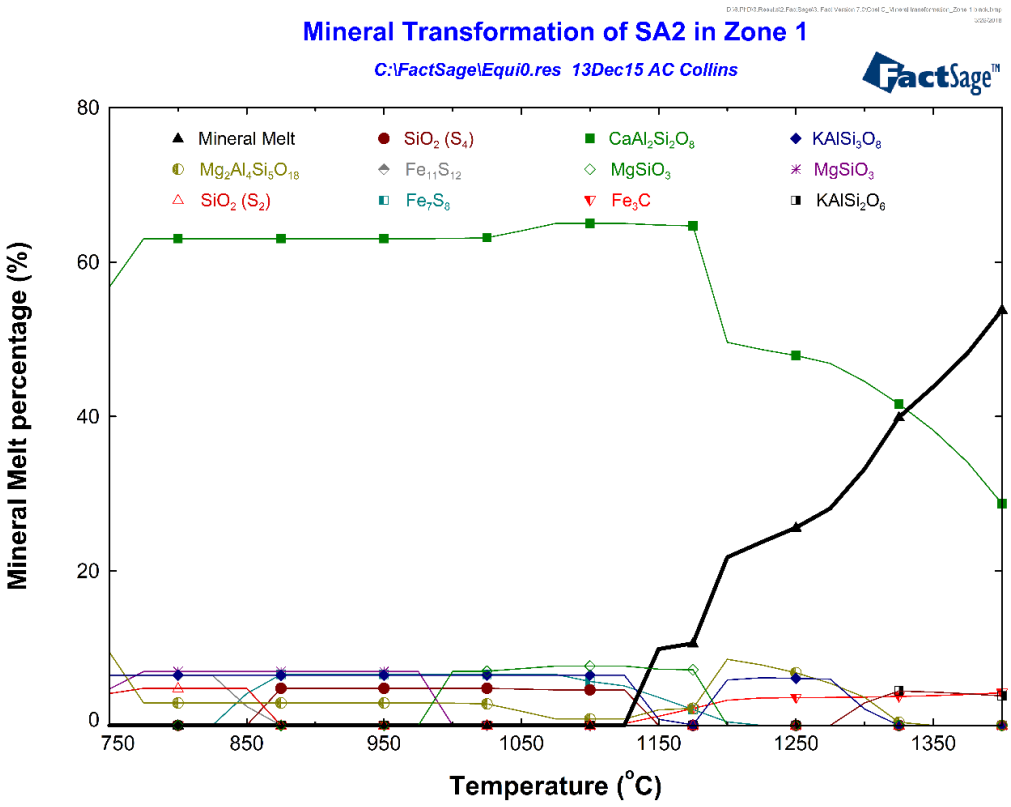

Figure 3-2: Calculated mineral transformations for SA2 in the reduction zone

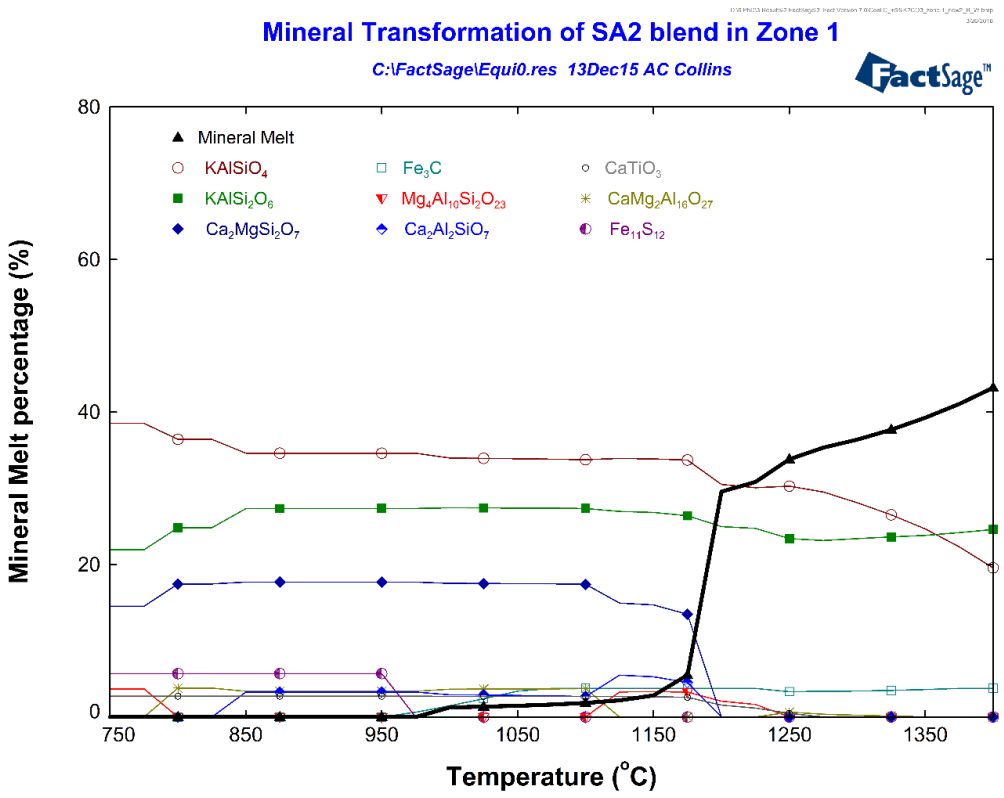

Figure 3-3: Calculated mineral transformations for SA2 blend in the reduction zone

3.3.3.2 Influence of added potassium salt on the slagging behaviour of coal

The modelled influence of added potassium (described in section 3.2.2) on slagging behaviour is presented in the following figures. From the SA1 slagging behaviour presented in Figure 3-4, an increase in the percentage melt with increasing potassium loading was observed. This increase in melt percentage may be caused by the additional potassium compound. Also noted from Figure 3-4 was the temperature at which the melt formation started remains the same for the feed coal and blended coal samples. This has also been observed in other studies (van Dyk, 2006). The same trend was observed for SA3, i.e. an increase in melt percentage, after the melt starting temperature was reached, with increasing potassium loading. The melt starting temperature was within 25°C for all the samples. From Figure 3-4 it can be seen that the extent to which the potassium loading influenced the slagging behaviour of the SA1, depended on the loading percentage. The influence of potassium loading on the coal was only observed after the melt formation temperature was reached.

Presented in Figure 3-5 are the simulation runs on the influence of added potassium on the slagging behaviour for SA2. A decrease in the melt percentage with increasing potassium loading was observed. Also seen in Figure 3-5 was an increase in the melt starting temperature for the 5 and 10 mass% K-blended samples. These same trends for melt percentage and melt starting temperatures were observed for US1. When comparing the melt formation results for SA2 blend (Figure 3-3) and the theoretical results calculated for SA2 (Figure 3-5), it can be seen that the percentage melt formation between the prediction simulations was comparable (within 5%). The melt formation temperature for the SA2 blend in Figure 3-3 was lower (975°C) than the theoretical prediction results (1150°C) in Figure 3-5.

Comparing the results obtained in Figure 3-4 with the results in Figure 3-5, the following can be stated: the addition of potassium carbonate to coal at different loading percentages had various influences on slagging behaviour. The slagging behaviour of coal is dependent on the mineral matter present in the coal. From the XRF results presented in Table 3-4, it can be seen that SA2 contained high percentages of basic compounds (K-, Ca-, Fe-, Na-, and Mg- containing compounds). The basic compounds influence the AFT (increasing or decreasing thereof) (Hanxu *et al.*, 2006) and is also known to be fluxing agents when present in certain percentages in the coal (Jak *et al.*, 1998; van Dyk *et al.*, 2008b). The concentration of these compounds, especially Ca-containing species, will determine their combined influence on the AFT. When a high percentage of basic mineral compounds (Ca^{2+}, K^{+} Na^{+}, and Fe^{2+}) are present within a coal sample, an increase in the AFT will (possibly) be observed. This increase is due to the sub-liquidus transformation of the mineral phases (Song *et al.*, 2009). This implies that high percentages of basic mineral compounds lead to maximum mineral formation/transformation and the stabilization of these mineral phases, which in turn increase the AFT (van Dyk *et al.*, 2008b). The high AFT will also be observed with low percentages of basic

mineral compounds present in the coal (Jak *et al.*, 1998). The influence of basic compounds, especially Ca, on the AFT has previously been found and described by van Dyk et al (van Dyk *et al.*, 2008b) and is presented in Figure 3-6. The curve presented in Figure 3-6 is a schematical representation of the influence of basic compounds on the AFT. Presented with the results (source A and B) obtained by van Dyk et al (van Dyk *et al.*, 2008b), are the coal samples used during this investigation (SA1, SA2, SA3, US1). The percentage of basic compounds in SA1 (4.9) was lower than that of SA2 (22.9). Using the curve in Figure 3-6, this indicates that SA2 would have a lower AFT than SA1. This influence of the basic compounds was also predicted by FACTSAGE™ modelling, and is presented in Figure 3-4 and Figure 3-5.

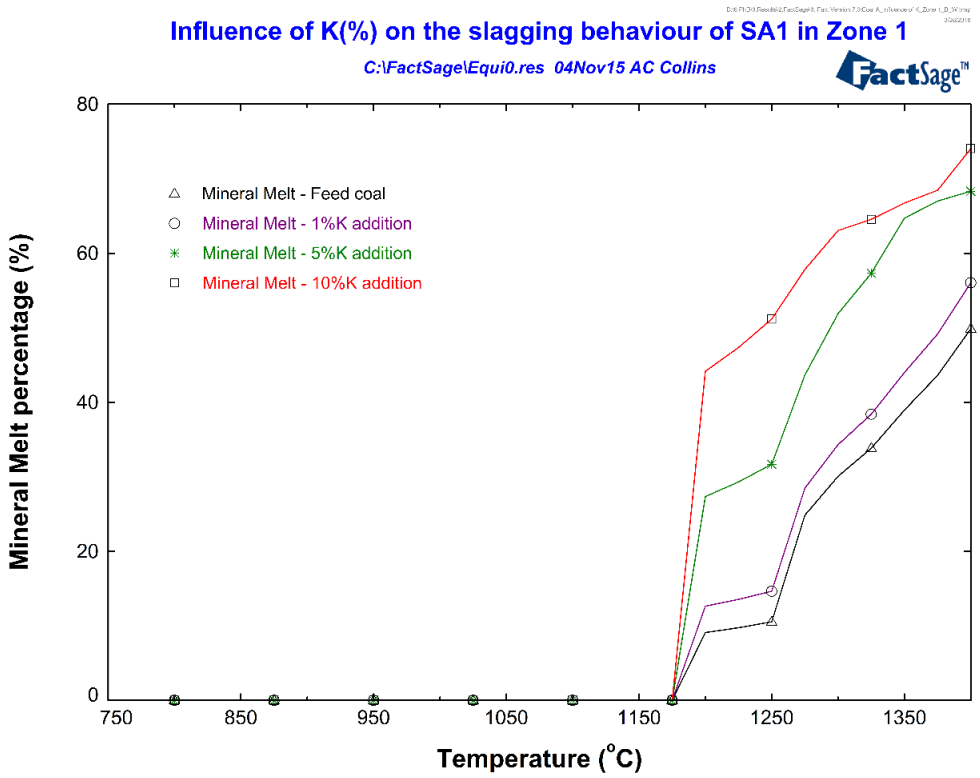

Figure 3-4: Calculated influence of K on the slagging behaviour of SA1 in the reduction zone

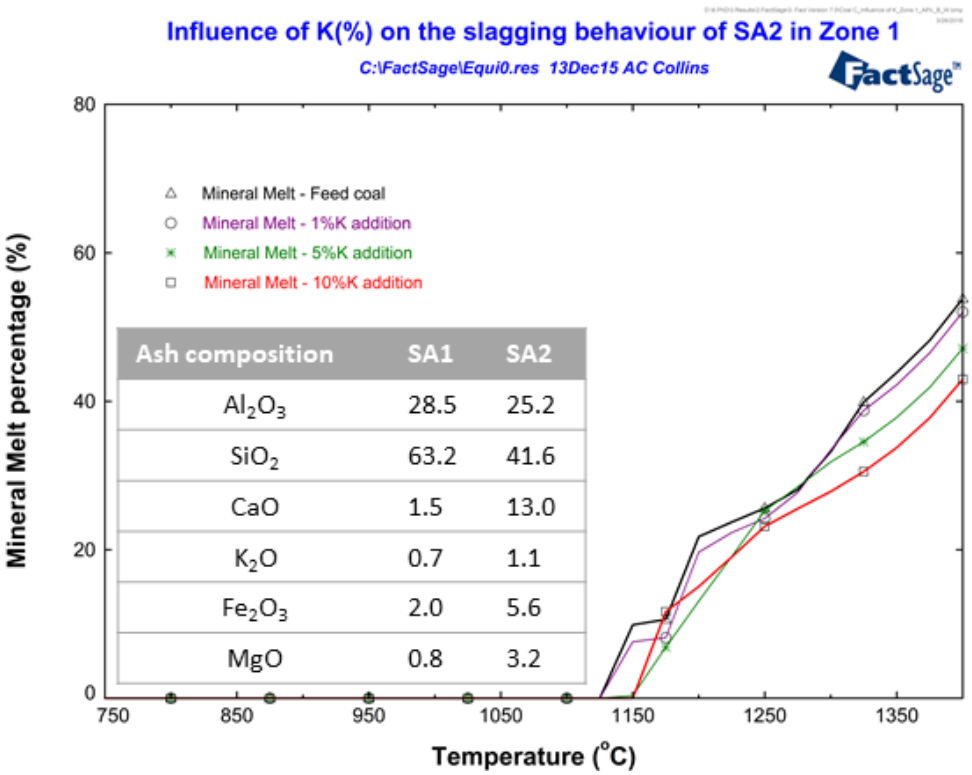

Figure 3-5: Calculated influence of K on the slagging behaviour of SA2 in the reduction zone

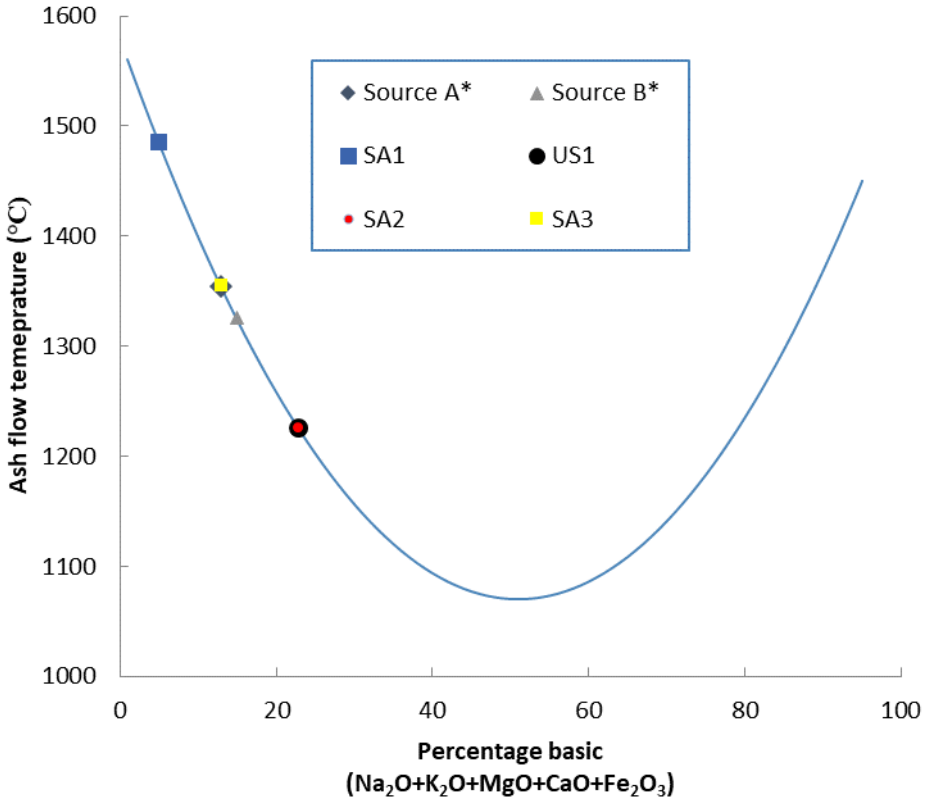

Figure 3-6: The ash-flow temperature versus the percentage of basic compounds *(Van Dyk *et al.*, 2008a)

3.3.4 Combustion and Ash (oxidation) Zone

Figures 3-7 to 3-9 presents the results obtained for the mineral transformation simulations for the different coal samples in the combustion and ash (oxidation) zone. It should be noted that the graphs should be read from right to left to better understand the flow of the material as it moves from the top to the bottom of the gasifier (cooling process). As the graph is read from right to left, the formation of mineral phases is observed, which may indicate crystallisation of mineral phases from the slag. Also seen in the figures is the decrease in melt percentages as the temperature of the operating process decreases.

3.3.4.1 Mineral transformation of the coal samples

The mineral transformation simulation for SA1 is presented in Figure 3-7. As the cooling process starts, sillimanite (Al_2SiO_5) and SiO_2 (S_4 and S_2) minerals are formed. Small percentages of other minerals are also predicted to form during cooling. The same trend of mineral formation was again observed for SA3. Simulation of mineral transformation for SA2 is presented in Figure 3-8. Crystallization of minerals, such as calcium feldspar ($CaAlSi_3O_8$), cordierite ($Mg_2Al_4Si_5O_{18}$), calcium sulphate ($CaSO_4$), SiO_2 (S_4 and S_2), and potassium feldspar ($KAlSi_3O_8$) were predicted to form as the temperature decreases. A similar trend was observed for US1. The simulation of mineral transformation for SA2 blend is presented in Figure 3-9. During the cooling process, crystallization of minerals, such as leucite ($KAlSi_2O_6$) and kalisilite ($KAlSiO_4$) was predicted as the temperature decreased. The influence of the potassium loading during the oxidizing zone will remain constant since slag formation was determined at the highest temperature in the reducing zone.

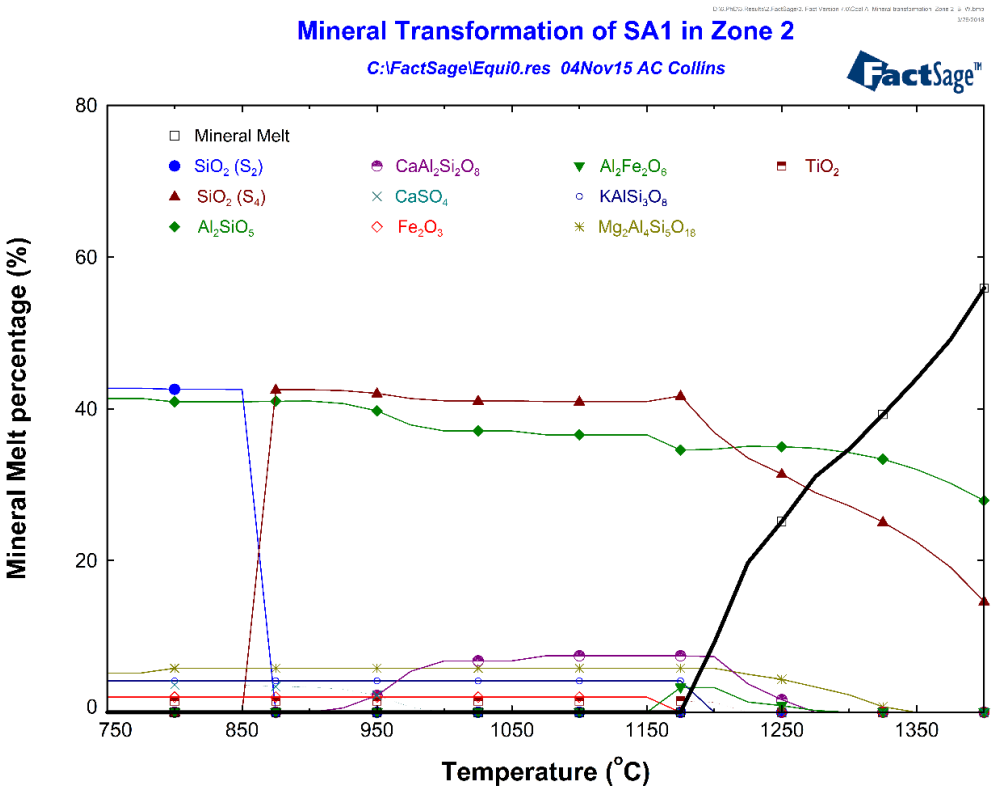

Figure 3-7: Calculated mineral transformations for SA1 in the oxidation zone

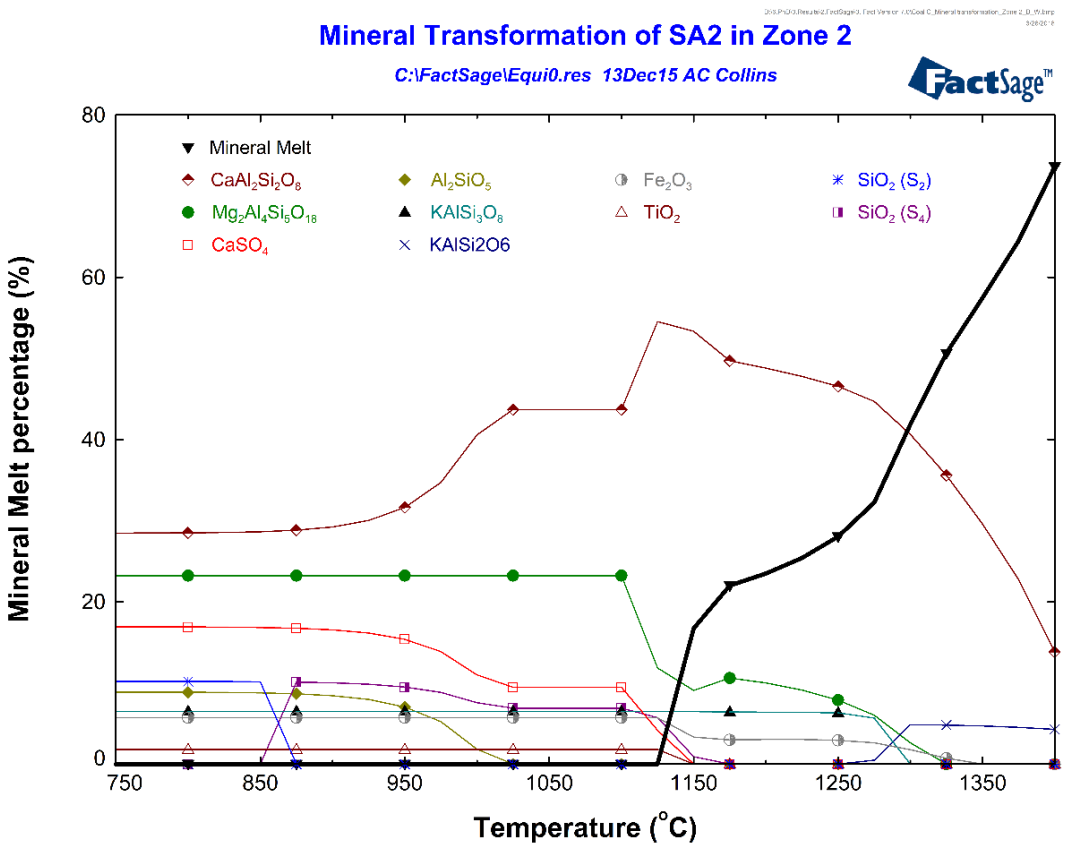

Figure 3-8: Calculated mineral transformations for SA2 in the oxidation zone

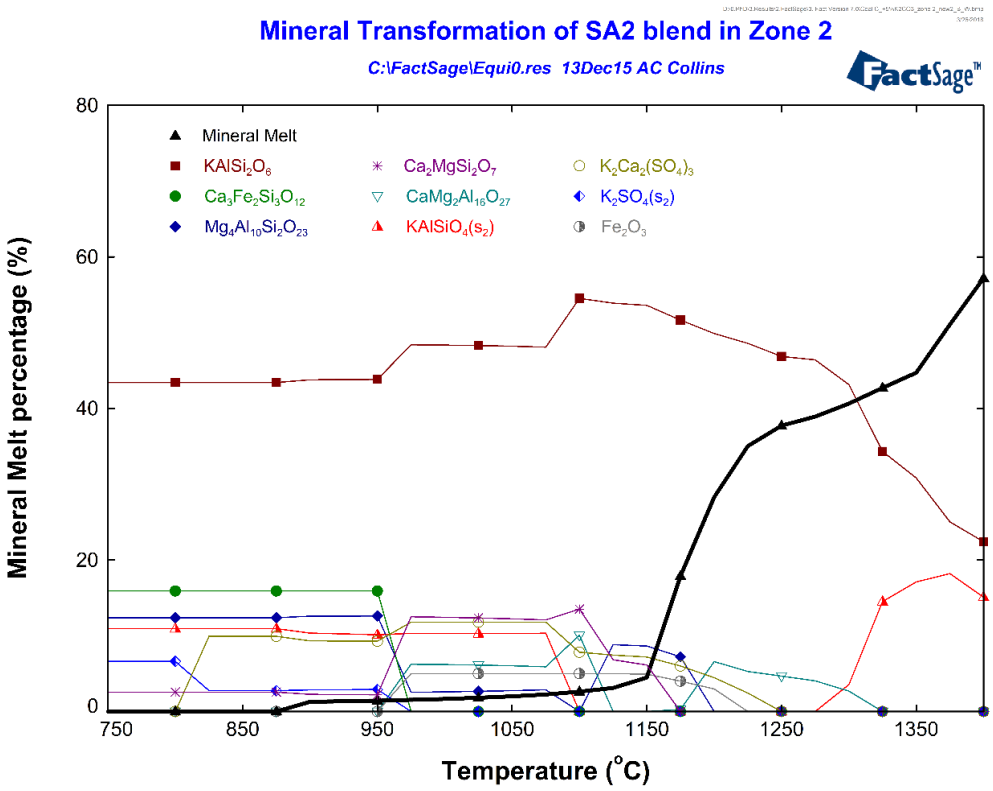

Figure 3-9: Calculated mineral transformations for SA2 blend in the oxidation zone

3.4 Conclusion

By using the FACTSAGE™ modelling database, predictions on the mineral transformation and slagging tendencies of different coal samples were investigated. The extent of melt formation increased with increasing operating temperature as more of the minerals present in the coal undergoes melting. A decrease in melting temperatures may result from the fluxing behaviour of basic components such as Ca-, Mg-, K-, and Fe-containing mineral compounds. The slagging tendencies of the coal samples were dependent on the specific mineral composition of the coal and the transformation of these minerals during thermal processing. The addition of potassium according to the mineral content yielded the following results: 1) an increase in melt formation with increased potassium loading for SA1 and SA3; 2) while US1 and SA2 indicated a decrease in melt formation with increased potassium loading. The last observation can be explained by the ratios of specific species and elemental composition and may be attributed to the already high percentages of basic components present in US1 and SA2.

The FACTSAGE™ simulations are modelled according to an equilibrium model for the gasifier, in which the equilibrium models predict mineral transformation on the assumption that all minerals present in the sample have reached equilibrium. Prediction studies are done on this basis, even though mineral transformations (reactions) do not reach equilibrium during thermal processing.

Although melt (slag) predictions have been modelled and verified with the use of this software, not all mineral interactions between phases can be predicted due to the software database limitations.

The following conclusions can be made:

→ Operating condition, i.e. the temperature at which thermal processing occurs, plays an important role in the extent of the melt formation, the mineral transformation, and also the recoverability of compounds from the ash.

→ The addition of potassium to the coal prior to thermal processing has an influence not only on the extent of melt formation but also the AFT, depending on the coal mineral composition.

→ Simulation predictions on the melt percentage from the theoretical (assumed) addition of potassium to the coal compared well to the simulation run of the blended sample (coal sample with potassium). The melt formation temperature between the simulation runs indicated a ±200°C difference. This may due to complex reactions taking place between the potassium and mineral phases in the coal, that could not be predicted by the equilibrium model conditions.

It needs to be remembered that FACTSAGE™ simulations are only a prediction on what might occur during thermal processing and that these predictions are done based on thermodynamic equilibrium conditions. These simulations only provide an indication of what might occur during thermal processing. Thus FACTSAGE™ modelling software can be a powerful prediction tool for coal behaviour, which can be used to optimize conditions for the different coal-burning technologies available.

Chapter 4

Sulphuric acid leaching of South African combustion ash – dissolution of Al, K, and Ti form laboratory coal ash

Anna C. Collins, Christien A. Strydom, Ratale H. Matjie,
John R. Bunt, Johannes C. van Dyk

The dissolution of Al- and K bearing mineral phases, present in the amorphous material and glassy structures, is investigated through sulphuric acid leaching of the coal ash. The influence of an added potassium salt to the coal, on the dissolution efficiencies of Al and K from the coal ash, was also investigated. The leaching conditions used in this investigation was similar to conditions used for the dissolution of Al from clay sources.

Abstract

South African coal ash generally contains about 30% aluminium oxide, which is constituted in the mullite ($Al_6Si_2O_{13}$); insoluble aluminium silicate in mineral acid solutions fraction. Most coal ash also contains other high-value inorganic elements that could be extracted during the recovery of soluble aluminium. The aim of this investigation was to determine if the aluminium present in amorphous material (metakaolinite ($Al_2O_3.2SiO_2$)); aluminium, potassium, and titanium in the amorphous aluminosilicate glasses and Ti in rutile/anatase (TiO_2) could be selectively dissolved from South African coal ash prepared at temperatures <1100°C by using sulphuric acid solutions. From the results obtained, it was observed that coal ash prepared at 700°C showed higher dissolution efficiencies for Al and K than coal ash prepared at 1050°C. The coal ash prepared at higher temperatures (≈1050°C) had lower dissolution efficiencies for Al, K, and Ti due to Al and K association with stable minerals phases (e.g. mullite, anorthite ($CaAl_2Si_2O_8$), and Na/K-feldspar ($Na/K\text{-}AlSi_3O_8$)) formed during thermal processing. Low sulphuric acid concentration leaching of the coal ash samples prepared at either 700°C or 1050°C showed low Al, K, and Ti dissolution efficiency values. These low dissolution efficiencies for the elements can be attributed to the formation of gelatinous calcium sulphate and silicic acid when the ash was leached with a low concentration of sulphuric acid solutions. Addition of potassium, to the selected coal prior to thermal processing, resulted in higher dissolution efficiencies of aluminium and potassium. The highest dissolution efficiency values of 87% Al and 89% K were achieved by leaching the ash sample prepared at 700°C with the 6.12M H_2SO_4 solution using a solid to liquid ratio of 1:5 at a temperature of 80°C for 8 hours. The ash sample prepared at 1050°C showed dissolution efficiency values of 73% Al and 67.2% K. The high dissolution efficiency values for these elements were achieved through formation of acid-soluble amorphous phases such as metakaolinite, K_2CO_3 melt, K_2CO_3, potassium alum ($KAl(SO_4)_2$ and potassium aluminosilicate glass in the coal ash sample. ICP-OES digestion results supported the dissolution efficiencies of Al, but results were less accurate for K and Ti. Complexometric titration of the leach liquors confirmed the presence of Al in the leach liquor samples. High dissolution efficiencies of Al and K, when using XRF analysis results, indicated that thermal processing of coal fines and the blend of coal fines and potassium carbonate at 700°C can be used to produce coal ash, which is suitable for the recovery of soluble aluminium and potassium species using sulphuric acid leaching procedures. Thermal processing (at 700°C) of South African coals, the addition of potassium carbonate and subsequent sulphuric acid leaching of the produced ash could, therefore, present an encouraging technology for the recovery of aluminium and potassium from low-temperature coal ash produce from South African coal fines.

Keywords: potassium, aluminium, titanium, sulphuric acid leaching, combustion ash, low-temperature ash

4.1 Introduction

The growth of industries and population numbers in developing countries has prompted the generation of more power to meet the increasing energy demands. Since coal-based power generation is still one of the most important, effective, and used methods (Izquierdo & Querol, 2012), increased power generation and the subsequent increase in waste products (coal fines, coal ash, gasses evolution etc.) results from energy demands being met (Nayak & Panda, 2010). Coal ash, which is comprised of bottom ash and coal fly ash, contains significant amounts of aluminium and other high-valued elements (elemental compounds); which is utilized in small percentages in other industrial applications such as brick manufacturing, building materials, ceramics, etc. (Dutta *et al.*, 2009; Nayak & Panda, 2010). This suggests that the ash by-products have the potential to be good source materials for the recovery of inorganic elements (Barry *et al.*, 2018; Matjie *et al.*, 2005b; Wu *et al.*, 2012). Around 80% of the aluminium present in coal fly ash, bottom ash, and ash produced through gasification and combustion of South African coal, are comprised of stable mullite ($Al_6Si_2O_{13}$) and feldspar ($Na/K\text{-}AlSi_3O_8$) mineral phases; with the other 20% aluminium present in the glassy phase (Matjie *et al.*, 2005b). The leachability of aluminium from the glassy phase will be influenced by the form in which the mineral is present (Seferinoglu, 2003) since surface-associated elements are more susceptible to leaching (Izquierdo & Querol, 2012). All inorganic elements which are associated with stable mineral phases formed at elevated temperatures (>900°C) are insoluble in basic solutions, and all mineral acids excluding hydrofluoric acid (Paul *et al.*, 2006). These stable phases are formed through partial or complete mineral transformation during thermal processing of the coal (Neupane & Donahoe, 2013).

Leaching of coal ash produced by gasification and combustion processes has achieved high aluminium extraction efficiency values in past investigations. These investigations consisted of acid and/or base leaching of coal ash or coal ash which was treated with lime or sodium/calcium/potassium carbonate. The pre-treatment of coal ash is done to form soluble aluminium compounds (Alguacil *et al.*, 1987; Phillips & Wills, 1982; Sangita *et al.*, 2017). Matjie *et al.* (2005b) used low-cost stable sulphuric acid in the leaching experiments when extracting aluminium from South African coal ash. Calcium oxide was used during the pre-treatment process of these ash samples. Extraction efficiencies for Al and Ti were 82% and 50% respectively when the ash pellets were leached for 4 hrs, at a temperature of 80°C, using an acid concentration of 6.12M (1:3½ and 1:5 ratios). Sangita *et al.* (2017) used sulphuric acid solutions to solubilize aluminium from coal fly ash, which contained 62% reactive amorphous aluminium silicate, to form a pure aluminium sulphate. The coal fly ash used in their investigation was produced by power stations located in China. The use of sulphuric acid is mostly due to its effectiveness, availability, and affordability as a leaching solution during recovery processes (Seidel, 1999). van der Merwe *et al.* (2017) applied a conventional hydrometallurgical process to selectively recover aluminium (47% Al

recovered) from the amorphous phase of the coal fly ash, consisting of ultrafine material (cenospheres), using a solution of ammonium sulphate. Other investigations included the use of chelating agents or organic acids during the leaching process and achieved varying degrees of success in the recovery of Al (Bai *et al.*, 2011; Kai *et al.*, 2011).

This paper reports on the utilization of a low cost, stable sulphuric acid (lixiviant) during the leaching of laboratory-prepared ash (prepared from coal fines), in an attempt to extract Al, K, and Ti from the amorphous materials and soluble elemental compounds present in the ash. The leaching methods and conditions used during this investigation have been applied in the recovery of aluminium from clay minerals (non-bauxite ores) (Ibrahim *et al.*, 2018; Mark *et al.*, 2019; Numluk & Chaisena, 2012), with dissolution efficiencies values reaching up to 90%.

Analytical techniques such as XRF, XRD, ICP-OES digestion analyses, and complexometric titration were utilized in determining the dissolution efficiencies after leaching. The mineral phases produced during the leaching process, such as aluminium sulphate, potassium sulphate, and titanium dioxide, can be utilized in other industries. Aluminium sulphate could be used in water treatment plants or could be purified through solvent extraction for the production of aluminium chemicals. Potassium sulphate could be used in potassium chemicals, or in the fertilizer industry; whereas a pure titanium dioxide could be used in the paint/paper industry. The ash residue after leaching is a co-product in this process and could be used as an aggregate in brick manufacturing and masonry concrete.

4.2 Material and Methods

4.2.1 Coal sample

Three South African coal samples were used during this investigation. The coal samples originated from coal mines situated in the Mpumalanga region. The coal samples will be identified as “SA1”, “SA2”, and “SA3” in the discussions that follow. The coal was collected and sampled by the employees at the mine, using standardized methods (ISO 1988:1975 and ISO139094:2016); from which a representative sample of 20 kg was taken and used in this investigation. Medium volatile bituminous coal samples were taken, and through characterization of the ash produced from the coal samples, were selected according to their aluminium- and potassium contents. The coal rank was determined using the ASTM D388-12 classification standard.

4.2.2 Sample Preparation

4.2.2.1 Coal Samples

The coal samples were prepared by air-drying for 2 days to reduce excess moisture, which is the moisture not associated with the coal structure. After the drying period, each sample was crushed, by first using a crusher and then a ball mill to obtain a particle size of <1 mm using standardized methods (ISO 1988:1975 and ISO139094:2016). A blended sample was prepared by adding a potassium compound (10 wt.% K_2CO_3) to the SA2 coal sample during the milling step. This blended sample is identified as "SA2 blend" in the discussions below. The addition was done during the ball milling step to ensure thorough mixing to obtain a homogeneous sample. The potassium carbonate was added to the SA2 coal sample to determine the recoverability of potassium after thermal processing of the coal sample, and whether potassium will influence the recovery of other inorganic elements.

4.2.2.2 Ash Samples

The coal samples used in this investigation were subjected to thermal processing, using specific conditions, to obtain the desired ash samples. The ash samples were produced by splitting the coal sample into four 5 kg sub-samples. The coal sub-samples were placed into clay fired sample trays and placed into the hot zone of a rotary kiln, where the temperature of the kiln was increased to 700°C at a heating rate of 10°C/min. A residence time of 3 hours at 700°C was set for all the sub-samples. The thermal step at 700°C was conducted under airflow to facilitate combustion of the organic compounds and the evolution of volatile matter. After the residence time was reached, the furnace was switched off, so that the cooling rate was generally the natural cooling of the furnace. The ash sub-samples were removed from the kiln once the samples reached ambient temperature; after which the four ash sub-samples were blended to form one homogenous ash sample. This bulk ash sample was again split into 4 sub-samples, from which one was kept to represent the ash sample prepared at 700°C. The other three sub-samples were placed in a muffle furnace where the temperature was increased at a heating rate of 10°C/min, to 850°C, 950°C, and 1050°C. A residence time of 3 hours was set for the ash samples in the muffle furnace after the desired temperature was reached. This process was repeated for all the coal samples used.

4.2.3 Analytical Methods

4.2.3.1 Ultimate and Proximate Analyses

Characterization of the coal samples used during this investigation was done according to specific ISO standard methods. The characterization method and the ISO standard method used is presented in Table 4-1.

Table 4-1: Characterization methods and ISO standard identification number

Analysis	Standard
Solid mineral fuels: Determination of moisture in general analysis test sample by drying in nitrogen	ISO 11722: 2013
Solid mineral fuels: Determination of ash	ISO 1171: 2010
Hard coal and coke: Determination of volatile matter	ISO 562: 2010
Fixed carbon	By calculation
Determination of total carbon, hydrogen and nitrogen content – international method. Oxygen content by calculation	ISO 29541: 2010

4.2.3.2 X-Ray Fluorescence (XRF) Analysis

Coal samples subjected to XRF analysis were ground until all particles could pass through a 75 µm sieve. Calcination of the powdered samples was conducted at 1000°C under airflow, with a residence time of 3 hours. This was done to remove all moisture and organic compounds, which might be present in the sample. After the calcination process, a solid solution was prepared by fusion of the calcined samples with lithium tetraborate: lithium metaborate (67:33). This solid solution, prepared from the calcined powder and the standard, was added into the casting dish with the measurement of 32 mm. The prepared fused beads (32 mm) were placed into the sample compartment of the XRF spectrometer (WROXI from PANalytical). The analysis was conducted according to the method proposed by Norrish and Hutton (1969). The concentration of the specific elements present in the ash sample was calculated from the intensity of the spectral line recorder by the analyser. These concentrations measured are expressed as elemental oxides.

4.2.3.3 X-Ray Diffraction (XRD) Analyses

Samples subjected to XRD analysis were ground to a particle size <75 µm with the use of a laboratory scale ball mill. The powdered samples and those containing the silicon standard were placed into sample holders. These holders were filled with the powdered sample, and the surplus removed with the use of a glass slide (50X70 mm and 5 mm thick). Simultaneous compression of the sample into the sample holder takes place as the excess sample is removed (Matjie, 2008). This step was repeated until a smooth surface of even texture was obtained. Each solid sample was spiked with 20% Si (Aldrich, 99.9% purity) and was subsequently micronized in a McCrone micronizing mill. The XRD analysis of the coal and ash samples were done using an X'Pert PRO PANalytical (Philips) – Unit 2 diffractometer system with Co Kα radiation. Identification of the

minerals present in the powdered samples was conducted with reference to the International Center for Diffraction Data (ICDD) Powder Diffraction File. Amorphous and crystalline phases in the powdered samples were identified and quantified with X'Pert Highscore plus software (Speukman, 2012) and the Rietveld method (Rietveld, 1969).

4.2.3.4 Inductively Coupled Plasma Spectrometry Optical Emission Spectroscopy (ICP-OES) digestion Analysis

The leach liquor samples produced in this investigation were subjected to ICP-OES analysis, using a model number Varian 700-ES. The analysis was conducted by SetPoint Laboratories and used to determine the concentrations of Al, K and Ti present in the liquid samples. The liquid samples obtained after acid leaching were dried; from which an aliquot of the sample was taken and fused with sodium peroxide and sodium hydroxide. This mixture was dissolved in hydrochloric acid in a 1:1 ratio. The digested samples were then made up to 100 ml in volumetric flasks using deionized water. The resulting solution was subjected to ICP-OES analysis. Duplicate runs were done on the experimental samples to ensure repeatability. Different standard samples, containing different concentrations of inorganic elements, were prepared and used as control samples during the ICP analysis of the leach liquor samples.

4.2.4 Experimental Methods

A schematic diagram presenting the experimental processes and analytical procedures used during the investigation on Al, K, and Ti recovery from coal ash, is presented in Figure 4-1.

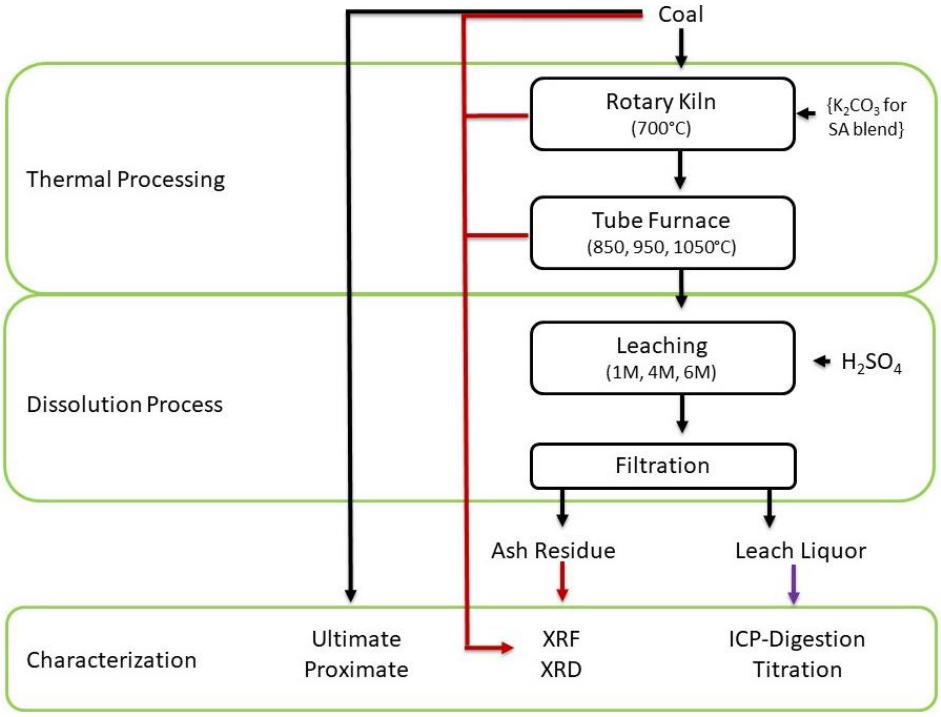

Figure 4-1: Schematic diagram of the experimental- and analytical procedures used during sulphuric acid leaching of the coal ash samples

4.2.4.1 Acid Leaching

Technical grade sulphuric acid (98% H_2SO_4) was used to make up the different concentration solutions used during the leaching experiments. A 500 ml round-bottomed container, with sealing lid and cooler, was used as a leaching vessel. An automatic overhead stirrer with a base plate (DESC 20 L) model 720, coupled with a temperature controller with a sensor probe, was used as a heat source. The leaching conditions used during this investigation are stated below:

a. Low sulphuric acid concentration leaching

Leaching of the coal ash samples with low sulphuric acid concentration solutions, all but two variables were kept constant during experimentation. Variables that were kept constant was the solid: liquid ratio at 1:10, and the leaching temperature at 45°C. The sulphuric acid concentration was varied between 1.02 M and 4.08 M; with the leaching, time-varying from 30 min to 180 min, with 30 min intervals. Experiments were carried out by weighing and placing the coal ash (10 g) into the leaching vessel. Sulphuric acid solution (100 ml) was added to the coal ash in the vessel to maintain the 1:10 solid to liquid ratio. Using an automatic overhead stirrer, the mixture was stirred (200 rpm) for the designated time. After completion of the leaching step, the sample was removed from the heat and the hot mixture was filtered. The ash residue was washed with deionized water to ensure that the soluble compounds were removed. The ash residue was placed in a vacuum furnace to dried overnight at 60°C. The filtrate was combined with the leach liquor to form a final leach liquor sample, used to determine the concentration of Al, K, and Ti through ICP-OES digestion analysis and Al concentration with complexometric titration.

b. High sulphuric acid concentration leaching

During high sulphuric acid concentration leaching of the coal ash samples, the influence of solid to liquid ratio on the recovery of the inorganic elements was investigated. The ratios used were 1:5 and 1:10 solid to liquid ratio. The coal ash sample (10 g) was weighed and placed into the leaching vessel. A 6.12 M H_2SO_4 solution was added to the coal ash sample in the vessel. The volume of sulphuric acid solution was added to maintain the solid to liquid ratio of the specific experiment. The mixture was stirred (200 rpm) with an automatic overhead stirrer for 8 hours at a temperature of 80°C. After the leaching time was reached, the sample was removed from the heat and the hot mixture filtered. The ash residue was washed with deionized water to ensure that the soluble compounds were removed. The ash residue was placed in a vacuum furnace and dried overnight at 60°C. The filtrate was combined with the leach liquor sample to form the final leach liquor sample; which was submitted for complexometric titration and ICP-OES digestion analysis.

4.2.4.2 Complexometric Titration

The concentration of aluminium in the aqueous solution after sulphuric acid leaching of the coal ash samples was determined through complexometric titration. The development and implementation of this method was done by Matjie (1997). The experimental method used is as follow:

Determination of Al concentration in the leach liquor

Complexometric titration of the liquid samples was done by taking a 5 cm^3 volume of the leach liquor and placing it into a 250 cm^3 beaker. An excess volume (25 cm^3) of an 0.1 M EDTA standard solution was added to the beaker containing the leach liquor. The volume of EDTA solution was measured accurately with a burette or a pipet. This solution (EDTA and leach liquor) was boiled on a heating mantle for 5 min. After this time period, the sample was removed from the heating mantle and left to cool to ambient temperature. The pH of the solution in the beaker was adjusted to 5 - 5.5 with the use of sodium acetate (anhydrite). Xylenol orange was used as an indicator during titration of the mixture. The xylenol orange indicator was prepared by adding 1 g xylenol orange to 99 g potassium nitrate. These chemicals were mixed until a homogenous mixture was obtained. A small amount (small spatula) of the indicator was added to the solution. The solution, containing the indicator, was titrated with a 0.1 M $ZnSO_4$ standard solution. The concentration of aluminium in the leach liquor was determined with the following equation:

$$\boldsymbol{c = V_1 - V_2 \times \frac{1000}{V_3} + \frac{F}{1000}} \quad (4\text{-}1)$$

where V_1 represents the volume of EDTA (in excess) added, V_2 the volume of titrant used during titration, V_3 the volume of the leach liquor (5 cm^3) used, and F the mass (mg) of aluminium present in the EDTA standard solution.

4.2.4.3 Dissolution Efficiencies

Dissolution efficiencies are calculated and used to indicate the solubility of a compound or compounds into a specific solution when using extraction methods. The dissolution efficiency of the inorganic elements in different concentration sulphuric acid solutions was determined through various analytical methods. These methods included XRF (ash and ash residue) analysis, ICP-OES digestion (leach liquor) analysis, and complexometric titration (leach liquor). Dissolution efficiencies for Al, K, and Ti were determined from the results obtained from these analytical methods.

4.2.4.3.1 Dissolution efficiencies determined from XRF analysis

The dissolution efficiencies for Al, K, and Ti were determined with the XRF analysis results by applying the following equation:

$$\eta(\boldsymbol{MO}) = \frac{\boldsymbol{m_{CA} - m_{RES}}}{\boldsymbol{m_{CA}}} \times \boldsymbol{100\%} \quad (4\text{-}2)$$

where η(MO) presents the dissolution efficiency of the specific inorganic compound (Al, K, or Ti) and m_{CA} and m_{RES} the mass of the inorganic element in the coal ash and ash residue (after leaching), respectively (Jiang *et al.*, 2015). The mass of the specific inorganic element in the coal ash and ash residue samples can be determined as follow:

$$\boldsymbol{m_{ash}} = (\frac{\%\boldsymbol{E}}{\boldsymbol{100}}) \times \boldsymbol{m_{sample}} \quad (4\text{-}3)$$

where m_{ash} is the mass (g) of inorganic element (Al, K, or Ti) in the coal ash or ash residue; %E the percentage of the inorganic element in the coal ash or ash residue, as determined in Equation 4-4; and m_{sample} the mass of the ash sample or ash residue. The percentage (%E) of the inorganic element present in each of the ash and ash residue samples was determined with the following equation:

$$\%\boldsymbol{E} = \%\boldsymbol{EO} \times \frac{\boldsymbol{M_{element}}}{\boldsymbol{M_{EO}}} \quad (4\text{-}4)$$

with %E the percentage of the element in the coal ash or ash residue sample; %EO the percentage elemental oxide in the sample (provided through XRF analysis); $M_{element}$ the molecular weight of the element in the oxide and M_{EO} the molecular weight of the elemental oxide.

4.2.4.3.2 Dissolution efficiencies determined from ICP-OES digestion analysis

The ICP-OES digestion analysis results were expressed as a weight percentage (wt.%) of the inorganic elements present in the leach liquor. To calculate the dissolution efficiency using these percentages, the following equation was used:

$$\boldsymbol{\beta} = \frac{\%\boldsymbol{E_{leachate}}}{\%\boldsymbol{E}} \times \boldsymbol{100}\% \quad (4\text{-}5)$$

with β representing the dissolution efficiency determined through ICP-digestion; $\%E_{leachate}$ the percentage of the inorganic element (Al, K, or Ti) determined to be in the leach liquor; and %E (Equation 4-4) the percentage of inorganic element (Al, K, or Ti) present in the original ash samples.

4.2.4.3.3 Dissolution efficiencies determined from complexometric titration experiments

The dissolution efficiencies for Al can be determined through complexometric titration of the leach liquor samples obtained after acid. The concentration Al in the leach liquor samples were determined by Equation 4-1; from which the mass of the inorganic element in the leach liquor was determined. Using these values, the dissolution efficiencies for Al was calculated with the following equation:

$$\boldsymbol{\alpha} = \frac{\boldsymbol{m_{leachate}}}{\boldsymbol{m_{ash}}} \times \boldsymbol{100\%} \quad (4\text{-}6)$$

where α presents the dissolution efficiency of Al determined from complexometric titration, $m_{leachate}$ the mass of the inorganic element (Al, K, or Ti) in the leach liquor, and m_{ash} (Equation 4-3) the mass of the inorganic element in the original ash sample.

4.3 Results and Discussion

4.3.1 Ultimate and Proximate Analyses

The proximate and ultimate analyses results obtained for the coal samples used in this investigation are presented in Table 4-2. The proximate analysis results are reported on an air-dried basis, whereas the ultimate analysis results are given on a dry-and ash-free basis. From the proximate results, high ash yields (>20%) and volatile content (>15%), accompanied by low moisture (<4%) percentages were found for the coal samples. The fixed carbon content for the samples was determined to be between 45% and 52%. The ultimate analysis of the coal samples indicated carbon contents ranging between 79% and 83%, and oxygen contents ranging between 10% and 13%. The results obtained from proximate and ultimate analyses for the coal samples used in this investigation are consistent with values found for other South African coal samples (Hattingh *et al.*, 2011; van Alphen, 2005; van Dyk *et al.*, 2009b).

Table 4-2: Ultimate and Proximate results for the coal samples

Sample	*SA1*	*SA2*	*SA2 Blend*	*SA3*
Proximate Analysis (air-dried basis)				
Moisture content (%)	3.3	3.7	4.6	4.0
Ash yield (%)	28.3	28.5	26.8	22.4
Volatile content (%)	18.2	21.2	21.5	21.9
Fixed Carbon (%)	50.2	46.5	47.1	51.7
Ultimate Analysis (dry-ash free basis)				
% Carbon Content	82.3	79.2	79.6	80.3
% Hydrogen Content	4.4	3.8	4.9	4.2
% Nitrogen Content	1.8	1.9	1.9	1.9
% Oxygen Content	10.8	13.1	12.4	12.1
% Sulphur Content	0.7	1.9	1.2	1.5

4.3.2 Ash composition of the coal samples – XRF results

The XRF results for the coal samples are presented in Table 4-3. The analysis was done on ash samples prepared, at 1000°C, from these coal samples. The values presented in the table are reported as elemental oxides and on a normalized basis. From these results, significant percentages of iron, sulphur, and calcium can be seen throughout all of the ashes derived from the coal samples used, with the SA2 ash sample containing more than 7% sulphur trioxide and 10% calcium dioxide. All the samples contained aluminium oxide percentages exceeding 20%, and silicon oxide concentrations between 36.6% and 63.2%. As expected, a high potassium oxide percentage of 18.9% was seen for the SA2 blend ash, due to spiking of the sample with K_2CO_3 before analysis. The XRF results determined for the coal samples, with the exception of the coal sample spiked with K_2CO_3, are in good agreement with XRF results determined for ash samples prepared from other South African coals (Hattingh *et al.*, 2011; Matjie *et al.*, 2008; van Alphen, 2005; van Dyk *et al.*, 2008b; van Dyk *et al.*, 2009b).

Table 4-3: Normalized XRF results (wt.%) for the coal samples (ash prepared at 1000°C)

Sample	*SA1*	*SA2*	*SA2 Blend*	*SA3*
SiO_2	63.2	41.6	37.7	55.2
Al_2O_3	28.5	25.2	22.3	25.9
CaO	1.5	13.0	11.1	5.1
SO_3	1.5	7.6	-	4.3
Fe_2O_3	2.0	5.6	4.2	5.5
MgO	0.8	3.2	2.1	1.8
TiO_2	1.5	1.8	1.7	1.3
K_2O	0.7	1.1	18.9	0.4
P_2O_5	0.1	0.3	0.3	0.1
SrO	-	0.3	-	0.1
BaO	-	0.2	-	0.1
Cr_2O_3	0.1	-	0.3	-
Na_2O	-	-	0.7	-

4.3.3 Mineralogy of the coal samples – XRD results

The mineral mass percentages from XRD analysis determined for the coal samples used are presented in Table 4-4. The results indicate that all of the coal samples consist mainly of amorphous (non-crystalline; organic carbon) material, with percentages exceeding 65%. The SA1 and SA3 samples contained kaolinite at 18% and 13.7% respectively, quartz (<10%) and small percentages of other crystalline phases (microcline, illite, calcite, pyrite, anatase). The SA2 blend (a mixture of K_2CO_3 and SA2) contained kaolinite (14%), dolomite (6.5%), and calcite (3.2%) phases. Other mineral phases are also present in small quantities. The XRD results determined for the coals evaluated in this investigation are in agreement with previous XRD data reported for other South African coals (Matjie *et al.*, 2008; van Alphen, 2005; van Dyk *et al.*, 2009b).

Table 4-4: XRD results (wt.%) for the coal samples

Sample	*SA1*	*SA2*	*SA2 Blend*	*SA3*
Amorphous (organic carbon)	66.2	71.4	67.9	73.2
Anatase	0.4	-	0.3	0.2
Calcite	-	2.5	3.2	0.7
Dolomite	1.3	6.2	6.5	4.4
Graphite	1.9	0.8	-	0.5
Illite	0.8	1	3.6	-
Kaolinite	18	13.8	14	13.7
Microcline	0.7	0.2	-	-
Muscovite	-	-	0.1	-
Pyrite	0.1	0.2	0.1	-
Quartz	10.6	3.8	4	7.3

4.3.4 Ash analysis and mineralogy of acid leached samples

The XRF results for the SA1 ash samples, before leaching, presented in Table 4-5, indicated small differences in composition after the ash preparation temperature was increased from 700°C to 1050°C. A difference of <2% was observed when these to ash samples were compared with one another. The XRD results in Table 4-6 indicate that the SA1 ash sample prepared at 700°C, consisted of 46.7% amorphous material (metakaolinite ($Al_2O_3.2SiO_2$)) and 44.3% quartz (SiO_2). This is supported by Bunt *et al.* (1998), where coal fines were subjected to thermal processing in a rotary kiln at 600°C; and the coal ash produced was comprised of metakaolinite and other crystalline phases. The metakaolinite is soluble in mineral acids such as HNO_3, HCl, and H_2SO_4, to form aluminium nitrate, aluminium chloride, and aluminium sulphate, respectively. The SA1 ash sample prepared at 1050°C consisted of 35.5% amorphous material, 43.5% quartz, 14.1% mullite, and 1.2% anorthite (stable mineral phases formed at elevated temperatures (>900°C)). Matjie (2008) found that mullite and anorthite phases crystallized from the molten solution at temperatures above 900°C during the gasification process of other South African coals. Other crystalline mineral phases such as mullite ($Al_6Si_2O_{13}$), hematite (Fe_2O_3), anhydrite ($CaSO_4$), anorthite ($CaAl_2Si_2O_8$), portlandite ($Ca(OH)_2$), and cristobalite (SiO_2) were also observed in the SA1 ash samples in percentages <5%. The detection limit for accurate mineral phase determination is >5% mineral presence in the sample.

The XRF results obtained for the SA2 blend (mixture of K_2CO_3 and SA2) ash samples showed similar compositions for both ash samples prepared at 700°C and 1050°C. The XRD results in Table 4-6 show a decrease in the amorphous phase concentration from 74.8% to 44.1% as the preparation temperature increased. This decrease suggests that mineral phase formation occurred at higher temperatures. This is supported as the decrease of the amorphous material is accompanied by an increase in the content of gypsum from 0.6% to 7.6%, K_2CO_3 from 0.9% to 14%, microcline from 0% to 9.7%, and mullite from 0% to 13.2%. Insoluble potassium feldspars (microcline) formed as the potassium ion from the K_2CO_3 melt or K_2O reacted with the reactive metakaolinite ($Al_2O_3.2SiO_2$), at elevated temperatures (>900°C) (Table 4-6). Metakaolinite is the transformed mineral product of kaolinite when coal is subjected to thermal processing. CaO (transformed product of calcite/dolomite associated with kaolinite) can react with metakaolinite to form anorthite, which is insoluble in the sulphuric acid solution. The remaining metakaolinite transforms at high temperatures >1050°C to form mullite, which is insoluble in sulphuric acid solutions. Small percentages of cristobalite (SiO_2) and diopside ($CaMgSi_2O_6$) were also observed in the SA2 blend samples. The cristobalite was probably formed from reactive amorphous silica (transformed product of kaolinite and illite), while diopside was formed from amorphous silica reacting with high-temperature carbonate products (calcite or dolomite) (Matjie, 2008).

The same observations made in regard to the XRF results for the SA1 ash samples can be applied to the SA3 ash samples. This suggests that the ash samples prepared at 700°C and 1050°C had similar compositional results, with <2% difference between the values obtained for the two ash temperature samples. The XRD results for the SA3 ash sample prepared at 700°C was mainly composed of 68.5% amorphous material and 20.3% quartz. The SA3 ash sample prepared at 1050°C showed the same makeup as that of the 700°C ash sample but with 39.3% amorphous material and 36.8% quartz. Other mineral phases present in both the 700°C and 1050°C ash samples, were present in percentages <5%. The XRD results obtained are in good agreement with XRF results for the ash samples evaluated in this investigation (Tables 4-5 and 4-6).

Table 4-5: Normalized XRF results for the coal ash samples prepared at 700°C and 1050°C

Sample	*SA1*		*SA2 Blend*		*SA3*	
Ash Temp	*700°C*	*1050°C*	*700°C*	*1050°C*	*700°C*	*1050°C*
SiO_2	62.1	62.6	36.3	36.1	57.7	56.9
Al_2O_3	28.3	28.3	22.6	22.2	27.5	27.1
CaO	2.7	2.3	8.9	8.6	5.4	5.2
Fe_2O_3	2.7	2.7	4.1	4.2	3.8	3.8
TiO_2	2.1	1.7	1.7	1.6	1.5	1.5
MgO	0.9	0.8	2.3	2.3	2.0	1.8
K_2O	0.8	0.8	18.4	18.6	0.4	0.7
SO_3	0.2	0.2	4.4	4.9	0.8	2.1
Cr_2O_3	0.1	-	0.1	0.1	0.1	0.1
Mn_3O_4	0.1	-	0.1	0.1	0.1	-
P_2O_5	0.1	-	0.2	0.2	0.1	0.1
BaO	-	0.2	0.4	0.4	0.3	0.4
Na_2O	-	-	0.1	-	-	-
SrO	-	-	0.3	0.3	0.1	0.1

Table 4-6: XRD results for the ash samples prepared at 700°C and 1050°C

Sample	*SA1*		*SA2 Blend*		*SA3*	
Ash Temp	*700°C*	*1050°C*	*700°C*	*1050°C*	*700°C*	*1050°C*
Amorphous	47.6	35.5	74.8	44.1	68.5	39.3
Quartz	44.3	43.5	3.9	-	20.3	36.8
Anhydrite	1.6	1.5	1.3	0.9	1	2.7
Mullite	1.5	14.1	-	13.2	0.1	3.3
Hematite	1.4	-	1.3	0.4	1	2.2
Anorthite	1.2	1.2	8.3	9	-	1.4
Portlandite	0.4	0.2	0.2	-	0.1	0.2
Magnetite	0.2	0.3	-	-	0.3	0.7
Cristobalite	0.1	0.4	0.1	-	0.1	0.5
Muscovite	-	-	-	-	0.3	0.7
Anatase	-	-	-	-	-	0.1
Microcline	-	-	-	9.7	-	-
Dolomite	-	-	-	-	0.1	1.2
Calcite	-	-	-	-	4.2	0.1
Gypsum	-	-	0.6	7.6	0.2	0.4
Graphite	-	-	2	-	3.2	8.3
Diopside	-	-	4.5	0.5	-	0.3
K_2CO_3	-	-	0.9	14	-	-
Kaolinite	-	-	0.6	-	-	0.2
Periclase	-	0.8	-	0.2	0.2	-
Pyrrhotite	-	0.3	0.3	-	0.1	-
Rutile	-	-	-	-	-	0.8
Silimanite	-	1.4	-	-	-	-

a. Low sulphuric acid concentration leaching

The XRF and XRD results for the ash residue samples leached with 1.02 M and 4.08 M H_2SO_4 solutions, at 45°C, for 180 min, using a solid to liquid ratio of 1:10, are presented in Tables 4-7 and 4-8 respectively. The XRF results showed that leaching of the SA1 ash sample prepared at 700°C with the 1.02 M and 4.08 M H_2SO_4 solutions, yielded leached residues with ash compositions resembling that of the original ash sample, presented in Table 4-5. A difference of <3% in elemental oxide percentages was observed when the results for the leached residues were compared with those of the original ash samples. The XRD results showed a decrease in the quartz content from 44.3% to 23.1% after the ash was leached with 1.02 M H_2SO_4 solution. The reduction of the concentration of quartz in the ash sample could be attributed to the increase in the amorphous material concentration from 47.7% to 63.6% (Tables 4-6 and 4-8). Small changes in the concentration of the minor mineral phases were seen, but the values were all <5%. These same

observations, regarding mineral composition (XRD) of the SA1 ash sample after being leached with the 1.02 M H_2SO_4 solution, could be applied to the SA1 ash sample leached with the 4.08 M H_2SO_4 solution. The SA1 ash sample prepared at 1050°C showed similar XRF results when compared to the residual ash samples, after being leached with the 1.02 M and 4.08 M H_2SO_4 solutions. The XRD results showed a lower concentration of quartz (33.7%) in the ash leached with the 1.02 M H_2SO_4 solution than the concentration of quartz (44.3%) in the original ash sample. This same trend was seen after the ash was leached with the 4.08 M H_2SO_4 solution. The leached ash residue contained 33.9% quartz, while the original ash (original material) prepared at 1050°C contained 43.5% quartz. The decreases in the quartz concentration, after leaching the ash sample prepared at 1050°C with 1.02 M and 4.08 M H_2SO_4 solutions, can be attributed to the formation of gypsum (gelatinous precipitates) and silicic acid (Equations 4-7 to 4-9) (Matjie *et al.*, 2005b). Sulphuric acid generally reacts with reactive silica to form unstable silicic acid, which will precipitate (gelatinous silicic) from the leach liquor at low temperature- and pH values (Matjie *et al.*, 2005b). The chemical reactions that lead to the formation of gelatinous precipitates interfere with reactions between sulphuric acid and aluminium species (metakaolinite). This interference will subsequently result in low dissolution efficiencies for Al, K, and Ti. These gelatinous precipitates also cause difficulty during the separation (filtration) of the leach liquor from the ash residue.

Possible reactions of gelatinous calcium sulphate and silicic precipitates (Torma, 1983) are as follow:

$$CaO + H_2SO_4 + H_2O \rightarrow CaSO_4.2H_2O \quad (4\text{-}7)$$

$$CaCO_3 + H_2SO_4 \rightarrow CaSO_4 + H_2O + CO_2 \quad (4\text{-}8)$$

$$CaO.Al_2O_3 + 4H_2SO_4 \rightarrow CaSO_4 + Al_2(SO_4)_3 + 4H_2O \quad (4\text{-}9)$$

$$(CaO)_x.\ SiO_2 + xH_2SO_4 \rightarrow xCaSO_4 + H_2SiO_3 + (x\text{-}1)H_2O \quad (4\text{-}10)$$

Available sulphuric acid could react with metakaolinite, potassium- and titanium species, to form alum ($Al_2(SO_4)_3$) (Equation 4-14), potassium alum ($AlK(SO_4)_2.12H_2O$), titanyl sulphate ($TiOSO_4$), and potassium sulphate. Potassium alum, potassium sulphate, and titanyl sulphate are soluble in a sulphuric acid solution (aqueous phase), whilst potassium aluminium silicate ($KAl2(Si_3O_{10})\ (OH)_2$ are insoluble in the aqueous phase.

Possible reactions between sulphuric acid, titanium dioxide and potassium carbonate are as follow:

$$H_2SO_4 + TiO_2 \rightarrow TiOSO_4 + H_2O \quad (4\text{-}11)$$

$$H_2SO_4 + K_2CO_3 \rightarrow K_2SO_4 + CO_2 + H_2O \quad (4\text{-}12)$$

$$4H_2SO_4 + Al_2O_3 + 2KOH \rightarrow Al_2(SO_4)_3.\ K_2SO_4 + 5H_2O \quad (4\text{-}13)$$

$$3H_2SO_4 + Al_2O_3.2SiO_2 + 2H_2O + 9H_2O \rightarrow Al_2(SO_4)_3.14H_2O + 2SiO_2 \quad (4\text{-}14)$$

Leaching the SA2 blend (a mixture of K_2CO_3 and SA2) with 1.02 M H_2SO_4 was unsuccessful and no samples could be submitted for analyses. Thus, no results for the ash samples prepared at 700°C and 1050°C are reported. Failure of the leaching experiment was caused by the formation of gelatinous gypsum (calcium sulphate), silicic acid, and reactions between potassium species and sulphuric acid to form potassium sulphate. The formation of these gelatinous substances was visibly observed; from which a highly viscous solution was obtained that could not be filtered.

The SA2 blend ash sample prepared at 700°C, and leached with the 4.08 M H_2SO_4 solution, contained decreased quantities of Al_2O_3 and K_2O, (9.2% and 3.4% respectively) when compared to the original ash samples with 22.6% Al_2O_3 and 18.4% K_2O (Table 4-5 and Table 4-7). This suggests the dissolution of aluminium and potassium species into the sulphuric acid solution occurred during the leaching process. The observed increase in SiO_2 concentration from 36.6% to 53.9% and CaO concentration from 8.9% to 16.2% may be due to the decrease of potassium and aluminium species concentrations after leaching. Whereas the increase in SO_3 concentration from 4.4% to 11% was caused by the formation of calcium sulphates (anhydrite and gypsum) after leaching the ash with sulphuric acid solutions (1.02 M and 4.08 M H_2SO_4). These changes were also observed in the XRD results (Table 4-8 and Table 4-10) obtained for the ash samples after leaching with sulphuric acid. An increase in the anhydrite concentration from 1.3% to 16.6% was accompanied by a decrease in anorthite concentration from 8.3% to 0%; a 5.6% illite concentration was observed in the leached residue. Potassium species could react with metakaolinite (transformed product of kaolinite) at elevated temperatures to form potassium aluminium silicate (microcline/muscovite/illite = potassium feldspars) (Matjie *et al.*, 2015) that are insoluble in sulphuric acid (Table 4-8). A concentration of 10.9% of potassium aluminium sulphate (potassium-alum) was seen in the ash residue after sulphuric acid leaching. The XRF results for the SA2 blend ash prepared at 1050°C, indicate a decrease in K_2O content from 18.4% to 6% and a decrease of Al_2O_3 content from 22.2% to 11% (Table 4-8), after leaching with the 4.08 M H_2SO_4 solution. The observed increase of the SiO_2 content from 36.1% to 54% may be due to the dissolution for the aluminium and potassium species from the amorphous material, during the leaching experiment. An increase in CaO content from 8.6% to 15.9% was seen; accompanied by the increase in anhydrite ($CaSO_4$) from 0.9% to 24.4% and a decrease in anorthite content from 9% to 0%. The decrease in mullite content from 13.2% to 0% could be attributed to the formation of calcium sulphates, thus minimizing the observed mullite. The presence of potassium aluminium sulphate (potassium-alum) at 15% was observed in the ash residue after leaching with the 4.08 M H_2SO_4 solution. Potassium alum forms during the reaction of aluminium- and potassium-containing species with sulphuric acid.

The same observations made with regards to the XRF results for the SA1 residual ash samples can be applied to the SA3 residual ash samples. This implies that after leaching of the SA3 ash samples, prepared at 700°C and 1050°C with the 1.02 M and 4.08 M H_2SO_4 solutions, that the XRF results differed by <6% when compared to the original ash samples. This tendency was also seen in the XRD results (Table 4-8) when comparing the residual ash samples to the original ash samples. The 4.2% calcite (Table 4-6) present in the SA3 ash sample dissolved in the 1.02 M H_2SO_4 to form a gypsum precipitate in the corresponding leached ash residue (Equation 4-8). The concentration of gypsum in this leached ash residue was determined to be 6.2% (Table 4-8). The SA3 ash prepared at 1050°C showed an increase in gypsum from 0.4% to 6.4% and mullite from 3.3% to 15.1% after the ash sample was leached with the 1.02 M H_2SO_4 solution. The observed increase in mullite percentage resulted from the dissolution of acid-soluble compounds. In Table 4-8, a lower percentage for gypsum was observed after leaching the SA3 ash sample with the 4.08 M H_2SO_4 solution. This occurrence is due to the digestion or re-dissolution of gypsum in the sulphuric acid, as the acid concentration is increased. Small changes in the mineral composition can be attributed to acid-soluble compounds being removed from the ash.

Table 4-7: Normalized XRF results (wt.%) for the coal ash samples leached with 1.02 M and 4.08 M H_2SO_4 solutions

Sample	*SA1*				*SA2 Blend*				*SA3*			
Ash Temp	*700°C*		*1050°C*		*700°C*		*1050°C*		*700°C*		*1050°C*	
Acid Conc.	*1.02M*	*4.08M*	*1.02M*	*4.08M*	*1.02M*	*4.08M*	*1.02M*	*4.08M*	*1.02M*	*4.08M*	*1.02M*	*4.08M*
SiO_2	64.6	65.2	63.1	63.1	-	53.9	-	54.0	63.5	60.7	59.3	60.0
Al_2O_3	29.0	28.4	29.6	29.3	-	9.2	-	11.0	27.5	28.7	28.7	27.7
Fe_2O_3	3.3	2.5	3.7	3.4	-	3.0	-	5.7	3.6	3.3	4.4	3.6
TiO_2	1.6	1.6	1.6	1.5	-	1.9	-	2.3	1.5	1.5	1.6	1.5
K_2O	0.7	0.7	0.7	0.7	-	3.4	-	6.0	0.4	0.4	0.4	0.4
CaO	0.3	0.9	0.6	1.2	-	16.2	-	15.9	2.3	4.1	3.9	5.4
MgO	0.3	0.3	0.3	0.3	-	0.2	-	1.6	0.3	0.2	0.5	0.3
SO_3	0.2	0.2	0.2	0.2	-	11.0	-	1.5	0.6	0.8	0.9	0.8
Cr_2O_3	0.1	0.1	0.1	0.1	-	0.1	-	0.1	0.1	0.1	0.1	0.1
P_2O_5	0.1	-	0.1	-	-	-	-	-	-	-	-	-
Na_2O	-	0.1	-	0.1	-	-	-	-	0.1	-	-	-

Table 4-8: XRD results (wt.%) for the coal ash samples leached with 1.02 M and 4.08 M H_2SO_4 solutions

Sample	*SA1*				*SA2 Blend*				*SA3*			
Ash Temp	*700°C*		*1050°C*		*700°C*		*1050°C*		*700°C*		*1050°C*	
Acid Conc.	*1.02M*	*4.08M*	*1.02M*	*4.08M*	*1.02M*	*4.08M*	*1.02M*	*4.08M*	*1.02M*	*4.08M*	*1.02M*	*4.08M*
Amorphous	63.6	64.6	39.8	34.3	-	55.6	-	50.3	65.6	69.5	32.8	39.5
Quartz	23.1	23.8	33.7	33.9	-	6.6	-	-	18.6	17.8	34.3	28.9
Anhydrite	-		-	-	-	16.6	-	24.4	-	-	-	-
Mullite	3.0	3.5	13.9	17.4	-	-	-	-	2.7	2.9	15.1	14.1
Hematite	0.8	0.6	1.8	0.9	-	2.9	-	6.4	0.9	0.7	1.6	1.7
Cristobalite	1.6	-	5.0	2.8	-	-	-	-	-	-	5.7	6.0
Anatase	1.4	1.8	1.3	2.7	-	0.3	-	0.4	1.0	3.3	2.5	7.9
Microcline	3.8	3.1	1.5	1.3	-	-	-	-	3.3	2.4	1.3	-
Illite	-	-	-	-	-	5.7	-	-	-	-	-	-
Dolomite	-	-	-	-	-	0.1	-	-	-	-	-	-
Calcite	-	-	-	-	-	-	-	0.1	-	-	-	-
Gypsum	1.1	1.3	1.6	5.8	-	1.2	-	1.3	6.2	2.7	6.4	1.4
Graphite	-	-	-	-	-	-	-	0.1	-	-	-	-
Diopside	-	-	1.3	0.6	-	-	-	-	-	-	-	-
Periclase	1.4	1.3	-	-	-	-	-	0.3	1.8	0.8	-	0.3
Rutile	-	-	-	-	-	-	-	0.9	-	-	0.4	0.3
Potassium-Alum	-	-	-	-	-	10.9	-	15.0	-	-	-	-

b. <u>High sulphuric acid concentration leaching</u>

The XRF and XRD results for the ash residue samples leached with the 6.12 M H_2SO_4 solution at 80°C, for 8 hours, while using different solid to liquid ratios (1:5 and 1:10), are presented in Tables 4-9 and 4-10 respectively. The ash composition results for the SA1 ash sample prepared at 700°C, after leaching with a 1:5 S/L ratio, showed a decrease in Al_2O_3 concentration from 28.3% to 12.5% and K_2O from 0.8% to 0.4%. The decrease in aluminium and potassium species, which would mainly be present in the amorphous materials but also other soluble compounds, suggest the dissolution of these species into the sulphuric acid solution. As expected, an increase in SiO_2 from 62.1% to 77% was observed with the decrease in aluminium and potassium percentages in the ash and leached ash samples. From the XRD results presented in Table 4-10, the concentration of quartz present in the original SA1 ash sample, prepared at 700°C, decreased from 44.3% to 26.8% after leaching. Accompanied with the decrease of quartz, an increase in amorphous materials (gelatinous calcium sulphate and silicic precipitates) formed during sulphuric acid of the ash samples (Matjie *et al.*, 2005b), from 47.6% to 66.5% was observed. Small changes in the quantities of the other minor mineral phases (presence <5%) was also seen. This same trend in XRF and XRD results was seen for the SA1 ash sample, prepared at 700°C, and leached with a 1:10 S/L ratio sulphuric solution. The difference in XRF and XRD values, when comparing the results of the ash residues after

leaching with the different S/L ratios, were <3%. The SA1 ash sample prepared at 1050°C and leached with the 1:5 and 1:10 S/L ratio sulphuric acid solutions, yielded ash composition (XRF) results that did not differ significantly (<5%) from those of the original ash sample (Table 4-5). The XRD results presented in Table 4-10 indicated a decrease in the concentration of mullite from 14.1% to 0.9% (Table 4-6), after leaching the SA1 ash sample with the sulphuric acid solution. A decrease in the minor crystalline phases was also noted for this sample. The dissolution of soluble elemental species/ minerals into the sulphuric acid solution, coupled with the formation of gelatinous calcium sulphate and silicic acid (Matjie *et al.*, 2005b), resulted in the dilution of the concentrations of mullite and quartz in the ash residues (Table 4-10). An increase in anhydrite concentration from 1.5% to 7.1% and amorphous material from 35.5% to 48.1% was observed (Table 4-6, Table 4-10), after leaching the SA1 ash sample. The same mineral composition (XRD results) was seen for the SA1 ash sample prepared at 700°C and leached with the 6.12 M H_2SO_4 solution, using the 1:10 S/L ratio. Crystalline phases and amorphous material in the ash sample were as follow: amorphous material was present with 48%, anhydrite, 6.5%, and mullite 1.3%.

Leaching the SA2 blend (mixture of K_2CO_3 and SA2) ash, prepared at 700°C with the 6.12 M H_2SO_4 using a 1:5 S/L ratio, led to a decrease in the concentrations of Al_2O_3 from 22.6% to 4.2%, and K_2O from 18.4% to 2.8% (Table 4-5, Table 4-9). The concentration of CaO in the SA2 blend ash sample increased from 8.9% to 14.9% after leaching of the ash sample. A large increase in SiO_2 concentration, from 36.3% to 66.7%, was observed in the SA2 blend ash residue after leaching of the ash sample. The increase in calcium and silicon concentrations is mainly due to the insolubility of these species in sulphuric acid, and the dissolution of aluminium and potassium species in the solution. Leaching of the soluble compounds from the coal ash subsequently resulted in a decrease in amorphous material concentration from 74.8% to 64.4%. The concentration of anhydrite in the SA2 blend ash, increased from 1.3% to 23.1%, after leaching of the ash sample with the sulphuric acid solution (Equation 4-8). This increase is due to the formation of gelatinous calcium sulphate (Matjie *et al.*, 2005b) (Freeman, 1993). The results obtained via XRF and XRD analyses for the SA2 blend ash sample prepared at 700°C, and leached with the 6.12 M H_2SO_4 solution using a 1:10 S/L ratio, showed a similar trend as when the ash sample was leached using a 1:5 S/L ratio. Comparing the XRF and XRD values determined for the ash residue samples, that is after leaching with the sulphuric acid solution using different solid to liquid ratios, differed with <5%.

The SA2 blend ash prepared at 1050°C and leached with the 6.12 M H_2SO_4 solution, using a 1:5 S/L ratio, showed a decrease in Al_2O_3 content from 22.2% to 5.3%. This decrease in Al_2O_3 corresponds with the decrease in Al-containing mineral phases within the ash sample; which is due to the formation of gelatinous calcium sulphate, silicic acid, gypsum, and anhydrite (Table 4-10). A decrease in K_2CO_3 content from 18.6% to 5.4%, was also observed for this ash sample. This decrease in potassium content was reflected in the XRD results, which showed a decrease of

crystalline K_2CO_3 content from 14% to 0% (Equation 4-12). An increase in the SiO_2 content from 36.2% to 46.1% is observed; which could be attributed to the dissolution of aluminium and potassium species from the ash during leaching. The increase in SO_3 content from 4.9% to 26.8% in the leached ash residue, is coupled with the increase in CaO content from 8.6% to 11.1%. This increase is due to reactions between the calcium and sulphate ions, from sulphuric acid, and the formation of calcium sulphate species. This is supported by the XRD results, which indicate an increase in the anhydrite concentration from 1.3 to 33.3% (Equation 4-8), after leaching of the ash sample. A decrease in mullite concentration from 13.2% to 0.3% and anorthite concentration from 9% to 1.8% was seen after leaching the ash sample with a 1:5 S/L ratio. The drop in concentrations of mullite and anorthite, which are insoluble in the sulphuric acid solution (Table 4-6; Table 4-10), is attributed to the formation of amorphous material and calcium sulphate minerals during the leaching experiments. Leaching of the SA2 blend ash sample prepared at 1050°C, with the 6.12 M H_2SO_4 solution using a 1:10 S/L ratio, yielded XRF and XRD results which followed the same trend as seen when the ash sample was leached using a 1:5 S/L ratio. Additionally, an increase in the microcline concentration from 9.7% to 17.7% was seen after leaching of the ash sample. The formation of microcline occurs when potassium species react with metakaolinite at elevated temperature to form these potassium aluminium silicate phases (insoluble potassium feldspars) (Matjie *et al.*, 2015). The increase observed may result from the dissolution of aluminium and potassium in the sulphuric acid solution. Comparison of the ash residue samples after being leached with the 1:5 and 1:10 S/L ratio sulphuric acid solutions yielded values that differed with ±10%.

The XRF results obtained for the SA3 ash sample, prepared at 700°C and leached with a 1:5 S/L ratio sulphuric acid solution, showed a decrease in the Al_2O_3 concentration from 27.5% to 13.6%, and an increase in the SiO_2 concentration from 57.7% to 78.1% (Table 4-5; Table 4-9). The decrease in Al concentration from this ash sample is attributed to the selective dissolution of Al species from the amorphous material (metakaolinite) during the leaching step. From the XRD results, a decrease in calcite from 4.2% to 0.1% was seen with a corresponding increase in anhydrite from 1% to 7.6% (Table 4-6; Table 4-10; Equation 4-8). Other changes seen in the XRD results were a decrease in quartz concentration from 20.3% to 16.1%, resulting in an increase in amorphous material from 68.5% to 73.6% after leaching of the SA3 ash sample. The SA3 ash sample prepared at 1050°C and leached with the 1:10 S/L ratio sulphuric acid solution, indicated similar trends in XRF results as that of the ash leached with the 1:5 S/L ratio sulphuric acid solution. A percentage difference of <4% was observed when comparing the results of the ash residues, after leaching the ash with both S/L ratios (in Table 4-9). The XRD results for SA3 leached with a 1:10 S/L ratio showed lower amorphous material (63.5%), and higher quartz (23.9%) and anhydrite (9.9%) percentages in the ash residue. Leaching of the SA3 ash prepared at 1050°C with both a 1:5 and 1:10 S/L sulphuric acid solutions, yielded ash residues with ash composition (XRF results) resembling that of the original ash sample (Table 4-5).

The results found for Al in the coal ash- and leached residue samples obtained during this investigation, is consistent with results found for other coal ash samples and their corresponding leached material (Alguacil *et al.*, 1987; Burnet *et al.*, 1984; Canon *et al.*, 1979; Freeman, 1993; Matjie *et al.*, 2005b; Nayak & Panda, 2010; Sangita *et al.*, 2017; van der Merwe *et al.*, 2017).

Table 4-9: Normalized XRF results (wt.%) for the coal ash samples leached with a 6.12 M H_2SO_4 solution, using 1:5 and 1:10 S/L ratios

Sample	*SA1*				*SA2 Blend*				*SA3*			
Ash Temp	*700°C*		*1050°C*		*700°C*		*1050°C*		*700°C*		*1050°C*	
S/L Ratio	*1:5*	*1:10*	*1:5*	*1:10*	*1:5*	*1:10*	*1:5*	*1:10*	*1:5*	*1:10*	*1:5*	*1:10*
SiO_2	77.0	79.6	66.0	65.6	66.7	70.4	46.1	56.1	78.1	76.8	57.7	60.9
Al_2O_3	12.5	13.6	27.1	27.7	4.2	5.4	5.3	8.0	13.6	12.6	24.9	26.3
CaO	5.3	2.1	2.0	1.6	14.9	14.5	11.1	11.4	5.3	6.4	5.9	5.0
TiO_2	2.0	1.8	1.5	1.5	1.8	1.9	1.1	1.	1.9	1.7	1.5	1.4
Fe_2O_3	1.1	1.3	1.4	1.2	2.6	3.7	3.0	4.8	0.8	1.1	1.3	1.4
SO_3	0.9	0.1	0.4	0.6	6.0	0.9	26.8	11.1	0.1	0.3	7.3	3.8
K_2O	0.4	0.5	0.7	0.7	2.8	2.2	5.4	5.8	0.4	0.4	0.8	0.6
Cr_2O_3	0.2	0.1	0.1	0.1	-	-	-	-	0.1	0.1	0.1	0.1
MgO	0.2	0.3	0.2	0.2	0.2	0.2	0.4	0.6	0.1	0.2	0.3	0.2
P_2O_5	0.1	0.2	-	-	-	-	-	-	-	-	-	-
BaO	-	-	0.1	0.3	0.3	0.2	0.3	0.3	-	0.1	0.1	0.2
Na_2O	-	-	-	-	-	0.1	-	0.1	-	-	-	-
SrO	-	-	-	-	0.4	0.3	0.3	0.3	0.1	0.1	0.1	0.1

Table 4-10: XRD results (wt.%) for the coal ash samples leached with a 6.12 M H_2SO_4 solution, using 1:5 and 1:10 S/L ratios

Sample	*SA1*				*SA2 Blend*				*SA3*			
Ash Temp	*700°C*		*1050°C*		*700°C*		*1050°C*		*700°C*		*1050°C*	
S/L Ratio	*1:5*	*1:10*	*1:5*	*1:10*	*1:5*	*1:10*	*1:5*	*1:10*	*1:5*	*1:10*	*1:5*	*1:10*
Amorphous	66.5	66.8	48.1	48	64.4	63.3	51.4	48	73.6	63.5	49.5	43.5
Quartz	26.8	26.7	41	40	7.9	7.4	0.5	0.6	16.1	23.9	25.3	32.3
Anhydrite	4.1	3.3	7.1	6.5	23.1	24.9	33.3	29.3	7.6	9.9	15.4	17.1
Microcline	-	-	0.8	0.9	-	0.3	-	17.7	-	-	-	0.9
Mullite	-	-	0.9	1.3	-	-	0.3	1.8	-	-	-	2.2
Hematite	-	-	-	-	-	-	0.1	-	-	-	-	-
Anorthite	-	-	-	-	-	-	1.8	-	-	-	-	-
Portlandite	0.1	-	0.2	0.3	0.1	-	0.1	-	-	-	-	0.4
Cristobalite	-	-	-	-	-	-	0.1	-	-	-	0.4	-
Muscovite	0.1	0.1	-	-	0.5	0.1	0.1	0.1	0.3	0.2	-	0.1
Anatase	-	-	-	-	-	0.3	1.3	-	-	-	-	-
Illite	-	0.1	-	-	-	0.5	-	0.7	-	0.4	-	0.3
Dolomite	0.3	-	0.4	0.5	0.3	0.2	5.7	0.6	0.8	0.1	1.2	0.7
Calcite	0.4	0.3	0.5	0.8	-	0.4	-	-	0.1	0.3	-	0.7
Gypsum	1	1.5	0.7	0.6	1.9	1.1	0.8	0.1	0.8	1	-	0.8
Graphite	-	-	-	-	0.7	-	0.9	-	0.2	-	-	-
K_2CO_3	0.8	1.2	-	0.5	0.8	1	1.3	-	0.5	0.7	-	0.5
Kaolinite	-	0.1	0.1	0.2	-	-	-	-	-	-	-	0.1
Periclase	-	-	0.2	0.1	-	-	-	-	-	-	-	0.2
Pyrrhotite	-	-	-	-	0.1	-	-	0.1	-	-	-	-
Rutile	-	-	-	-	0.1	0.2	-	0.8	-	-	0.4	0.1
Silimanite	-	-	-	-	-	-	0.2	-	-	-	7.4	-

The results for the ash samples leached with the 6.12 M H_2SO_4 solution using a 1:5 S/L ratio are discussed in the following sections, and not the results obtained after acid leaching using a 1:10 S/L ratio. This is due to the similarity of XRF results after leaching of the ash samples with the 6.12 M H_2SO_4 solution using 1:5 and 1:10 S/L ratios.

4.3.5 ICP-OES digestion

ICP-digestion analysis was done on the leach liquor samples obtained after sulphuric acid leaching of the coal ash samples. In the first set of experiments, the coal ash samples were leached with the 1.02 M and 4.08 M H_2SO_4 solutions, at a temperature of 45°C, using a 1:10 S/L ratio for 180 min. In the second set of experiments, the coal ash samples were leached with a 6.12M H_2SO_4 solution, at a temperature of 80°C, for 8 hours using a 1:5 S/L ratio. The ICP results from the digestive analysis method (Section 4.2.3.4) are presented in Table 4-11. The values from this analytical method are reported as weight percentages (wt.%) of the inorganic elements present in the leach liquor. This

percentage of Al in the leach liquor accounts for the organic and inorganic elements present. Analysis results of the leach liquors obtained after leaching the SA1 ash samples with the 1.02 M and 4.08 M H_2SO_4 solutions, showed that no Al, K, or Ti was detected in the leach liquors. This was seen for both the ash samples prepared at 700°C and 1050°C. The leach liquor obtained after leaching the SA1 ash sample, prepared at 700°C, with the 6.12 M H_2SO_4 solution (1:5 S/L ratio) contained 11.6% Al, 0.4% K, and 0.1% Ti. The SA1 ash prepared at 1050°C, and leached with the 6.12 M H_2SO_4 solution (1:5 S/L ratio), contained 4.3% Al, 0.1% K, and 0.3% Ti.

The leach liquors obtained after leaching of the SA2 blend (mixture of K_2CO_3 with SA2) ash samples, prepared at 700°C and 1050°C, with the 4.08 M H_2SO_4 solution contained values of <1% Ti and 6% and 8% of Al respectively. The percentage of K in the leach liquors were 10.3% and 11.1% for the SA2 ash prepared at 700°C and 1050°C, respectively. The leach liquors samples produced by leaching the SA2 ash samples with the 6.12 M H_2SO_4 solution using a 1:5 S/L ratio, contained 7.9% Al and 4.4% K from the 700°C ash, and 7.2% Al and 5.8% K from the 1050°C ash.

Analysis of the leach liquor samples produced by leaching the SA3 ash samples, prepared at 700°C and 1050°C with the 1.02 M and 4.08 M H_2SO_4 solutions, showed a <4% presence of Al and K in solution, with Ti <1%. Leaching the ash prepared at 700°C and 1050°C SA3 with the 6.12 M H_2SO_4 solution (1:5 S/L ratio), yielded Al percentages of 11.2% and 0% respectively. The percentages of K and Ti in the two leach liquor samples were determined to be <1% in value.

Table 4-11: ICP-OES digestion results (wt.%) for Al, K, and Ti present in the leach liquors

		SA1 700°C	*SA1 1050°C*	*SA2 Blend 700°C*	*SA2 Blend 1050°C*	*SA3 700°C*	*SA3 1050°C*
Al	1.02M	0	0	-	-	3.6	2.8
	4.08M	0	0	6.9	7.9	0	3.9
	6.12M (1:5)	11.6	4.3	7.9	7.2	11.2	0
K	1.02M	0	0	-	-	0.1	2.9
	4.08M	0	0	10.3	11.1	0	0.5
	6.12M (1:5)	0.4	0.1	4.4	5.8	0.2	0
Ti	1.2M	0	0	-	-	0.1	0.1
	4.08M	0	0	0.2	0.1	0	0.1
	6.12M (1:5)	0.1	0.3	0.3	0.4	0.2	0

4.3.6 Complexometric titration

Complexometric titration of the leach liquor samples obtained after acid leaching of the coal ash samples was used to determine the concentration of aluminium in the leach liquor samples. The coal ash samples were leached with 1.02 M and 4.08 M H_2SO_4 solutions, at a temperature of 45°C, using a 1:10 S/L ratio for 180 min during the first set of experiments. The second set of experiments were done by leaching the coal ash samples with a 6.12 M H_2SO_4 solution, at a temperature of 80°C, for 8 hours, using a 1:5 S/L ratio. The volume of $ZnSO_4$ used during each titration experiments was measured and is presented in Table 4-12. The volume of $ZnSO_4$ used, the leach liquor volume, and Equation 4-1 was used to determine the concentration of Al in each of the liquid samples. The Al concentrations calculated are also presented in Table 4-12. Titration of the leach liquor samples showed low concentrations of Al <2 g/ dm^3 in the solution for the SA1 and SA3 ash samples prepared at 700°C and 1050°C when leached with the 1.02 M H_2SO_4 solution. The concentration of Al in the leach liquor samples were <2 g/ dm^3 for SA1 and SA3 samples, and <4 g/ dm^3 for SA2 blend sample after leaching the ash samples, prepared at 700°C and 1050°C, with the 4.08 M H_2SO_4 solution. Higher concentrations of Al were observed in the leach liquor samples obtained after leaching the coal ash samples with the 6.12 M (1:5 S/L ratio) H_2SO_4 solution. The concentration of Al in the leach liquor samples were determined to be 6.8 g/ dm^3 and 1.8 g/ dm^3, for the SA1 ash sample, prepared at 700°C and 1050°C and with the 6.12 M H_2SO_4 solution, respectively. The leach liquor samples obtained after leaching the SA3 ash samples, prepared at 700°C and 1050°C with a 6.12 M H_2SO_4 solution, contained Al concentrations of 5.1 g/ dm^3 and 2.1 g/ dm^3 respectively. The leach liquor samples obtained by leaching the SA2 blend, prepared at 700°C and 1050°C with the 6.12 M H_2SO_4 solution (1:5 S/L ratio), concentrations >8.5 g/ dm^3 for Al was obtained.

Table 4-12: Volume of $ZnSO_4$ (cm^3) and Al concentrations calculated for the leach liquors (g/ dm^3)

	SA1 700°C	*SA1 1050°C*	*SA2 Blend 700°C*	*SA2 Blend 1050°C*	*SA3 700°C*	*SA3 1050°C*
			Volume $ZnSO_4$ (cm^3)			
1.02 M	24.6	22.3	-	-	22	22.1
4.08 M	22.4	22.4	17.9	18.5	22.5	22.1
6.12 M (1:5)	12.5	21.7	8.3	9.2	15.5	21.1
			Concentration Al (g/ dm^3)			
1.02 M	0.2	1.5	-	-	1.6	1.6
4.08 M	1.4	1.4	3.8	3.5	1.4	1.6
6.12 M (1:5)	6.8	1.8	9.0	8.5	5.1	2.1

4.3.7 Dissolution efficiencies

4.3.7.1 Dissolution efficiencies of Al, K, and Ti as determined from XRF analysis results

a. Low sulphuric acid concentration leaching

The dissolution efficiencies for Al, K, and Ti as calculated from the XRF results obtained after leaching of the coal ash samples, with the 1.02 M and 4.08 M H_2SO_4 solutions at a temperature of 45°C for 180 min, using a solid/liquid ratio of 1:10, are presented in Figure 4-2. The calculation method used to determine the dissolution efficiencies is discussed in Section 4.2.4.3.1. Leaching of the SA1 ash sample, prepared at 700°C with the 1.02 M and 4.08 M H_2SO_4 solutions, yielded the following low dissolution efficiencies; 2.7% Al, 16.9% K, and 27.6% Ti for the 1.02 M H_2SO_4 solution; and 4.2% Al, 16.4% K, and 27.2% Ti for the 4.08 M H_2SO_4 solution. The difference in dissolution efficiency for Al was <2% when comparing the results calculated for the two concentrations used; while identical dissolution efficiencies for K and Ti were observed. The SA1 ash sample prepared at 1050°C achieved dissolution efficiencies of <1% Al, 17% K, and 15% Ti when the ash was leached with the 1.02 M H_2SO_4 solution; and <1% Al, 15.5% K, and 14.8% Ti when the ash was leached with the 4.08 M H_2SO_4 solution. The difference in dissolution efficiencies determined for Al, K, and Ti are <5% when comparing the results obtained for the two concentrations used.

Leaching the SA2 blend (mixture of K_2CO_3 and SA2) ash prepared at 700°C, with the 4.08 M H_2SO_4 solution, produced dissolution efficiencies of 65% Al, 84% K, and 4.6% Ti; while the ash sample prepared at 1050°C yielded dissolution efficiencies of 58% Al and 72.5% K. According to the calculations, very low to no Ti was leached from this sample. The low dissolution efficiencies are reflected in the negative value seen in Figure 4-2.

Dissolution efficiencies <7% for Al, K, and Ti were observed after leaching the SA3 ash sample, prepared at 700°C, with both the 1.02 M and 4.08 M H_2SO_4 solutions. The specific values can be seen in Figure 4-2. Leaching the SA3 ash sample prepared at 1050°C, with the 1.02 M and 4.08 M H_2SO_4 solutions, yielded dissolution efficiencies <8% for both Al and Ti. Moderate dissolution efficiencies of 45.9% and 47% for K were obtained when leached with 1.02 M and 4.08 M H_2SO_4 solutions, respectively.

From the results in Figure 4-2, it can be seen that the use of low acid concentrations during direct leaching yields low dissolution efficiencies. This is mainly due to the formation of gelatinous calcium sulphate and silicic acid precipitates (amorphous materials). The reactions of these gelatinous materials will consume more sulphuric acid, preventing the dissolution of other soluble Al- and K compounds. This is especially true for ash samples containing high concentrations of CaO and subjected to sulphuric acid leaching. Also seen in Figure 4-2, is an increase in Al dissolution efficiency with the addition of potassium carbonate to the coal prior to thermal processing.

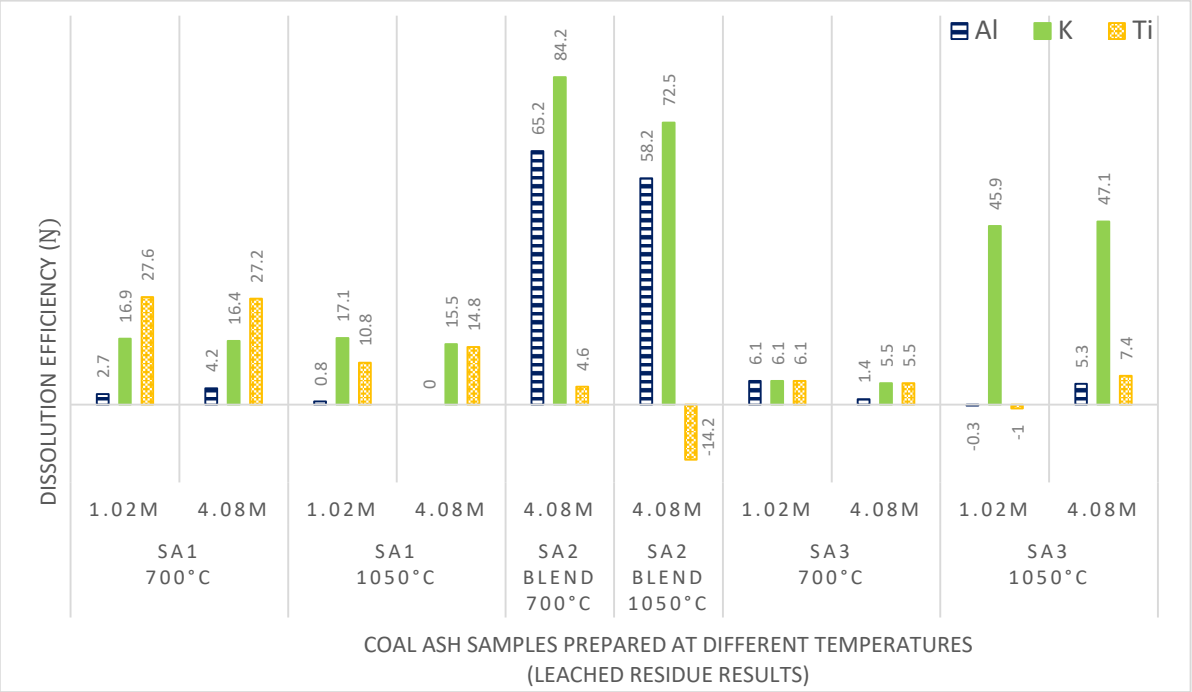

Figure 4-2: Dissolution efficiencies (ŋ) for Al, K, and Ti as determined from XRF analysis of leached and original ash samples (leaching conditions: 1.02 M and 4.08 M H_2SO_4 solutions, 45°C, 180 min, 1:10 S/L ratio)

b. <u>High sulphuric acid concentration leaching</u>

The dissolution efficiencies for Al, K, and Ti as calculated from the XRF results obtained after leaching of the coal ash samples with the 6.12 M H_2SO_4 solution, at a temperature of 80°C for 8 hours, using 1:5 and 1:10 as solid to liquid ratios, is presented in Figure 4-3. The calculation method used to determine the dissolution efficiencies are discussed in Section 4.2.4.3.1. Leaching the SA1 ash, produced at 700°C with the 6.12 M H_2SO_4 solution using a 1:5 S/L ratio, yielded dissolution efficiencies of 59.9% Al, 54.6% K, and 13.4% Ti; while the 1:10 S/L ratio showed dissolution efficiencies of 56.1% Al, 42.9% K, and 21.4% Ti. The difference in dissolution efficiency values was <5% for Al, 12% for K, and 8% for Ti when comparing the results calculated for the ash samples leached with the different solid to liquid ratios. The formation of significant amounts of gelatinous calcium sulphate (precipitate), when leaching coal ash samples with sulphuric acid solutions, can reduce the dissolution efficiency of the elemental species. Also, as the volume/ concentration of sulphuric acid (lixiviant) is increased, precipitation of the gelatinous calcium sulphate increases within the leaching vessel; subsequently resulting in low dissolution efficiencies for Al and K species form the coal ash. The SA1 ash sample prepared at 1050°C, showed dissolution efficiencies of 0% Al, 3.8% K, and 3% Ti when leached with the 6.12 M H_2SO_4 solution using a 1:5 S/L ratio; and 0% Al, 6.8% K, and 6% Ti when using a 1:10 S/L ratio. The negative values seen in Figure 4-3, suggests that little to no leaching of that specific element took place. A 3% difference in K and Ti dissolution efficiencies was observed when comparing the results obtained after leaching with the different S/L ratios. Low or zero dissolution of Al and K was expected for the ash samples prepared at 1050°C.

This is due to mullite (transformed product of metakaolinite) and Ca-K anorthite/ microcline (feldspars) (transformed products of association minerals (calcite/dolomite/K_2CO_3 and kaolinite), formed at temperatures at >1000°C. These mineral phases (containing Al and K) are insoluble in sulphuric acid (Matjie *et al.*, 2008; Matjie *et al.*, 2006; van Alphen, 2005). The low Ti dissolution efficiencies could be associated with Ti being capture in mullite and anorthite crystalline phases during recrystallization of the phases from the molten solution formed during thermal processing.

The SA2 blend (mixture of K_2CO_3 and SA2) ash sample prepared at 700°C showed dissolution efficiencies of 86.5% Al, 88.9% K, and 23.2% Ti when leached with the 6.12 M H_2SO_4 solution using a 1:5 S/L ratio; and 82.3% Al, 91.1% K, and 16.6% Ti using a 1:10 S/L ratio. The difference in dissolution efficiency for Al and K were <4% when comparing the calculated results for the two solid to liquid ratios. Leaching of the SA2 blend ash prepared at 1050°C with the 6.12 M H_2SO_4 solution, while using a 1:5 S/L ratio, yielded dissolution efficiencies of 73% Al, 67.2% K, and 22.3 Ti; while 70.6% Al, 74.6% K, and 33.7% Ti was observed when using a 1:10 S/L ratio. The difference in dissolution efficiencies observed, when the ash was leached with the 6.12M H_2SO_4 solution using the two solid to liquid ratios, was <5% for Al, 8% for K, and 11% for Ti. The high dissolution efficiency obtained for Al and K from the SA2 blend ash sample was achieved through the dissolution of Al- and K containing phases from the amorphous material (metakaolinite and amorphous K_2CO_3 or soluble K species) present in the ash samples. The high dissolution efficiency values of Al, determined from ash containing metakaolinite, is in good agreement with results found by Matjie *et al.* (2005b) when coal pellets, lime, and ash was subjected to thermal processing (>1000°C) and subsequently leached with 6.12 M H_2SO_4.

Leaching of the SA3 ash sample prepared at 700°C, with the 6.12 M H_2SO_4 solution using a 1:5 S/L ratio, yielded dissolution efficiencies of 64.5% Al, 28% K, and 9.1% Ti; whilst leaching of the ash sample with a 1:10 S/L ratio yielded dissolution efficiencies of 59.5% Al, 11.5% K, and 0% Ti. The difference in dissolution efficiency values calculated after leaching the ash samples with the 1:5 and 1:10 S/L ratios were <5% for Al, 17% for K, and 9% for Ti. The SA3 ash sample prepared at 1050°C showed no dissolution of Al, K, and Ti when leached with the 6.12 M H_2SO_4 solution when using a 1:5 S/L ratio. Low dissolution efficiencies of 7.3% Al, 18.1 K, and 10.9% Ti were obtained when the ash sample was leached using a 1:10 S/L ratio. The dissolution efficiencies calculated and presented in Figure 4-3, showed that leaching the SA2 blend ash samples with the 6.12 M H_2SO_4 solution while using a 1:5 S/L ratio, yielded better dissolution efficiencies; when compared to the results obtained after leaching the ash with a 1:10 S/L ratio. This is attributed to the formation of significant amounts of gelatinous calcium sulphate and silicic acid precipitates; formed when the ash was leached with the 6.12 M H_2SO_4 solution using a 1:10 S/L ratio. The formed precipitates will prevent the sulphuric acid from dissolving aluminium species from the ash sample.

The SA2 blend (mixture of SA2 and K_2CO_3) ash prepared at 700°C showed the best dissolution of Al and K from this ash; after leaching the ash with the 6.12 M H_2SO_4 solution at a temperature of 80°C for 8 hours. The K-containing species in the ash reacted with sulphuric acid to form soluble potassium sulphate (Klopper *et al.*, 2012); which in turn prevented the formation of gelatinous calcium sulphate precipitate. An Al dissolution efficiency of 85% was reached by Matjie *et al.* (2005b), when sintered pellets of another South African coal, South African fly ash, and quicklime (CaO) was leached with a 6.12 M H_2SO_4 solution at a temperature of 80°C for 8 hours. Torma (1983) achieved the highest Al dissolution efficiency of 99% after leaching calcined pellets, which comprised of fly ash from an overseas power station and calcium carbonate, with sulphuric acid. van der Merwe *et al.* (2017) showed a low dissolution efficiency of 47% for Al when using a conventional hydrometallurgy process to selectively solubilize Al from an ultrafine South African coal fly ash, by means of an ammonium sulphate solution.

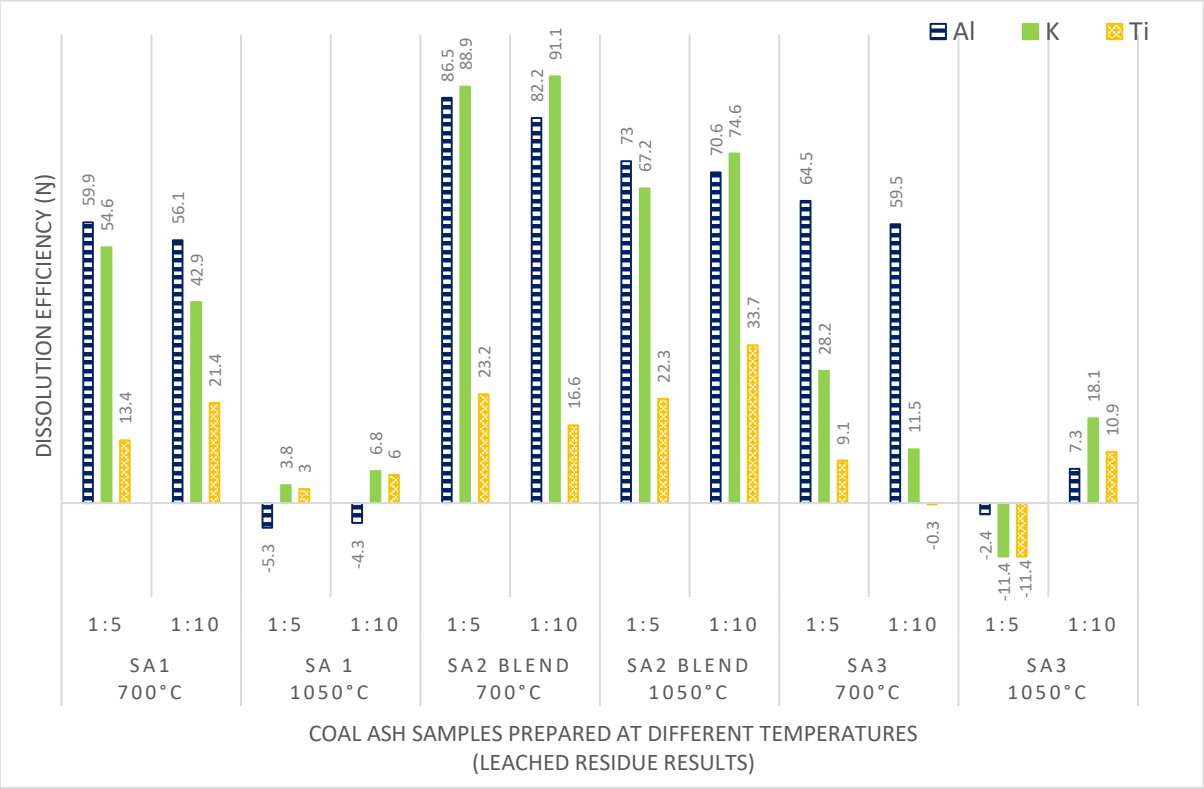

Figure 4-3: Dissolution efficiencies (ŋ) for Al, K, and Ti as determined from XRF analysis of leached and original ash samples (leaching conditions: 6.12 M H_2SO_4 solution, 80°C, 8 hrs., 1:5 and 1:10 S/L ratio)

The results for the ash samples leached with the 6.12 M H_2SO_4 solution using a 1:5 S/L ratio are discussed in the following sections while excluding the results obtained after leaching the ash samples using a 1:10 S/L ratio. This is due to the similarities of the XRF results obtained; coupled with the similarities in the calculated dissolution efficiencies.

4.3.7.2 Dissolution efficiencies of Al, K, and Ti as determined from ICP-OES digestion results

The dissolution efficiencies (β) for Al, K, and Ti calculated from the results obtained through ICP-OES digestion analysis (of the leach liquors), is presented in Figure 4-4. The calculation method for determining the dissolution efficiencies are discussed in Section 4.2.4.3.2. From the analysis results Al, K, and Ti were not detected in the leach liquor samples obtained after leaching of the SA1 ash samples, prepared at 700°C and 1050°C, with the 1.02 M and 4.08 M H_2SO_4 solutions. The ash sample prepared at 700°C yielded dissolution efficiencies of 77.6% Al, 54.5% K, and 6.4% Ti; whilst the ash sample prepared at 1050°C yielded dissolution efficiencies of 28.7% Al, 7.6% K, and 33.3% Ti, when leached with the 6.12 M H_2SO_4 solution (1:5 S/L ratio).

The SA2 blend (mixture of K_2CO_3 and SA2) ash samples prepared at 700°C, yielded dissolution efficiencies of 58.3% Al, 67.2% K, and 20.6% Ti when leached with the 4.08 M H_2SO_4 solution; and 66.2% Al, 28.6% K, and 29.4% when leached with the 6.12 M H_2SO_4 solution (1:5 S/L ratio). The ash samples prepared at 1050°C showed dissolution efficiencies of 67.6% Al, 72.3% K, and 10.8% Ti when leached with the 4.08 M H_2SO_4 solution, and 60.9% Al, 37.9% K, and 41.2% Ti when leached with the 6.12 M H_2SO_4 solution (1:5 S/L ratio).

The leach liquor samples obtained after leaching the SA3 ash sample, prepared at 700°C with the 1.02 M H_2SO_4 solution, yielded relatively low dissolution efficiencies of 24.9% Al, 39.4% K, and 13.3% Ti. Dissolution efficiencies for Al, K, and Ti could not be calculated for the leach liquor obtained after leaching the SA3 ash sample with the 4.08 M H_2SO_4 solution. A high Al dissolution efficiency of 76.9% was calculated for the leach liquor obtained by leaching the SA3 ash sample, prepared at 700°C, with a 6.12 M H_2SO_4 solution (1:5 S/L ratio); with dissolution efficiencies for K and Ti reaching percentages of 42.4% and 18.9% respectively. Low dissolution efficiencies of Al, K, and Ti were calculated for the leach liquor samples obtained after leaching the SA3 ash sample prepared at 1050°C. Dissolution efficiencies of 19.8% Al, 1.7% K, and 4.4% Ti were observed when the ash was leached with the 1.02 M H_2SO_4 solution; and 26.9% Al, 21.1% K, and 15.6% Ti when leached with the 4.08 M H_2SO_4 solution. Al, K, and Ti dissolution efficiencies could not be calculated for the leach liquor sample obtained by leaching the ash prepared at 1050°C with the 6.12 M H_2SO_4 solution (1:5 S/L ratio).

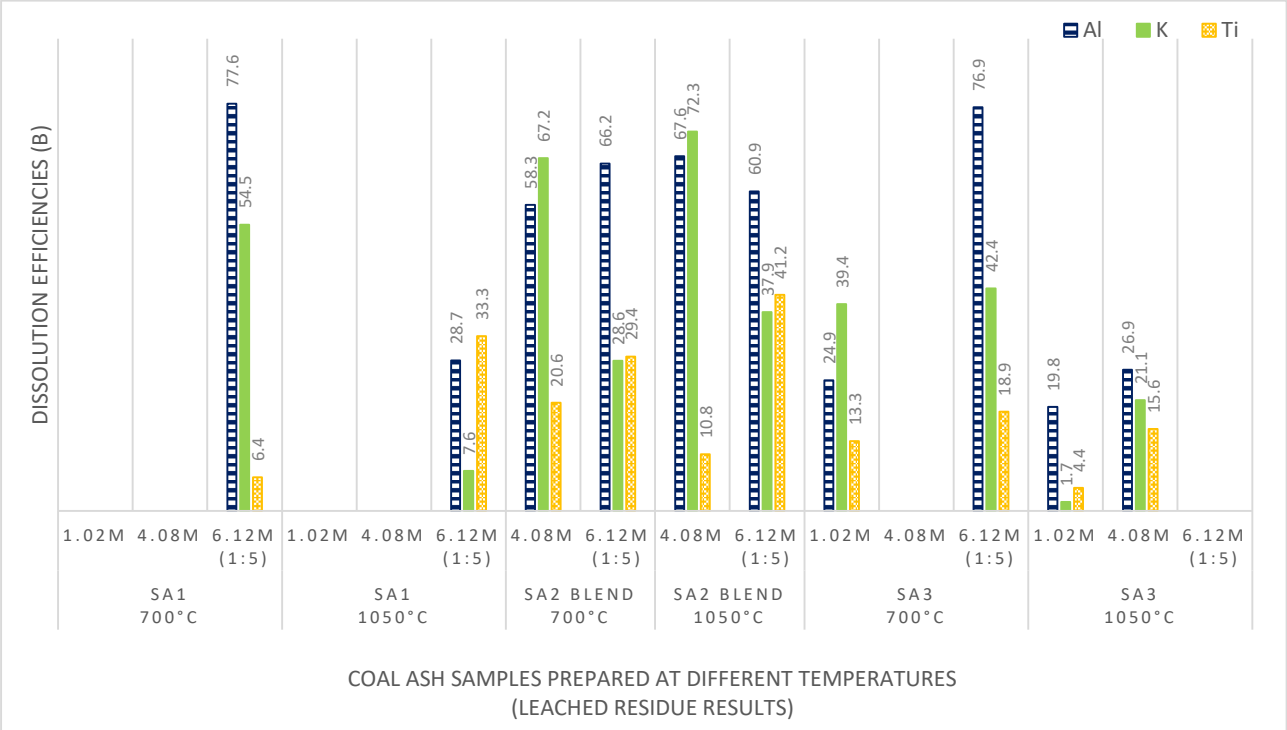

Figure 4-4: Dissolution efficiencies (β) for Al, K, and Ti as determined by ICP-OES digestion analysis of leach liquors (leaching conditions: 1.02 M and 4.08 M H_2SO_4 solutions, 45°C, 180 min, 1:10 S/L ratio; and 6.12 M H_2SO_4 solution, 80°C, 8 hrs., 1:5 S/L ratio)

4.3.7.3 Dissolution efficiencies of Al as determined from complexometric titration

The dissolution efficiencies (α) of Al calculated through complexometric titration of the leach liquor samples obtained after leaching of the coal ash samples are presented in Figure 4-5. The calculation methods for determining the dissolution efficiencies are discussed in Section 4.2.4.3.3. Titration of the leach liquor samples obtained after leaching the SA1 ash sample (produced at 700°C) with the 1.02 M and 4.08 M H_2SO_4 solutions, yielded Al dissolution efficiencies of less than 10%. A dissolution efficiency of 45% Al was observed for the leach liquor produced by leaching the SA1 ash sample, prepared at 700°C, with the 6.12 M H_2SO_4 solution using a 1:5 S/L ratio. Dissolution efficiencies <12% was observed for the leach liquor samples obtained by leaching the SA1 ash sample, prepared at 1050°C, with the 1.02 M, 4.08 M, and 6.12 M H_2SO_4 solutions.

The Al dissolution efficiencies determined for the leach liquors obtained by leaching the SA2 blend ash samples, produced at 700°C and 1050°C with the 4.08 M H_2SO_4 solution, were 32% and 29.8% respectively. When the SA2 blend ash sample was leached with the 6.12 M H_2SO_4 solution (1:5 S/L ratio), dissolution efficiencies of 75.3% and 72.5% were obtained for the ash samples produced at 700°C and 1050°C respectively.

The same trend in Al dissolution observed for the SA1 ash samples was also seen for the SA3 ash samples. Dissolution efficiencies for Al were <11% for the leach liquors obtained by leaching the ash sample (prepared at 700°C) with the 1.02 M and 4.08 M H_2SO_4 solutions, and 35.2% when leached with the 6.12 M H_2SO_4 solution (1:5 S/L ratio). The dissolution efficiencies of Al were <15% for the leach liquor samples obtained after leaching the SA3 ash sample, prepared at 1050°C, with the 1.02 M, 4.08 M, and 6.12 M H_2SO_4 solutions.

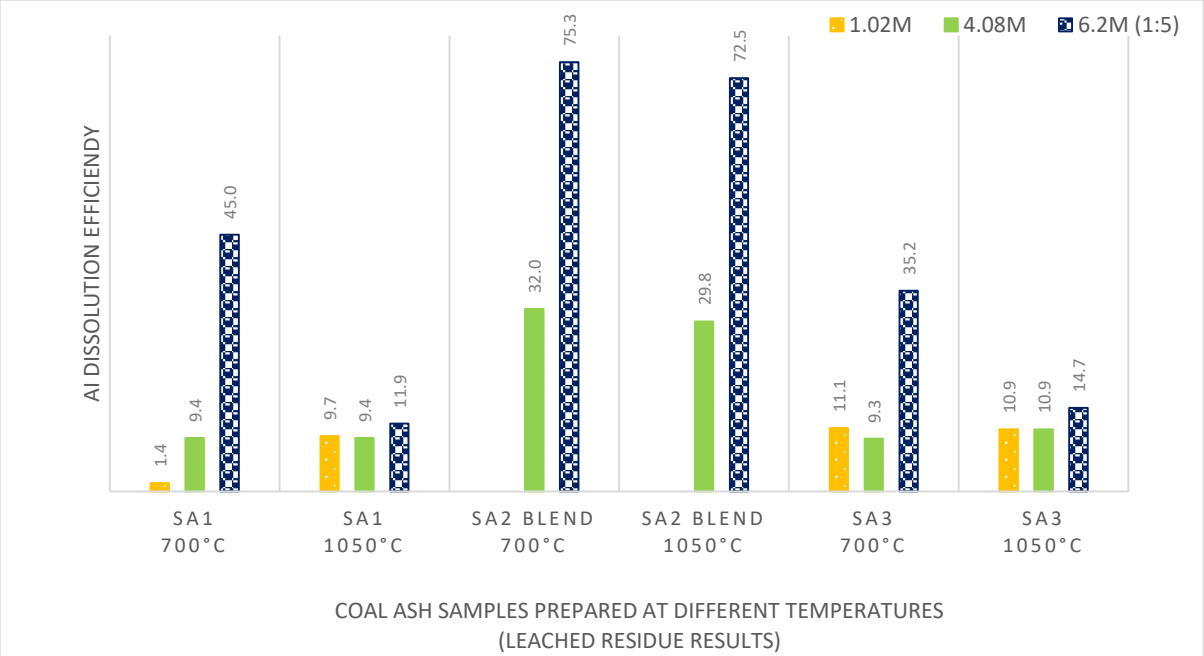

Figure 4-5: Dissolution efficiencies (α) of Al as determined by complexometric titration

4.3.7.4 Comparison of dissolution efficiencies determined by different analytical techniques

Different analytical techniques (see Sections 4.3.7.1, 4.3.7.2, and 4.3.7.3) were used to determine the dissolution efficiencies of Al, K, and Ti from the coal ash, when subjected to sulphuric acid leaching experiments. Comparison of the Al dissolution efficiencies determined through these techniques is presented in Figure 4-6. From the figure it follows that the dissolution efficiencies determined from the XRF results (of ash residues) and ICP-OES digestion results (of leach liquors), showed similar trends in the dissolution percentages (<20%), with complexometric titration indicating larger differences in dissolution efficiency values.

The dissolution efficiency values determined from XRF analysis results may be more accurate than those determined by ICP-OES digestion- and complexometric titration of the leach liquors. XRF analysis of the solid samples is a non-destructive method, requiring little to no sample preparation. The sample composition is determined with an analyser and standard analysis program; with a known equipment error, which was taken into account. This eliminates/ minimizes the occurrence of human errors. Extensive sample preparation is needed for ICP-OES digestion analysis, coupled with specialized standard solutions. This is also true for complexometric titration experiments of the

leach liquor samples, suggesting a higher possibility for human error, and thus influencing the accuracy of the method. This same trend, when comparing the dissolution efficiencies calculated from the different methods, was seen for potassium and titanium.

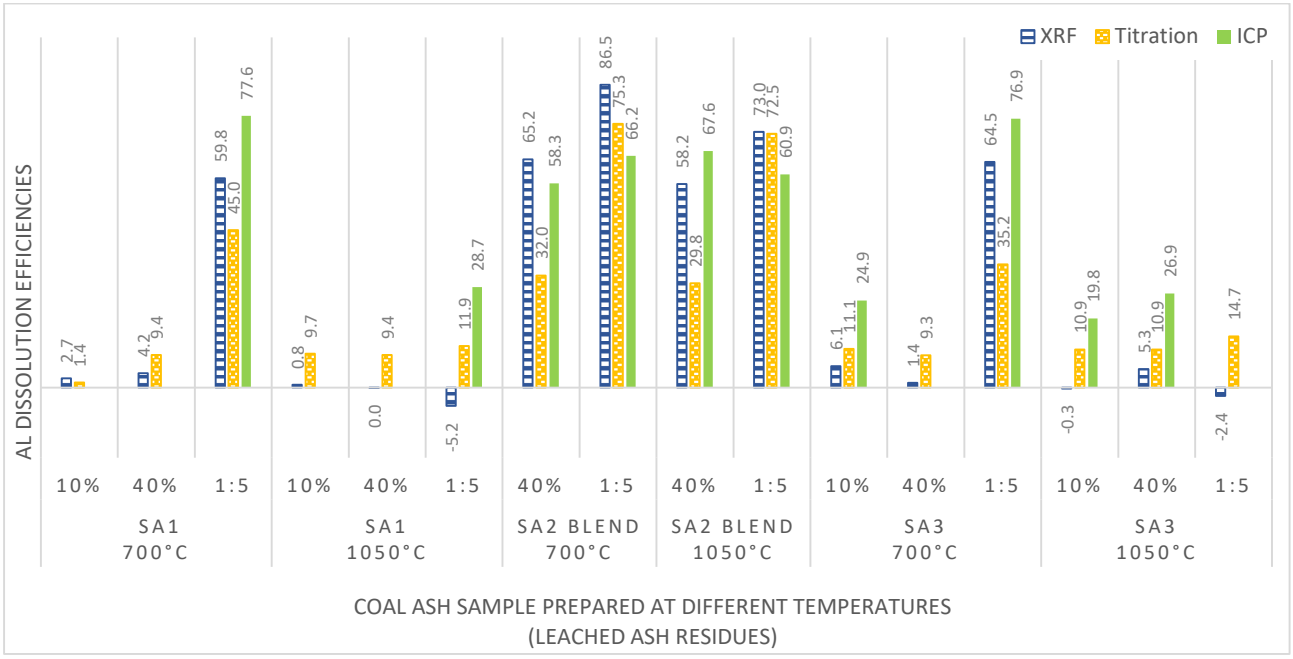

Figure 4-6: Comparison of different techniques used to determine Al dissolution efficiencies

4.4 Conclusion

The dissolution of Al, K, and Ti bearing inorganic compounds from laboratory-produced coal ash, by means of sulphuric acid leaching, was investigated. From the results obtained, leaching the SA1 ash samples prepared at 700°C and 1050°C, with 1.02 M and 4.08 M H_2SO_4 solutions, yielded dissolution efficiencies <5% for Al and ±17% for K; with the dissolution efficiency for Ti approximately ±17% for the ash sample prepared at 700°C, and <15% for the ash prepared at 1050°C. The low dissolution efficiencies observed were caused by the formation of gelatinous calcium sulphate and silicic acid precipitates; which lead to insufficient sulphuric acid to react with the Al- and K containing compounds. XRD analysis of the ash residues detected sulphuric acid-soluble compounds, which included potassium alum, potassium carbonate and amorphous materials (potassium aluminosilicate glass, metakaolinite and potassium melt). The XRD analysis results also indicated the concentrations of compounds insoluble in sulphuric acid such as potassium/calcium aluminium silicates (anorthites), mullite and calcium sulphate salts. The SA3 ash samples, prepared at 700°C and 1050°C and leached with the 1.02 M and 4.08 M H_2SO_4 solutions, showed similar trends in the dissolution efficiencies of Al, K, and Ti as seen for the SA1 ash samples. The dissolution efficiencies of Al, K, and Ti determined for the SA3 ash samples were <10%; with the exception of potassium in the ash prepared at 1050°C (±45%). This would suggest that acid-soluble potassium salts, potassium melt, potassium in the aluminosilicate glass, or metakaolinite phase reacted with sulphuric acid, resulting in higher dissolution efficiencies. Leaching the SA2 blend ash samples (prepared at 700°C and 1050°C) with the 1.02 M H_2SO_4 solution was not successful due to reactions between the sulphuric acid and Ca-containing compounds; which lead to the formation of gelatinous precipitates. The high viscosity of these gelatinous materials in solution made filtering and analysis of the ash residue and leach liquor impossible. The SA2 blend ash samples, prepared at 700°C and 1050°C and leached with the 4.08 M H_2SO_4 solution, yielded dissolution efficiencies up to 65% Al and 84% K. The increase in sulphuric acid concentration lead to digestion of gelatinous precipitates that may have formed.

Due to low dissolution efficiencies obtained from low sulphuric acid concentration leaching; leached parameters were changed and investigated. Leaching the SA1 ash sample prepared at 700°C, with the 6.12 M H_2SO_4 solution using 1:5 and 1:10 S/L ratios, yielded moderately high Al dissolution efficiencies of 59% and 56% respectively; while dissolution efficiencies observed for K were 54% and 42.9% respectively. The dissolution efficiencies obtained were due to an increase in sulphuric acid concentration, and subsequently an increase in sulphate ion present in the aqueous phase (low pH values); which lead to the formation of soluble compounds. The dissolution efficiencies of titanium determined were <20% when 1:5 and 1:10 S/L ratios were used. Leaching the SA1 ash prepared at 1050°C with the 6.12 M H_2SO_4 solution using 1:5 and 1:10 S/L ratios, dissolution efficiencies <10% for Al, K, and Ti were observed. This is due to the formation of more stable mineral

phases (mullite, anorthite, Na/K- feldspar) and the presence of anatase/ rutile in the ash samples. This same trend in Al, K, and Ti dissolution efficiencies observed for the SA1 ash samples could be applied to the SA3 ash samples, with similar values. High dissolution efficiencies for Al and K were obtained by leaching the SA2 blend ash with the 6.12 M H_2SO_4 solution and 1:5 and 1:10 S/L ratios. The SA2 blend ash prepared at 700°C yielded Al dissolution efficiencies of 86.5% and 82.2%, and 88.9% and 91% for K when leached with the 1:5 and 1:10 S/L ratios, respectively. High dissolution efficiencies of these elements can be attributed to the metakaolinite, amorphous potassium species, potassium carbonate and potassium aluminium sulphate; which are soluble in the sulphuric acid solutions. Titanium dissolution efficiencies were determined to be <25% when leached under these conditions. This trend in the dissolution of Al, K, and Ti from the ash prepared at 700°C was also observed for the ash prepared at 1050°C, with high Al and K dissolution efficiencies.

The ICP-OES digestion results correlated with the dissolution efficiencies determined for aluminium from the XRF results. However, discrepancies were found when this analysis method was used to determine the concentration of potassium and titanium in solution. Complexometric titration of the leach liquor solutions supported the trend of aluminium dissolution from the ash samples, if not the exact percentages. These observations on the ICP-OES digestion and complexometric titration results were observed for all the leaching experiments investigated in this paper. The accuracy of these analytical analyses methods may be questioned, due to the possibility of human error during sample preparation, experimental steps, and judgement calls.

The recovery of aluminium and potassium compounds from coal ash, and also ash with a potassium additive, is possible with sulphuric acid leaching. These compounds produced during the leaching experiments can be utilized in a variety of industrial applications such as fertilizer, water treatment, or chemical industries.

Chapter 5

Ammonium sulphate sintering of South African combustion ash: Recovery of Al, K, and Ti from laboratory prepared ash

Anna C. Collins, Christien A. Strydom, Ratale H. Matjie,
John R. Bunt, Johannes C. van Dyk

The dissolution of Al-, K-, and Ti bearing mineral phases from the sintered ash residue formed after ammonium sulphate sintering process is discussed in this chapter. The ash was produced by low-temperature combustion of South African coals. The influence of an added potassium compound on the dissolution of Al, K, and Ti from the sintered ash residue was also investigated

Abstract

The aim of this investigation was to determine if aluminium, present in the amorphous material and crystalline phases along with potassium and titanium in the glassy phases, could be recovered by subjecting low-temperature combustion ash to an ammonium sulphate sintering procedure. The ash used in the investigation was prepared from South African coal samples at a temperature of 700°C. Characterization of the two coal samples showed similar ash yields (28%) and volatile content. XRF analysis of the coal samples indicated similar Al_2O_3 percentages (25%-28%), but differing in basic compound content. The SA1 sample contained 1.5% CaO and 0.7% K_2O, while the SA2 blend sample, to which a potassium compound was added, contained 11% CaO and 19% K_2O. Sintering the coal ash samples with $(NH_4)_2SO_4$ yielded dissolution efficiencies of 43.4% Al and 56% K for the SA1 ash sample. This was due to the formation of soluble ammonium/potassium aluminium sulphates. Sintering the SA2 blend (SA2 ash + K_2CO_3) with the $(NH_4)_2SO_4$, yielded dissolution efficiencies of 29% Al and 59% K. The lower dissolution efficiency value observed for the SA2 blend ash sample was due to the formation of potassium aluminium silicates (potassium-alum); which was insoluble in this specific dissolution procedure. By using another dissolution procedure, potassium-alum could be leached from the ash residue, thus increasing the overall dissolution efficiencies for Al and K. Due to the stable and unreactive nature of Ti-bearing mineral phases, no dissolution of Ti took place. The dissolution efficiency values obtained for Al and K, indicate ash derived through coal fines could be used for the recovery of these elements.

Keywords: potassium, aluminium, titanium, ammonium sulphate, sintering, low-temperature ash

5.1 Introduction

Bauxite deposits are the main source material from which aluminium is extracted and distributed worldwide. The decrease in bauxite deposits has prompted the search for alternative source material from which alumina could be recovered (Wang *et al.*, 2014b). Coal ash and fly ash, consisting mainly of alumina and silica (Li *et al.*, 2012), is such a source material (Barry *et al.*, 2018), containing up to 55% Al_2O_3 depending on the coal source (Blissett & Rowson, 2012; Vassilev & Vassileva, 2007); and is considered a waste product produced by coal combustion. Using coal ash, either from power plants or produced from coal fines, or coal fly ash as an aluminium source can have a positive financial influence since bauxite ore has to be imported (van der Merwe *et al.*, 2017; Xu *et al.*, 2016).

Ammonium sulphate sintering of coal ash or coal fly ash is a recovery method considered to be less corrosive than acid or alkaline leaching procedures, with fewer waste products produced (Wu *et al.*, 2014). The ammonium sulphate sintering process and subsequent dissolution of the sintered ash residue is a non-selective extraction method which may lead to the extraction of other elements found in the ash sample. van der Merwe *et al.* (2017) found that the sintering temperature had the largest influence on the sulphate mineral phases. Other factors that may influence the extraction of aluminium from the coal ash or coal fly ash was particle size, the ash preparation temperature, specific mineral content, and ammonium sulphate: ash ratio used (Wu *et al.*, 2014). According to Li *et al.* (2012), ammonium sulphate is needed in excess during the sintering process because it is a solid phase reaction. During the sintering process, the ammonium sulphate reacts with the alumina (glassy phase) in the ash sample, which leads to the formation of soluble ammonium aluminium sulphate and aluminium sulphate (Wu *et al.*, 2014).

Li *et al.* (2012) found a 95% aluminium extraction efficiency after sintering the coal fly ash and ammonium sulphate and subjecting the sintering residue to the dissolution process. Doucet *et al.* (2016) achieved a 95% aluminium extraction from the glassy phase in ultra-fine coal fly ash. Doucet *et al.* (2016) also found that increased sintering temperature (above 500°C), coupled with increased Al extraction, showed decreased extraction of elements such as Ca, Ti and Fe. Hanxu *et al.* (2006) reached an aluminium extraction of 91% by sintering coal fly ash with a ammonium sulphate and sulphuric acid mixture.

Potassium carbonate is a known catalyst used during gasification and combustion of coal (Tang & Wang, 2016). The potassium carbonate was added to one of the coal samples prior to ash preparation. The aim of this investigation was to determine the dissolution of aluminium from the amorphous material and glassy phases present in low-temperature combustion ash. The influence of the added potassium carbonate on the extraction of aluminium was also investigated. The sintering and dissolution conditions used in this investigation was as described by Doucet *et al.* (2016), with minor changes to some of the conditions. Analytical techniques such as XRF and XRD

were utilized in the determination of the dissolution efficiencies after the ash samples had been subjected to the sintering and dissolution procedures. The inorganic elements, Al and K, can be converted to the desired products through various analytical methods (Doucet *et al.*, 2016); while the ash residue left after the dissolution process could be used in brick manufacturing.

5.2 Material and Methods

5.2.1 Coal Samples

Two medium volatile bituminous South African coal samples were used during this investigation. The coal samples were collected from different coal mines within the Mpumalanga region. The coal samples will be identified as "SA1" and "SA2" in the discussions that follow. Using standardized procedures (ISO 1988:1975 and ISO 139094:2016), the coal was sampled and collected at the respective mines; and a representative sample of 20 kg was used. Coal selection was based on the aluminium and potassium contents of each sample; which was determined through characterization of the ash samples produced from the coals. The coal rank was determined using the ASTM D388-12 classification standard.

5.2.2 Sample Preparation

5.2.2.1 Coal Samples

The coal samples were air-dried for 2 days to ensure evaporation of the excess moisture, i.e. moisture not associated with the coal structure. The coal sample was crushed with a crusher followed by crushing with a ball mill to obtain a particle size of <1 mm. This was done to each of the coal samples investigated. A blended sample was prepared by adding potassium carbonate (10 wt.% K_2CO_3) to the SA2 coal sample. Addition of the compound was done during the milling step, to ensure that a homogenous mixture was obtained. This blended sample will be identified as "SA2 blend" in the discussions that follow. The potassium was added to the coal sample to determine the recoverability of potassium after thermal processing, and whether the added potassium salt will influence the recovery of other the inorganic elements investigated.

5.2.2.2 Ash Samples

The coal samples were subjected to thermal processing in order to obtain the ash samples at the desired temperatures. Each of the coal samples was split into four 5 kg sub-samples; which were then individually placed into the hot zone of a rotary kiln. Clay fired trays were used as sample holders. The temperature of the kiln was increased to 700°C while using a heating rate of 10°C/ min. A residence time of 3 hours was set; while thermal processing was conducted under airflow conditions. This was to facilitate combustion of the organic components and evolution of volatile matter. After the residence time had been reached, the furnace was switched off; to which the cooling rate was generally the natural cooling of the furnace. The sub-samples were removed from

the furnace and blended to form a homogenous ash sample. This was done for each of the coal samples investigated.

5.2.3 Analytical Methods

5.2.3.1 Ultimate and Proximate Analysis

Characterization analyses of the coal samples used in this investigation were done according to specific ISO standardized methods. The characterization methods and corresponding ISO standard numbers are presented in Table 5-1.

Table 5-1: Characterization methods and ISO standard identification number

Analysis method	Standard Number
Solid mineral fuels: Determination of moisture in general analysis test sample by drying in nitrogen	ISO 11722: 2013
Solid mineral fuels: Determination of ash	ISO 1171: 2010
Hard coal and coke: Determination of volatile matter	ISO 562: 2010
Fixed carbon	By calculation
Determination of total carbon, hydrogen and nitrogen content – international method.	ISO 29541: 2010
Oxygen content by calculation	

5.2.3.2 X-Ray Fluorescence (XRF) Analysis

Coal samples subjected to XRF analysis were ground until all particles could pass through a 75 µm sieve. Calcination of the powdered samples was conducted at 1000°C under airflow, with a residence time of 3 hours. This was done to remove all moisture and organic compounds, which might be present in the sample. After the calcination step, a solid solution was prepared by fusion of the calcined samples with lithium tetraborate: lithium metaborate (67:33). This solid solution, prepared from the calcined powder and the standard, was added into the casting dish with the measurement of 32 mm. The prepared fused beads (32 mm) were placed into the sample compartment of the XRF spectrometer (WROXI from PANalytical). The analysis was done according to the method proposed by Norrish and Hutton (1969). Results obtained from this analysis method are expressed as percentages of the major elemental oxides present in each sample. The concentration of the specific elements present in the ash sample was calculated from the intensity of the spectral lines recorded by the analyser. These concentrations measured are expressed as elemental oxides.

5.2.3.3 X-Ray Diffraction (XRD) Analysis

Samples subjected to XRD analysis were ground to a particle size <75 µm with the use of a laboratory scale ball mill. The powdered samples and those containing the silicon standard were placed into sample holders. These holders were filled with the powdered sample, and the surplus removed with the use of a glass slide (50X70 mm and 5 mm thick). Simultaneous compression of the sample into the sample holder takes place as the excess sample is removed (Matjie, 2008). This step was repeated until a smooth surface of even texture was obtained. Each solid sample was

spiked with 20% Si (Aldrich, 99.9% purity) and was subsequently micronized in a McCrone micronizing mill. XRD analysis of the coal and ash samples were done using an X'Pert PRO PANalytical (Philips) – Unit 2 diffractometer system with Co Kα radiation. Identification of the minerals present in the powdered samples was done with reference to the International Center for Diffraction Data (ICDD) Powder Diffraction File. Amorphous and crystalline phases in the powdered samples were identified and quantified with X'Pert Highscore plus software (Speukman, 2012) and the Rietveld method (Rietveld, 1969).

5.2.4 Experimental Methods

A schematic representation of the experimental- and analytical procedures used during this investigation on ammonium sulphate sintering of coal ash is presented in Figure 5-1.

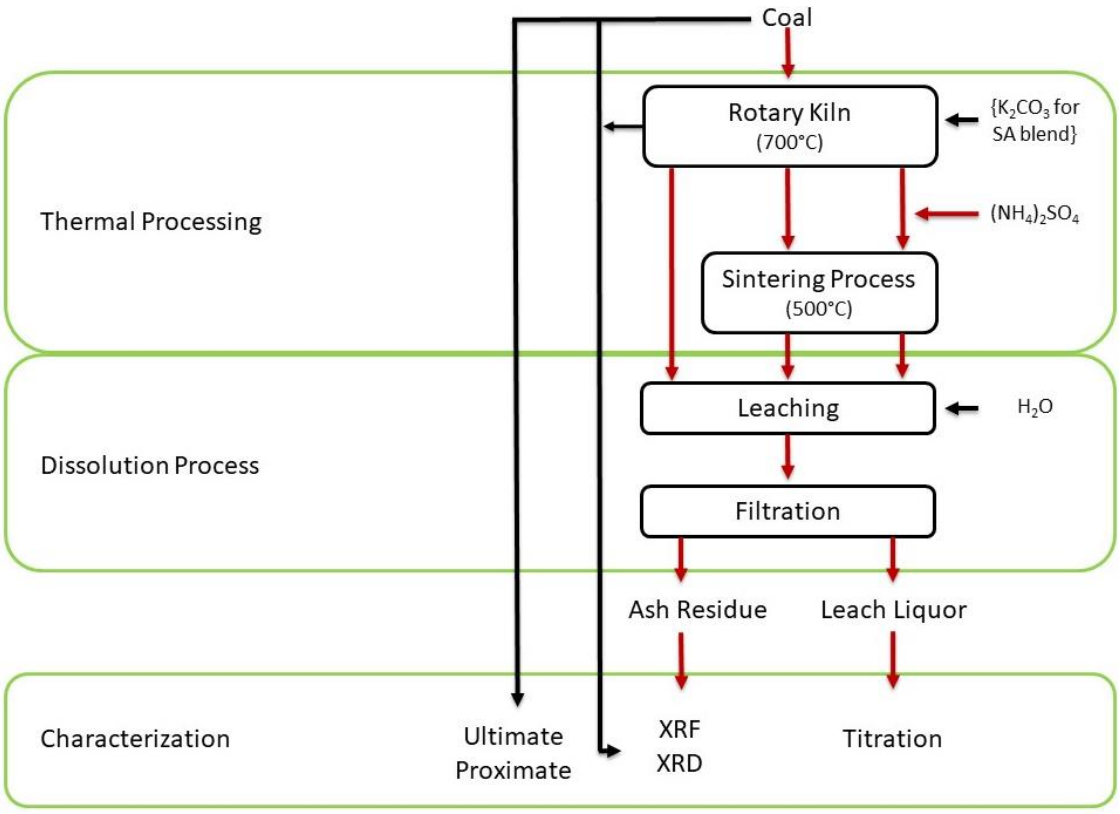

Figure 5-1: Schematic representation of the experimental- and analytical procedures used during ammonium sulphate sintering and dissolution processes

5.2.4.1 Sintering and Dissolution Experiments

5.2.4.1.1 Sintering Procedure

The coal ash and ammonium sulphate salt were mixed (manually) until a homogenous mixture was obtained. A mixture ratio of 2:6, coal ash: $(NH_4)_2SO_4$, was used during the experimental procedure. The ash-and-ammonium sulphate salt mixture was placed into deep crucibles; which were positioned in the middle of a muffle furnace. The temperature of the furnace was increased to 500°C at a heating rate of 10°C/ min. Doucet *et al.* (2016) found that these parameters yielded good aluminium extraction results. The residence time for the samples in the muffle furnace was set for 6 hours (360

min). After this allotted time was reached, the furnace was switched off and left to cool until ambient temperature. Visual analysis of the samples when removed from the furnace, showed that a sintered residue was formed. The sample was removed from the crucibles, weighed, and subjected to the dissolution procedure (Section 5.2.4.1.2). The sintering procedure was also done on the coal ash samples, without the addition of the ammonium sulphate salt. This was to serve as one of the controls.

5.2.4.1.2 Dissolution Procedure

The dissolution experiments on the sintered residue were done by stirring the ash or sintered ash residues with deionized water. A 500 ml round-bottomed container, with sealing lid and cooler, was used as a leaching vessel. An automatic overhead stirrer with a base plate (DESC 20 L) model 720, coupled with a temperature controller with a sensor probe, was used as a heat source. Deionized water was added to the ash or sintered ash residues in a solid to liquid ratio of 1 g: 50 ml. The mixture in the leaching vessel was stirred for 18 hours. The leaching time was chosen to ensure dissolution of all aqueous soluble compounds. Separation of the leached residue and aqueous solution was done by means of vacuum filtering. The ash residue was washed with 60 ml of deionized water to remove residual soluble compounds. The ash residue was placed in a vacuum oven and dried overnight at 60°C. The dried residues were characterized by XRF and XRD analyses. The dissolution procedure was applied to the sintered ash residues, both with and without the ammonium sulphate salt, and also on the original ash sample.

5.2.4.2 Dissolution Efficiencies

The solubility of inorganic compound(s) into a specific solution can be determined by the dissolution efficiencies; which in turn can be determined through various analytical analyses. The dissolution efficiencies for the inorganic elements Al, K, and Ti investigated, was calculated from the XRF analysis results of the coal ash and ash residue samples. The following equation was used:

$$\eta(MO) = \frac{m(MO)_{CA} - m(MO)_{RES}}{m(MO)_{CA}} \times 100\% \quad (5\text{-}1)$$

where η(MO) represents the Al, K, or Ti dissolution efficiency, $m(MO)_{CA}$ and $m(MO)_{RES}$ the mass (Equation 5-2) of the inorganic element in the coal ash and ash residue, respectively (Jiang *et al.*, 2015). The mass of the specific inorganic element in the coal ash and ash residue samples can be determined as follow:

$$\boldsymbol{m(MO)_{ash} = (\frac{\%E}{100}) \times m_{sample}} \quad (5\text{-}2)$$

where $m(MO)_{ash}$ is the mass (g) of inorganic element (Al, K, or Ti) in the coal ash or ash residue; %E the percentage of the inorganic element in the coal ash or ash residue, as determined by Equation 5-3; and m_{sample} the mass of the ash sample or ash residue. The percentage (%E) of the inorganic element in each of the ash and ash residue samples was determined with the following equation:

$$\%\boldsymbol{E} = \%\boldsymbol{EO} \times \frac{\boldsymbol{M_{element}}}{\boldsymbol{M_{EO}}} \quad (5\text{-}3)$$

with %E the percentage of the element in the coal ash or ash residue sample; %EO the percentage elemental oxide in the sample (provided through XRF analysis); $M_{element}$ the molecular weight of the element in the oxide and M_{EO} the molecular weight of the elemental oxide.

5.3 Results and Discussion

5.3.1 Coal composition

The proximate and ultimate analyses, of the coal samples used in this investigation, are presented in Table 5-2. The proximate results are reported on an air-dried basis showed moisture contents <5% for all coal samples. This was coupled with high ash yields (>25%) and volatile contents (>18%). The fixed carbon contents ranged between 45% and 51% for the different samples.

Ultimate analysis of the coal samples are reported on a dry-ash-free basis, indicated carbon contents ranging between 79% and 83%, and oxygen contents between 10% and 13%. Hydrogen, nitrogen, and sulphur contents were <5% in all the coal samples investigated. The proximate and ultimate analysis results obtained for the coal samples used in this investigation are consistent with results reported for other South African coal samples (Hattingh *et al.*, 2011; van Alphen, 2005; van Dyk *et al.*, 2009b).

Table 5-2: Ultimate and Proximate analyses results of the coal samples

Sample	*SA1*	*SA2*	*SA2 Blend*
Proximate Analysis (air-dried basis)			
Moisture content (%)	3.3	3.7	4.6
Ash yield (%)	28.3	28.5	26.8
Volatile content (%)	18.2	21.3	21.5
Fixed Carbon (%)	50.2	46.5	47.1
Ultimate Analysis (dry-ash-free basis)			
% Carbon Content	82.3	79.2	79.6
% Hydrogen Content	4.4	3.8	4.9
% Nitrogen Content	1.8	1.9	1.9
% Oxygen Content	10.8	13.2	12.4
% Sulphur Content	0.7	1.9	1.2

5.3.2 XRF and XRD analyses of the coal samples

The XRF results for the coal samples are presented in Table 5-3. The analysis was done on the ash samples produced at 1000°C, from these coal samples. The results are reported as elemental oxides and presented on a normalized basis. The results show that silicon oxide percentages ranging from 37% to 63%; with aluminium oxide percentages ranging between 22% and 29%. Significant percentages of iron, sulphur, and calcium were observed in the SA2 sample, with percentages exceeding 7% for sulphur trioxide and 10% for calcium dioxide. The high potassium oxide percentage seen for the SA2 blend sample is expected; as this is due to the spiking of the

sample with K_2CO_3 before analyses. The results obtained, with the exception of the coal sample spiked with the K_2CO_3, are in good agreement with XRF results determined for ash samples prepared from other South African coal samples (Hattingh *et al.*, 2011; Matjie *et al.*, 2008; van Alphen, 2005; van Dyk *et al.*, 2008b; van Dyk *et al.*, 2009b).

Table 5-3: Normalized XRF results (wt.%) for the coal samples (ash prepared at 1000°C)

Sample	*SA1*	*SA2*	*SA2 Blend*
SiO_2	63.2	41.6	37.7
Al_2O_3	28.5	25.2	22.3
CaO	1.5	13.0	11.1
SO_3	1.5	7.6	-
Fe_2O_3	2.0	5.6	4.2
MgO	0.8	3.2	2.1
TiO_2	1.5	1.8	1.7
K_2O	0.7	1.1	18.9
P_2O_5	0.1	0.3	0.3
SrO	-	0.3	-
BaO	-	0.2	-
Cr_2O_3	0.1	-	0.3
Na_2O	-	-	0.7

The XRD analysis results determined for the coal samples are presented in Table 5-4. The results indicate that the coal samples primarily consist of amorphous material (organic carbon), with values exceeding 66%. The crystalline mineral phases present in the SA1 sample were 18% kaolinite, 10.6% quartz, and small percentages of crystalline phases such as microcline, illite, calcite, pyrite, anatase. The SA2 and SA2 blend samples showed similar composition trends. The SA2 blend (a mixture of K_2CO_3 and SA2) contained kaolinite (14%), dolomite (6.5%), and calcite (3.2%) phases, and small quantities of other mineral phases. The XRD results determined for the coals evaluated in this investigation are in agreement with previous XRD data reported for other South African coals (Matjie *et al.*, 2008; van Alphen, 2005; van Dyk *et al.*, 2009b).

Table 5-4: XRD results (wt.%) for the coal samples

Sample	*SA1*	*SA2*	*SA2 Blend*
Amorphous/organic carbon	66.2	71.4	67.9
Anatase	0.4	-	0.3
Calcite	-	2.5	3.2
Dolomite	1.3	6.2	6.5
Graphite	1.9	0.8	-
Illite	0.8	1	3.6
Kaolinite	18	13.8	14
Microcline	0.7	0.2	-
Muscovite	-	-	0.1
Pyrite	0.1	0.2	0.1
Quartz	10.6	3.8	4

5.3.3 Analyses of ash and ash residue samples

5.3.3.1 Ash analyses results

The XRF results for the SA1 ash sample in Table 5-5, showed that the chemical composition for the sample was mainly comprised of SiO_2 (62.1%) and Al_2O_3 (28.3%). The other oxide compounds present in the sample were <3%. The XRD results in Table 5-5 indicate that the ash sample consisted of 46.7% amorphous material (metakaolinite ($Al_2O_3.2SiO_2$)) and 44.3% quartz (SiO_2). This is supported by Bunt *et al.* (1998), where coal fines were subjected to thermal processing in a rotary kiln at 600°C. The coal ash produced was comprised of metakaolinite along with other crystalline phases.

The XRF results for the SA2 blend (mixture of K_2CO_3 and SA2) ash sample in Table 5-5 showed that the ash sample was comprised of SiO_2 (36.3%), Al_2O_3 (22.6%), and K_2O (18.4%). The high potassium oxide value observed, is due to the addition of potassium carbonate to the coal before thermal processing. The XRD results showed that the ash is mainly comprised of amorphous material (74.8%). Small percentages of crystalline phases such as quartz (3.9%), anorthite (8.3%), and diopside (4.5%) were present. CaO (transformed product of calcite/dolomite associated with kaolinite) can react with metakaolinite to form anorthite, while diopside was formed from amorphous silica reacting to give high-temperature carbonate products (calcite or dolomite) (Matjie, 2008). Metakaolinite is the transformed product of kaolinite when coal is subjected to thermal processing.

Table 5-5: XRD (normalized) and XRD results (wt.%) for the coal ash samples prepared at 700°C

Sample	*SA1*	*SA2 Blend*	*Sample*	*SA1*	*SA2 Blend*
SiO_2	62.1	36.3	Amorphous	47.6	74.8
Al_2O_3	28.3	22.6	Quartz	44.3	3.9
CaO	2.7	8.9	Anhydrite	1.6	1.3
Fe_2O_3	2.7	4.1	Mullite	1.5	-
TiO_2	2.1	1.7	Hematite	1.4	1.3
MgO	0.9	2.3	Anorthite	1.2	8.3
K_2O	0.8	18.4	Portlandite	0.4	0.2
SO_3	0.2	4.4	Magnetite	0.2	-
Cr_2O_3	0.1	0.1	Cristobalite	0.1	0.1
Mn_3O_4	0.1	0.1	Gypsum	-	0.6
P_2O_5	0.1	0.2	Graphite	-	2
BaO	-	0.4	Diopside	-	4.5
Na_2O	-	0.1	K_2CO_3	-	0.9
SrO	-	0.3	Kaolinite	-	0.6
			Pyrrhotite	-	0.3

5.3.3.2 H_2O Dissolution of the coal ash samples

The XRF and XRD results obtained after the SA1 and SA2 blend ash samples had been subjected to the dissolution procedure (Section 5.2.4.1.2), are presented in Table 5-6. Subjecting the SA1 ash sample to the dissolution procedure, produced an ash residue resembling that of the original ash sample (Table 5-5), as determined with XRF analysis. The changes in the XRF results were <2%, which might be caused by the dissolution of small percentages of aqueous soluble compounds. The XRD results showed a decrease in the quartz concentration from 44.3% to 29.8% after leaching the SA1 ash sample. This decrease was accompanied by an increase in the amorphous material from 47.6% to 62.2%. Other changes in the mineral composition were <5%.

The XRF results for the SA2 blend (mixture of K_2CO_3 and SA2) ash residue, showed an increase in SiO_2 concentration from 36.3% to 43.4% and Al_2O_3 concentration from 22.6% to 25.8%. The increases seen in alumina and silica concentration may be due to decreases in the following concentrations; K_2O from 18.4% to 14% (as given in equation 5-4), CaO from 8.9% to 8.2%, MgO from 2.3% to 1.6%, and SO_3 from 4.4% to 0.3 (as given in equation 5-5). The XRD results showed an increase in calcite concentration from 0% to 6.8%, a decrease in amorphous material from 74.8% to 69.9% and diopside from 4.5% to 2.1%.

$$K_2CO_3 + 2H_2O \rightarrow 2KOH + H_2O + CO_2 \quad (5\text{-}4)$$

$$SO_3 + H_2O \rightarrow H_2SO_4 \quad (5\text{-}5)$$

Table 5-6: XRF (normalized) and XRD results (wt.%) for the ash residues after H_2O dissolution

Sample	*SA1*	*SA2 Blend*	*Sample*	*SA1*	*SA2 Blend*
SiO_2	61.1	43.4	Amorphous	62.3	69.9
Al_2O_3	28.5	25.8	Quartz	29.8	5.4
K_2O	0.7	14.0	Calcite	0.6	6.8
Fe_2O_3	4.7	3.8	Anorthite	0.5	8.7
TiO_2	1.7	2.1	Hematite	3.7	3.7
CaO	2.2	8.2	Silimanite	-	0.2
MgO	-	1.6	Rutile	0.2	0.1
SO_3	0.3	0.3	Pyrrhotite	-	0.2
BaO	0.5	0.2	Portlandite	-	0.1
SrO	-	0.3	Periclase	0.1	0.5
Mn_3O_4	-	0.1	Mullite	-	1
P_2O_5	0.1	0.3	Magnetite	0.2	0.1
ZrO_2	0.1	-	Maghemite	0.3	-
Cr_2O_3	0.1	-	Kaolinite	0.2	-
			Illite	1.3	-
			Diopside	-	2.4
			Cristobalite	-	0.4
			Anhydrite	0.1	0.1
			Anatase	0.7	0.2

5.3.3.3 Sintering and dissolution of coal ash – without $(NH_4)_2SO_4$

The XRF and XRD results for the SA1 and SA2 blend ash samples, after sintering and dissolution experiments, are presented in Table 5-7. The ash composition provided by XRF analysis of the SA1 ash residue resembled the composition of the original ash sample used (Table 5-5). This suggests that sintering of the ash did not have an influence on its composition. The XRD results showed a decrease in quartz concentration from 44.3% to 29.9%, accompanied by an increase in the amorphous material from 47.6% to 63.1%.

The XRF results for the SA2 blend (mixture of K_2CO_3 and SA2) ash residue showed an increase in the SiO_2 concentration from 36.6% to 41.7% and Al_2O_3 concentration from 22.6% to 25%. These observed increases resulted from the decrease in K_2O concentration from 18.4% to 15.8% (Equation 5-4) and SO_3 from 4.4% to 0.4% (equation 5-5); as these components are soluble in aqueous solution. The XRD results showed a decrease in amorphous material from 74.8% to 59.9% with a corresponding increase in calcite concentration from 0% to 14.3%. The increase in calcite concentration may be due to reactions between unreacted K_2CO_3 and Ca-containing compounds during the sintering process. Minor changes (<5%) in the other mineral phases present in the ash sample was also observed.

Table 5-7: XRF (normalized) and XRD results (wt.%) for the ash residues after sintering and H_2O dissolution

Sample	*SA1*	*SA2 Blend*	*Sample*	*SA1*	*SA2 Blend*
SiO_2	60.7	41.7	Amorphous	63.1	59.9
Al_2O_3	28.1	25.0	Quartz	29.9	8.4
K_2O	0.7	15.8	Calcite	0.5	14.3
Fe_2O_3	4.7	3.8	Anorthite	-	8.9
TiO_2	1.7	2.0	Hematite	3.8	5.5
CaO	2.0	8.7	Rutile	0.1	-
MgO	0.8	1.6	Pyrrhotite	-	0.3
SO_3	0.5	0.4	Periclase	0.1	0.7
BaO	0.5	0.2	Mullite	-	0.9
SrO	-	0.3	Mascagnite	0.1	-
Mn_3O_4	-	0.1	Magnetite	0.2	0.4
P_2O_5	0.1	0.3	Kaolinite	0.1	-
ZrO_2	0.1	-	Illite	1.5	-
Cr_2O_3	0.1	-	Cristobalite	-	0.5
			Anhydrite	-	0.1
			Anatase	0.5	-

5.3.3.4 Sintering and dissolution of coal – with $(NH_4)_2SO_4$ addition

The XRF and XRD results for the SA1 and SA2 blend ash samples; after $(NH_4)_2SO_4$ addition, sintering, and dissolution experiments, are presented in Table 5-8. The XRF results for the SA1 ash residue showed a similar composition as that observed in the original ash sample (Table 5-5). The XRD results showed an increase in amorphous material from 47.6% to 61.1%, with a decrease in the quartz concentration from 44.3% to 34%. The increase in amorphous material concentration may be due to the formation of gelatinous calcium sulphate, as ammonium sulphate reacts with the calcium bearing minerals during the sintering process. These mineral phases form part of the amorphous material.

Possible reactions of ammonium sulphate as given by Wu *et al.* (2014) (5-6) and Bayer *et al.* (1982) (5-7 to 5-9), are presented below:

$$4(NH_4)_2SO_4 + Al_2O_3 \rightarrow 2NH_4Al(SO_4)_2 + 6NH_3 + 3H_2O \quad (5\text{-}6)$$

$$Al_2O_3{\cdot}2SiO_2{\cdot}2H_2O + 6(NH_4)_2SO_4 \rightarrow 2(NH_4)_3Al(SO_4)_3 + 2SiO_2 + 6NH_3 + 5H_2O \quad (5\text{-}7)$$

$$2(NH_4)_3Al(SO_4)_3 \rightarrow 2(NH_4)Al(SO_4)_2 + 4NH_3 + 2H_2O + 2SO_2 + O_2 \quad (5\text{-}8)$$

$$2(NH_4)Al(SO_4)_2 \rightarrow Al_2(SO_4)_3 + 2NH_3 + H_2O + SO_2 + \tfrac{1}{2}O_2 \quad (5\text{-}9)$$

$$Al_2O_3 + (NH_4)_2SO_4 \rightarrow Al_2(SO_4)_3 + (NH_4)_2O \quad (5\text{-}10)$$

$$Al_2(SO_4)_3 + 6H_2O \rightarrow 2Al(OH)_3 + 3H_2SO_4 \quad (5\text{-}11)$$

The XRF results for the SA2 blend ash sample; after $(NH_4)_2SO_4$, sintering, and dissolution experiments, an increase in SiO_2 concentration from 36.3% to 54.7% was observed. The increase in SiO_2 is due to the decreases in Al_2O_3 concentration from 22.6% to 19.2% (Equation 5-1, Equation 5-10), decrease in K_2O concentration from 18.4% to 9.1% (Equation 5-12, Equation 5-14), and decrease in CaO concentration from 8.9% to 3.9% (Equation 5-15). The XRD results showed a decrease in the amorphous material from 74.8% to 51.2%, a decrease in anorthite concentration from 8.3% to 1.1%, and diopside concentration from 4.5% to 0%. These decreases were mainly due to the formation of potassium-alum, as an increase in this mineral phase concentration from 0% to 38% was observed.

Possible reactions for the dissolution of potassium and calcium from the ash sample are:

$$(NH_4)_2SO_4 + K_2CO_3 \rightarrow (NH_4)_2CO_3 + K_2SO_4 \quad (5\text{-}12)$$

$$K_2SO_4 + H_2O \rightarrow H_2SO_4 + KOH \quad (5\text{-}13)$$

$$(NH_4)_2SO_4 + H_2O \rightarrow H_2SO_4 + NH_4O \quad (5\text{-}14)$$

$$H_2SO_4 + K_2CO_3 \rightarrow K_2SO_4 + CO_2 + H_2O \quad (5\text{-}15)$$

$$H_2SO_4 + CaO + H_2O \rightarrow CaSO_4.2H_2O \quad (5\text{-}16)$$

Table 5-8: XRF (normalized) and XRD results for the ash residues after sintering (with $(NH_4)_2SO_4$) addition and H_2O dissolution

Sample	*SA1*	*SA2 Blend*	*Sample*	*SA1*	*SA2 Blend*
SiO_2	64.2	54.7	Amorphous	61.1	51.2
Al_2O_3	27.3	19.2	Quartz	34	5.7
K_2O	0.6	9.1	Anorthite	0.3	1.1
Fe_2O_3	5.2	4.4	Potassium-alum	-	38
TiO_2	1.8	2.6	Hematite	1.9	0.5
CaO	0.3	3.9	Sodalite	0.1	-
MgO	-	0.5	Silimanite	-	0.1
SO_3	-	5.1	Periclase	0.1	-
BaO	0.3	-	Mullite	-	-
SrO	-	0.1	Mascagnite	0.2	0.8
Mn_3O_4	-	-	Magnetite	0.1	-
P_2O_5	0.1	0.4	Maghemite	0.1	-
ZrO_2	0.1	-	Kaolinite	0.4	-
Cr_2O_3	0.1	-	Illite	1.7	1.4
			Dolomite	-	0.3
			Anhydrite	-	0.9
			Anatase	0.2	-

5.3.4 Dissolution efficiencies of Al, K, and Ti as determined by XRF analysis

The dissolution efficiencies of Al, K, and Ti as determined from the XRF results of the coal ash and ash residues (obtained after dissolution experiments), are presented in Figure 5-2. The calculation method used to determine the dissolution efficiencies is described in Section 5.2.4.3.2. Subjecting the SA1 ash sample to the dissolution procedure, showed dissolution efficiencies of 2.8% Al, 15.6% K, and 21.9% Ti. The dissolution percentages seen suggests the presence of aqueous soluble compounds in the ash; while titanium may have been present in non-crystalline phases. The SA2 blend had a potassium dissolution efficiency of 30% after dissolution of the ash sample. This indicates that unreacted K_2CO_3, the compound that was added to the coal sample, may still have been present in the ash sample. The negative values observed for Al and Ti in Figure 5-2, indicates that no dissolution efficiency values were calculated for these inorganic elements.

Sintering and dissolution of the SA1 ash sample, without $(NH_4)_2SO_4$, showed dissolution efficiencies of 2.7% Al, 14.3% K, and 20.7% Ti. The dissolution efficiency values resembled those obtained after subjected the SA1 ash sample to the dissolution procedure. This suggests that sintering of the SA1 sample did not change the composition of the ash sample or promote dissolution of the inorganic compounds. The SA2 blend ash sample had dissolution efficiencies of 12.6% Al, 32.2% K, and 7.1% Ti. The increase in the aluminium dissolution efficiency value may be due to the dissolution of metakaolinite and soluble potassium species K_2CO_3 (additive). The low dissolution efficiency of Al and K may be due to the formation of potassium aluminium silicate mineral phases, which are insoluble in water (dissolution procedure).

The dissolution efficiencies determined from the XRF results obtained after $(NH_4)_2SO_4$ addition, sintering and dissolution of the sintered residue, yielded dissolution efficiencies of 43.4% Al, 56% K, and 49.7% Ti. This increase in the Al dissolution efficiency was due to the formation of ammonium/potassium aluminium sulphates (alums) (Equations 5-6 to 5-8); which could be extracted from the ash during the dissolution procedure. An increase in Al and K dissolution efficiencies was also observed from the SA2 blend ash sample, when $(NH_4)_2SO_4$ was added to the ash sample prior to sintering. The dissolution efficiencies were determined to be 29.5% for Al and 59% for K. The increase in potassium dissolution efficiency was due to the formation of soluble potassium sulphate (Equation 5-12). The formation of potassium-alum (Table 5-8) during the sintering process, resulted in lower dissolution efficiencies for Al and K than expected. This is due to the insolubility of potassium-alum when subjected to this specific dissolution procedure. No dissolution efficiency was determined for titanium.

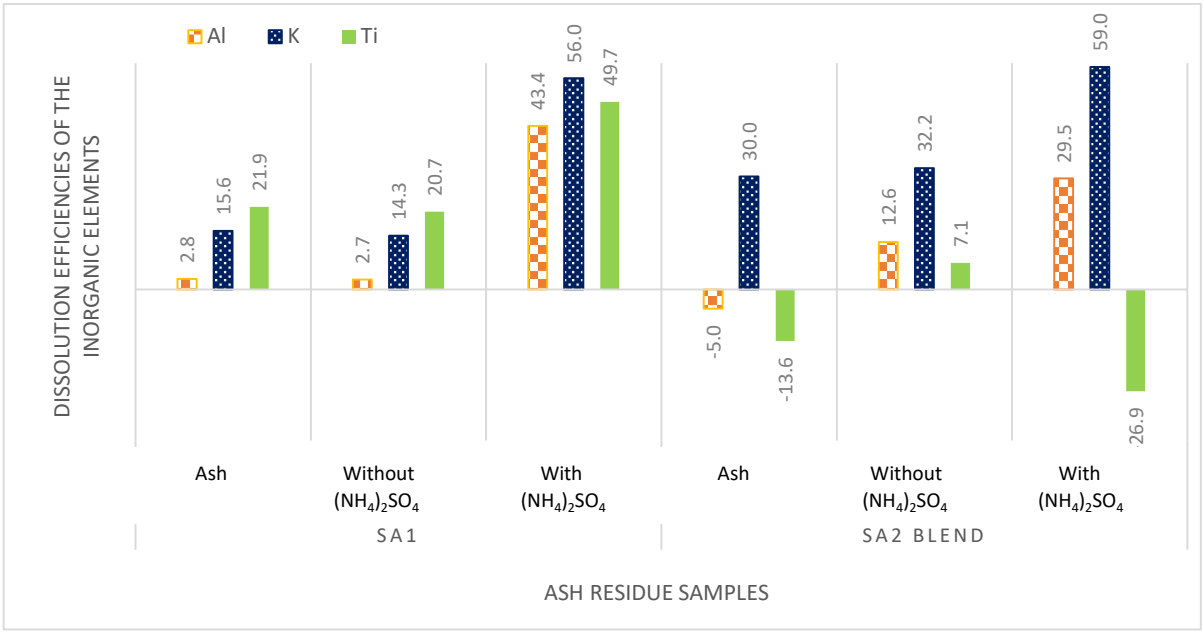

Figure 5-2: Dissolution efficiencies of Al, K, and Ti as determined by XRF analysis of the coal ash and ash residues

5.4 Conclusion

The dissolution of Al-, K-, and Ti- bearing mineral phases was investigated, by subjecting the low-temperature combustion ash samples to an ammonium sulphate sintering procedure. The coal samples used in this investigation showed similar characteristics, i.e. the ash yields determined were 28% and volatile content <20%. Ash composition results showed that the coal samples also contained approximately the same percentage Al_2O_3 (±26%). The ash composition results showed that the SA2 and SA2 blend samples contained higher CaO, SO_3, and K_2O concentrations. These basic compounds reacted with the $(NH_4)_2SO_4$ during the sintering process to produce calcium sulphates and potassium sulphates. As expected, low dissolution efficiencies of the inorganic compounds were obtained by dissolution of the SA1 and SA2 blend ash samples. This is due to the insolubility of the mineral phases in aqueous solution. Dissolution efficiencies of 2.8% Al, 15.6% K and 21.9% Ti were obtained for the SA1 ash sample; while the SA2 blend ash yielded no dissolution of Al and Ti, and 30% for K. The K dissolution percentage may be due to unreacted K_2CO_3, which was added to the coal sample prior to thermal processing, being leaching out of the ash sample.

Sintering of the SA1 and SA2 blend ash samples, without the addition of $(NH_4)_2SO_4$, yielded dissolution efficiencies similar to those obtained by subjecting the ash to the dissolution procedure (without sintering). This suggests that no changes in the mineral phases took place during the sintering process.

Sintering of the SA1 ash sample with $(NH_4)_2SO_4$, yielded dissolution efficiencies of 43.4% Al, 56% K, and 49.7% Ti; which is due to the formation of soluble ammonium/potassium aluminium sulphates during the sintering process. An increase in the K and Al dissolution efficiencies was also observed for the SA2 blend ash sintered with $(NH_4)_2SO_4$. The dissolution efficiencies obtained were 29.5% Al and 59% K. Higher dissolution efficiencies were expected, but the formation of potassium-alum in the leached ash residue influenced the dissolution efficiency values. The potassium-alum can be recovered from the leached ash residue by using another dissolution procedure. The method used in this investigation was inadequate for solubilisation of the mineral phase.

Results from this investigation indicated that sintering of coal ash samples with ammonium sulphate, promoted the dissolution of Al and K through the formation of soluble ammonium/potassium aluminium sulphate and water-soluble potassium species. The presence of high concentrations of potassium resulted in the formation of potassium-alum; which could be recovered from the leached ash residue by subjecting the sample to another dissolution procedure. This will increase the overall dissolution efficiencies for Al and K from the coal ash. Aluminium can be precipitated from the leach liquors generated; while the solid residue can be used in the production of carbon black, or used for chemical production, due to the high silica content of the ash residue.

Chapter 6

Alkaline dissolution of laboratory-produced South African coal ash containing potassium species

Anna C. Collins, Christien A. Strydom, Ratale H. Matjie,
John R. Bunt, Johannes C. van Dyk

Alkaline leaching of coal ash samples, prepared by low-temperature combustion of coal, was done to determine the dissolution of Al from the amorphous material and glassy phases. The influence of an added potassium salt to the coal, on the dissolution of Al from the ash, was also investigated. Sodalite (zeolite A) formation, when using different leaching methods and NaOH concentration solutions, was determined.

Abstract

The aim of this investigation was to determine whether aluminium in the amorphous phase; and aluminium, potassium, and titanium in the glassy phase may be dissolved from South African coal ash prepared at 700°C using sodium hydroxide solutions. The influence of K_2CO_3 addition on the dissolution efficiencies for Al, K, and Ti was investigated; along with the formation of zeolites during the leaching experiments. The results obtained after leaching of the ash showed dissolution efficiencies of <16% of Al for the ash sample; and <5% Al for an ash sample containing added potassium carbonate (K_2CO_3). This is due to the dissolution of metakaolinite, soluble potassium species and potassium aluminosilicate which formed precipitates of sodium or potassium sodalite ($Na_8Al_6Si_6O_{24}(OH)_2(H_2O)_2$) (17%) in the ash residues as well as soluble potassium species in the leach liquor. The highest dissolution efficiency obtained for potassium was found to be 89% for the ash sample containing added K_2CO_3 and 59% for the ash sample without added K_2CO_3; through sequential leaching of the ash samples at a leaching time of 4 hours and a temperature of 80°C, using a 1:5 solid to liquid ratio. The Inductively coupled plasma optical emission spectrometry (ICP-OES) results did not coincide with the exact dissolution efficiency values determined through X-ray fluorescence (XRF) analysis, but a trend supporting the dissolution of aluminium and potassium was achieved. The high dissolution efficiency values obtained for potassium, as determined from the XRF analysis results, indicate that the ash derived from of a blend of coal fines and K_2CO_3 prepared at 700°C can be used for the recovery of soluble potassium present in the amorphous material and soluble potassium compounds, through alkaline leaching. The formed zeolite phase and potassium-containing liquid could possibly be utilized in industrial applications, such as water purification, or used as molecule separators and fertilisers.

Keywords: potassium, aluminium, titanium, sodium hydroxide, zeolite, sodalite

6.1 Introduction

Coal is the most abundant fossil fuel in the world, used for the production of electricity in many countries around the world (Bukhari *et al.*, 2015). Increased population and industry growth have prompted the generation of more power to meet these demands (Izquierdo & Querol, 2012). Energy production occurs when the pulverized coal is burned at coal-fired power plants, resulting in a number of by-products (Nayak & Panda, 2010). Coal ash which is comprised of coal fly ash (the main constituent) and bottom ash produced during coal combustion, is one of these by-products (Bukhari *et al.*, 2015). However, utilization of these by-products in other industrial applications is limited (Nayak & Panda, 2010), with the bulk of the ash being discarded in landfills (Murayama *et al.*, 2002). The coal ash and coal fly ash have the potential to be a starting material in the production of $Al(OH)_3$, due to its high aluminium content (Su *et al.*, 2011; Yang *et al.*, 2014). The recovery of aluminium from bottom coal ash and coal fly ash has been the main focus of many investigations (King *et al.*, 2018; Li *et al.*, 2014; Matjie *et al.*, 2005a; Yang *et al.*, 2014).

Recovery methods include acid leaching (Matjie *et al.*, 2005a; Sangita *et al.*, 2017), alkaline leaching (Li *et al.*, 2014; Su *et al.*, 2011), ammonium sulphate roasting (van der Merwe *et al.*, 2017), and in some investigations a combination of these methods. Investigations of alkaline leaching showed that the concentration and type of alkaline solution used during leaching will influence the dissolution of the inorganic components. Alumina and silica precursors, which are the starting point for a variety of compounds, are mostly obtained by mixing of the coal fly ash with an alkaline solution (Comrie & Kriven, 2004). Adrian and McCulloch (1966) found that 90% recovery of Al from Sasol fly ash was possible, with the use of high extraction temperatures and concentrations, through multiple NaOH leaching of the fly ash. Even with the high dissolution, the process was not considered economical. Matjie *et al.* (2005a) found that 89% aluminium recovery was possible during alkaline leaching of calcined spent catalyst, derived from the Fischer-Tropsch process. Elevated temperature- and pressure conditions were used during this leaching procedure. The investigation conducted by Yang *et al.* (2014) stated that dissolution efficiencies up to 92% of aluminium can be achieved, through the formation of $NaCaHSiO_4$ which captures the silica and inhibits zeolite formation. Su *et al.* (2011) used a two-step leaching method for the extraction of aluminium from coal fly ash; from which an 89% aluminium dissolution efficiency was determined. The formation of sodalite occurred during the first step of the leaching procedure. Aside from being used as a recovery method for inorganic elements; this method has also been used for the synthesizing of zeolite crystals (Fukasawa *et al.*, 2017). During hydrothermal treatment of coal fly ash, aluminium- and silica mineral phases are dissolved in the alkaline solution to form silicate- and aluminate ions. These ions precipitate on the surface of the coal fly ash particles; from which crystal growth takes place (Jiang *et al.*, 2015). Leaching conditions such as reaction temperature, lixiviant concentration and leaching time, influence the dissolution efficiencies of aluminium and silicon, but also zeolite formation. Fukasawa *et al.* (2017) found that pulverization of the ash prior to hydrothermal treatment, increased the surface

area; this, in turn, increased the dissolution of alumina and silica, if these species do not form part of inert mullite and feldspars and increased zeolite formation.

Alkali carbonates are known catalysts and is frequently used during gasification and combustion of coal (Tang & Wang, 2016). Catalyst are used to lower the operating temperature during gasification (Green *et al.*, 1988), contribute in the conversion of carbonaceous material to the desired product, and promote methane production (Nahas, 1983). When potassium carbonate is used as a catalyst, it provides a good source material for the recovery of spent catalyst (Ge *et al.*, 2014). Thus the aim of this investigation was to report on the use of alkaline solutions in an attempt to dissolve Al, K, and Ti from the amorphous material in laboratory prepared combustion ash. The influence of potassium carbonate addition on the dissolution efficiency of Al, K, and Ti along with zeolite formation was investigated. Analytical techniques such as XRF, XRD and ICP-OES analyses were utilized in determining the dissolution efficiencies and zeolite formation after leaching of the ash samples with sodium hydroxide solutions. The ash residue after leaching is a by-product but could be used for brick manufacturing and concrete (Nayak & Panda, 2010). The zeolites could be used in industrial applications such as water- and gas purification (Cheung & Hedin, 2014). In addition, the leach liquor containing potassium species could possibly be used as a liquid fertiliser.

6.2 Material and Methods

6.2.1 Coal Samples

Two medium volatile bituminous South African coal samples, from different coalfields, were used during this investigation. The coal mines are situated in the Mpumalanga region. The coal samples will be referred to as “SA1” and “SA2” in the discussions that follow. The coal samples were collected and sampled by the mine using standardized procedures (ISO 1988:1975 and ISO 139094:2016); from which a representative sample of 20 kg was taken and used in this investigation. The coal samples were selected according to their aluminium and potassium content, which was determined through characterization of the coal samples. The coal rank was determined using the ASTM D388-12 classification standard.

6.2.2 Sample Preparation

6.2.2.1 Coals samples

The coal samples were prepared by air drying for 2 days to reduce excess moisture not associated with the coal structure. After the drying period, each sample was crushed, by first using a crusher and then a ball mill to obtain a particle size of <1 mm using standardized methods (ISO 1988:1975 and ISO 139094:2016). A blended sample was also prepared by adding a potassium compound (10 wt. % K_2CO_3) to the SA2 coal sample during the milling step. This blended sample is identified as “SA2 blend” in the discussions below. The addition was done during the ball milling step to ensure

thorough mixing and to obtain a homogeneous sample. K_2CO_3 was added to the SA2 coal sample to increase the concentration of potassium (K) in the ash, to determine the recoverability of potassium after thermal processing of the coal sample, and whether K will influence the recovery of other inorganic elements.

6.2.2.2 Ash Samples

The coal samples used in this investigation were subjected to thermal processing to obtain the desired ash samples. These ash samples were produced by splitting each coal sample into four 5 kg sub-samples. The sub-samples were placed into clay fired trays and placed in the hot zone of a rotary kiln, where the temperature of the kiln furnace was increased to 700°C at a heating rate of 10°C/min. A residence time of 3 hours at 700°C was set for all the sub-samples. This thermal step, in the kiln furnace, was conducted under airflow to facilitate combustion of the organic components. At the end of the test duration, the furnace was switched off, so that the cooling rate was generally the natural cooling of the furnace. The ash sub-samples were removed from the kiln furnace once the samples reached ambient temperature. From this, the four ash sub-samples were blended to form one homogenous ash sample.

6.2.3 Analytical Methods

6.2.3.1 Proximate and Ultimate Analysis

Characterization of the coal samples used during this investigation was done according to specific ISO standard methods. The characterization method and the ISO standard methods used are presented in Table 6-1.

Table 6-1: Characterization methods and ISO standard identification number

Analysis	*Standard Number*
Solid mineral fuels: Determination of moisture in general analysis test sample by drying in nitrogen	ISO 11722: 2013
Solid mineral fuels: Determination of ash	ISO 1171: 2010
Hard coal and coke: Determination of volatile matter	ISO 562: 2010
Fixed carbon	By calculation
Determination of total carbon, hydrogen and nitrogen content – international method. Oxygen content by calculation	ISO 29541: 2010

6.2.3.2 X-Ray Fluorescence (XRF) Analysis

Samples subjected to XRF analysis were ground until all particles could pass through a 75 µm sieve. Calcination of the powdered samples was conducted at 1000°C under airflow, with a residence time of 3 hours. This was done to remove all moisture and organic compounds, which might be present in the sample. After the calcination process, a solid solution was prepared by fusion of the calcined

samples with lithium tetraborate: lithium metaborate (67:33). This solid solution, prepared from the calcined powder and the standard, was added into the casting dish with the measurement of 32 mm. The prepared fused beads (32 mm) were placed into the sample compartment of the XRF spectrometer (WROXI from PANalytical). The analysis was conducted according to the method proposed by Norrish and Hutton (1969). Results obtained from this analysis method are expressed as percentages of the major elemental oxides present in each sample.

6.2.3.3 X-Ray Diffraction (XRD) Analysis

Samples subjected to XRD analysis were ground to a particle size <75µm with the use of a laboratory scale ball mill in order to liberate the minerals. The powdered samples and those containing the silicon standard were placed into sample holders. These holders were filled with the powdered sample, and the surplus removed with the use of a glass slide (50X70 mm and 5 mm thick). Simultaneous compression of the sample into the sample holder takes place as the excess sample is removed (Matjie, 2008). This step was repeated until a smooth surface of even texture was obtained. Each solid sample was spiked with 20% Si (Aldrich, 99.9% purity) and was subsequently micronized in a McCrone micronizing mill to further liberate the minerals. The XRD analyses of the coal and ash samples were done using an X'Pert PRO PANalytical (Philips) – Unit 2 diffractometer system with Co Kα radiation. Identification of the minerals present in the powdered samples was conducted with reference to the International Center for Diffraction Data (ICDD) Powder Diffraction File. Amorphous and crystalline phases in the powdered samples were identified and quantified with X'Pert Highscore plus software (Speukman, 2012) and the Rietveld method (Rietveld, 1969).

6.2.3.4 Inductively Coupled Plasma Spectrometry Optical Emission Spectroscopy (ICP-OES) Analysis

The leach liquor samples produced in this investigation were subjected to the ICP-OES, model number Varian 700-ES, which was supplied by SMM, currently known as Chemetrix. The analysis was conducted at SetPoint Laboratories used to determine the concentrations of Al, K, Ti, and Si in the leach liquor. Duplicate runs were performed on the leach liquor samples to ensure repeatability. Different standard samples, containing different concentrations of inorganic elements, were prepared (Settle, 1997) and used as control samples during ICP-OES analysis of the leach liquor samples.

6.2.4 Experimental Methods

A schematic diagram to show the experimental- and analytical methods used on the coal, coal ash, and ash residue samples during alkaline leaching is given in Figure 6-1.

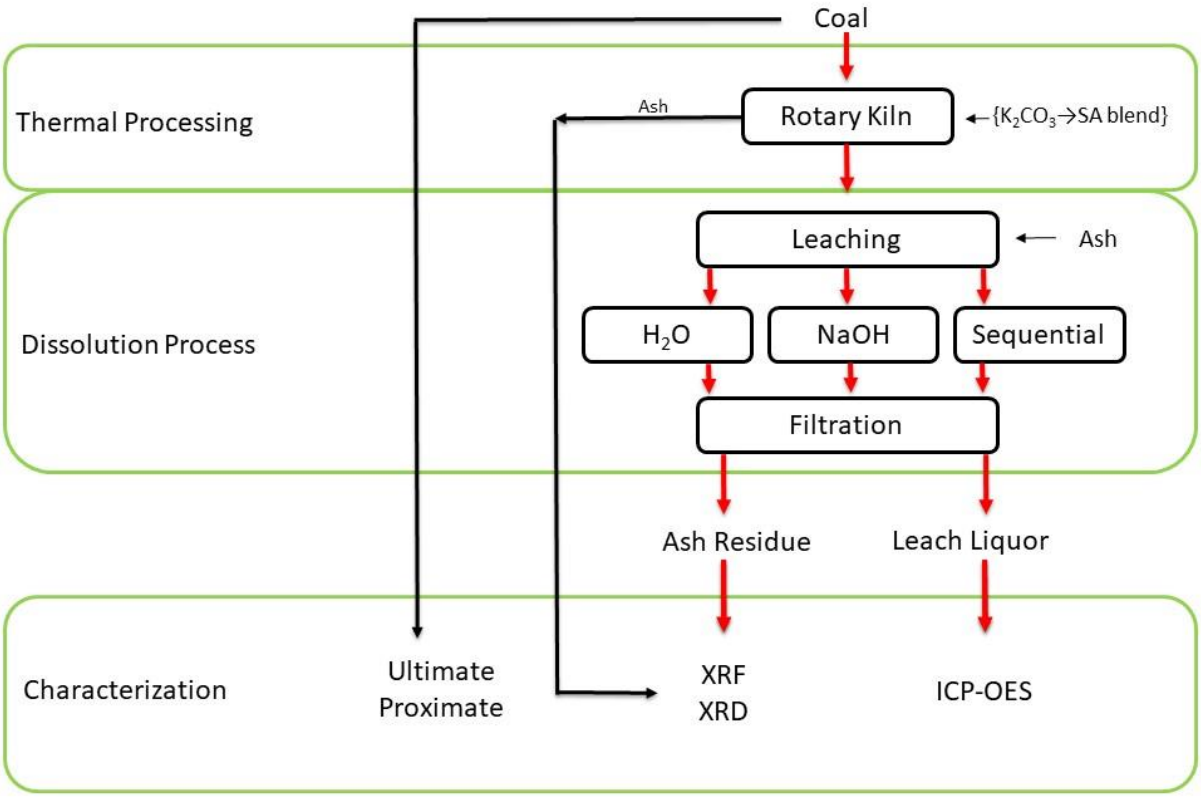

Figure 6-1: Schematic diagram of experimental- and analytical procedures used during alkaline leaching of the coal ash samples

6.2.4.1 Leaching Experiments

Leaching experiments were done by using a 500 ml round-bottomed container, with sealing lid and cooler, as a leaching vessel. An automatic overhead stirrer with a base plate (DESC 20 L) model 720, coupled with a temperature controller (with a sensor probe), was used as a heat source.

6.2.4.1.1 H_2O Leaching

The solubility of inorganic (Al, K, And Ti) compounds in an aqueous solution was determined through leaching of the coal ash samples with H_2O. The leaching experiments were done by weighing and placing the coal ash (20 g) into the leaching vessel. Deionized water (100 ml) was added to the leaching vessel to maintain a 1:5 solid to liquid ratio, which was used in these experiments. With the use of an automatic stirrer, the mixture was stirred (200 rpm) for 4 hours at a temperature of 80°C. After the leaching time was completed, the mixture was removed from the heat and filtered. Filtering of the hot mixture was followed by washing of the ash residue with deionized water, to remove all residual soluble components. The leach liquor was collected and combined with the

filtrate to produce the final leach liquor sample. ICP-OES analysis was done on the final leach liquor sample, while the ash residue was placed in a vacuum furnace and dried overnight at 60°C.

6.2.4.1.2 Alkaline Leaching

The solubility of inorganic (Al, K, and Ti) compounds in an alkaline solution was determined through leaching the coal ash with sodium hydroxide (NaOH) solutions. The coal ash (20 g) was weighed and placed into the leaching vessel. The NaOH solution (100 ml) was added to the leaching vessel to maintain a 1:5 solid to liquid ratio that was used in these experiments. The concentration of the sodium hydroxide solutions used in these leaching experiments were 1 M- and 8 M NaOH. With the use of an automatic stirrer, the mixture was stirred (200 rpm) for 4 hours at a temperature of 80°C. After the leaching time was completed, the mixture was removed from the heat and filtered. Filtering of the hot mixture was followed by washing of the ash residue with deionized water to remove all residual soluble components. The leach liquor was collected and combined with the filtrate to produce the final leach liquor sample. ICP-OES analysis was conducted on the final leach liquor sample, while the ash residue was placed into a vacuum furnace and dried overnight at 60°C.

6.2.4.1.3 Sequential Leaching

The sequential leaching procedure used in determining the solubility of inorganic (Al, K, and Ti) compounds from the coal ash consisted of two leaching steps. The leach liquor collected after each leaching step was added together to form one sample.

First sequential leaching procedure:

In this case, the coal ash was weighed (20 g) and placed into the leaching vessel. In step 1, 100 ml of H_2O (deionized) was added to the coal ash sample, to maintain a 1:5 S/L ratio. Using an automatic stirrer; the mixture was stirred (200 rpm) for 4 hours at a temperature of 80°C. After the leaching time had been completed, the hot mixture was filtered and washed with deionized water, to remove residual soluble compounds from the ash residue. The leach liquor was collected and stored. The ash residue was placed back into the leaching vessel. For step 2, 100 ml of an 8 M NaOH solution was added to the ash residue. The mixture was stirred (200 rpm) for 4 hours at a temperature of 80°C. After the leaching time was completed, the hot mixture was filtered and washed with deionized water. The leach liquor was collected and added to the leach liquor obtained during the first leaching step. The ICP-OES analysis was done on this combined leach liquor sample. The ash residue was placed in a vacuum oven and dried overnight at 60°C.

Second sequential leaching procedure:

In this instance, the coal ash (20 g) was weighed and placed in the leaching vessel. In step 1, 100 ml of a 1 M NaOH solution was added to the coal ash, to maintain a 1:5 S/L ratio. Using an automatic stirrer, the mixture was stirred (200 rpm) for 4 hours at a temperature of 80°C. After completion of the leaching time, the hot mixture was filtered and washed with deionized water to remove all residual

soluble compounds. The leach liquor was collected and stored. The ash residue was placed back into the leaching vessel. In step 2, 100 ml of an 8 M NaOH solution was added to the ash residue. The mixture was stirred (200 rpm) for 4 hours at a temperature of 80°C. After the leaching time was completed, the hot mixture was filtered and washed with deionized water. The leach liquor was collected and added to the leach liquor obtained during the first leaching step. This combined leach liquor sample was subjected to the ICP-OES analysis. The ash residue was placed in a vacuum oven and dried overnight at 60°C.

6.2.4.2 Dissolution Efficiencies

The solubility of a single inorganic compound, multiple compounds and amorphous phases can be determined through calculation of the dissolution efficiencies after the dissolution experiments. The dissolution of inorganic (Al, K and Ti) compounds into aqueous- and the alkaline solution was determined through XRF and ICP-OES analyses.

6.2.4.2.1 Dissolution efficiencies of Al, K, and Ti as determined from XRF analysis

The dissolution efficiencies for Al, K, and Ti were calculated from the XRF results. This calculation was done with the following equation:

$$\eta(MO) = \frac{m\,(MO)_{CA} - m\,(MO)_{RE}}{m\,(MO)_{CA}} \times 100\% \qquad (6\text{-}1)$$

where η(MO) is the dissolution efficiency for the specific inorganic (Al, K and Ti) compound, and $m(MO)_{CA}$ and $m(MO)_{RES}$ the mass (Equation 6-2) of inorganic compound in the coal ash and coal ash residue respectively (Jiang *et al.*, 2015). The mass of the specific inorganic element in the coal ash and ash residue samples can be determined as follow:

$$\boldsymbol{m\,(MO)_{ash}} = \left(\frac{\%\boldsymbol{E}}{\mathbf{100}}\right) \times \boldsymbol{m_{sample}} \qquad (6\text{-}2)$$

where $m(MO)_{ash}$ is the mass (g) of the inorganic element (Al, K, or Ti) in the coal ash (CA) or ash residue (RE); %E (Equation 6-3) the percentage of the inorganic element in the coal ash or ash residue; and m_{sample} the mass of the ash sample or ash residue. The percentage (%E) of the inorganic element present in each of the ash and ash residue samples was determined with the following equation:

$$\%\boldsymbol{E} = \%\boldsymbol{EO} \times \frac{\boldsymbol{M_{element}}}{\boldsymbol{M_{EO}}} \qquad (6\text{-}3)$$

with %E the percentage of the element in the coal ash or ash residue sample; %EO the percentage elemental oxide in the sample (provided through XRF analysis); $M_{element}$ the molecular weight of the element in the oxide and M_{EO} the molecular weight of the elemental oxide.

6.2.4.2.2 Dissolution efficiencies of Al, K, and Ti as determined from ICP-OES analysis

The ICP-OES analysis results for each of the inorganic elements investigated, are given as mg/L or ppm for each leach liquor sample. To determine the dissolution efficiency for each of these elements in solution, the following equations were used:

$$\alpha = \frac{m\,(E)_{LEACH}}{m\,(E)_{CA}} \times 100\% \qquad (6\text{-}4)$$

where α is the dissolution efficiency of inorganic elements calculated from the ICP-OES results; $m(E)_{LEACH}$ m $(E)_{CA}$ the mass of the element (Al, K, or Ti) in the leach liquor and coal ash respectively.

6.3 Results and Discussion

6.3.1 Coal Composition

The proximate and ultimate results obtained after analysis of the coal samples are presented in Table 6-2. The proximate results (reported on an air-dried basis) indicate low moisture content (<5%), along with high ash yields (>25%) and volatile contents (>18%). The fixed carbon contents of the coal samples were determined to range between 45% and 51%.

The ultimate results (reported on a dry-ash-free basis) showed carbon contents ranging between 79% and 83% for the coal samples; while the oxygen contents ranged between 10% and 13%. The hydrogen, nitrogen and sulphur contents were found to be <5% for all the coal samples. The results found for these coal samples are consistent with the ultimate and proximate results reported for other South African coal samples (Hattingh *et al.*, 2011; van Alphen, 2005; van Dyk *et al.*, 2009b).

Table 6-2: Proximate and Ultimate analyses results for the coal samples

Sample	*SA1*	*SA2*	*SA2 Blend*
Proximate Analysis (air-dried basis)			
Moisture content (%)	3.3	3.7	4.6
Ash yield (%)	28.3	28.5	26.8
Volatile content (%)	18.2	21.3	21.5
Fixed Carbon (%)	50.2	46.5	47.1
Ultimate Analysis (dry-ash-free basis)			
% Carbon Content	82.3	79.2	79.6
% Hydrogen Content	4.4	3.8	4.9
% Nitrogen Content	1.8	1.9	1.9
% Oxygen Content	10.8	13.2	12.4
% Sulphur Content	0.7	1.9	1.2

6.3.2 Ash and Mineralogy analyses for the coal samples – XRF and XRD

XRF analysis results of the ash prepared from the coal samples is presented in Table 6-3. The XRF results given in the table are presented on a normalized basis. From the results, it can be seen that the coal ash samples contained silicon measures as silicon oxide in percentages ranging from 37% to 63%; while the aluminium oxide percentages ranged from 22% to 29%. Significant percentages of iron, sulphur and calcium can be seen throughout all the coal ash samples used, with the SA2 sample containing >10% calcium oxide and >7% sulphur oxide. The high potassium oxide content seen for the "SA2 blend" sample was due to the spiking of the SA2 sample with K_2CO_3. The results found for SA1 and SA2 are in good agreement with results obtained for other South African coal ash samples (Hattingh *et al.*, 2011; Matjie *et al.*, 2008; van Alphen, 2005; van Dyk *et al.*, 2008b; van Dyk *et al.*, 2009b).

Table 6-3: Normalized XRF results (wt.%) for the coal samples (ash prepared at 1000°C)

Sample	*SA1*	*SA2*	*SA2 Blend*
SiO_2	63.2	41.6	37.7
Al_2O_3	28.5	25.2	22.3
CaO	1.5	13.0	11.1
SO_3	1.5	7.6	-
Fe_2O_3	2.0	5.6	4.2
MgO	0.8	3.2	2.1
TiO_2	1.5	1.8	1.7
K_2O	0.7	1.1	18.9
P_2O_5	0.1	0.3	0.3
SrO	-	0.3	-
BaO	-	0.2	-
Cr_2O_3	0.1	-	0.3
Na_2O	-	-	0.7

The XRD results determined for the coal samples are presented in Table 6-4. The results indicate that the coal samples were comprised mainly of amorphous (organic carbon) material with percentages exceeding 66%. The SA1 sample contained kaolinite (18%), quartz (10.6%), and small percentages of other crystalline phases. The SA2 coal sample consisted of kaolinite (13.9%), quartz (3.8%), dolomite (6.2%), and calcite (2.5%). The SA2 blend had a similar mineral composition as the SA2 coal sample even after the addition of 10% K_2CO_3. The high proportion of organic carbon, which is amorphous material in the coal, could affect the accuracy of the XRD analysis of the coal. The XRD results are in agreement with the XRD results reported for other South African coals samples (Matjie *et al.*, 2008; van Alphen, 2005; van Dyk *et al.*, 2009b).

Table 6-4: XRD results (wt.%) for the coal samples

Sample	*SA1*	*SA2*	*SA2 Blend*
Amorphous (organic carbon)	66.2	71.4	67.9
Anatase	0.4	-	0.3
Calcite	-	2.5	3.2
Dolomite	1.3	6.2	6.5
Graphite	1.9	0.8	-
Illite	0.8	1.0	3.6
Kaolinite	18.0	13.8	14.0
Microcline	0.7	0.2	-
Muscovite	-	-	0.1
Pyrite	0.1	0.2	0.1
Quartz	10.6	3.8	4.0

6.3.3 Analysis of ash and leached ash residues

The XRF and XRD results obtained for the ash from the SA1 and SA2 blend ash samples prepared at 700°C are presented in Table 6-5. The XRF results for the SA1 ash sample indicated that the composition was mainly comprised of SiO_2 (62.1%) and Al_2O_3 (28.3%). The remaining elemental oxides were present in percentages <3%. The XRD results showed that the SA1 ash sample contained quartz (44.3%), amorphous material (47.6%), and small percentages (<2%) of other crystalline phases. The amorphous material consists primarily of metakaolinite ($Al_2O_3 \cdot 2SiO_2$), which is the transformed mineral product of kaolinite after heating coal at elevated temperatures under oxidising condition. This is supported by the results found by Bunt *et al.* (1998); where the ash obtained after subjecting coal fines to thermal processing in a rotary kiln at 600°C, consisted of metakaolinite and other crystalline phases.

The XRF results obtained for the SA2 blend (mixture of K_2CO_3 and SA2) ash sample, showed that the ash sample was composed of SiO_2 (36.3%), Al_2O_3 (22.6%), K_2O (18.4%), and CaO (8.9%). The high potassium oxide percentage observed is due to the addition of K_2CO_3 to the coal before heating of the coal at elevated temperatures under air. The ash of the SA2 blend sample contained amorphous material (74.8%) with small percentages of quartz (3.9%), anorthite (8.3%), and diopside (4.5%). Calcium oxide can react with metakaolinite to form anorthite, while diopside was formed from amorphous silica reacting to high-temperature carbonate products (calcite or dolomite) (Matjie, 2008).

Table 6-5: XRF (normalized) and XRD results (wt.%) for the coal ash samples prepared at 700°C

Sample	*SA1*	*SA2 Blend*	*Sample*	*SA1*	*SA2 Blend*
Ash Temp	*700°C*	*700°C*	*Ash Temp*	*700°C*	*700°C*
SiO_2	62.1	36.3	Amorphous	47.6	74.8
Al_2O_3	28.3	22.6	Quartz	44.3	3.9
K_2O	0.8	18.4	Calcite	-	8.3
CaO	2.7	8.9	Anhydrite	1.6	1.3
Fe_2O_3	2.7	4.1	Mullite	1.5	-
TiO_2	2.1	1.7	Hematite	1.4	1.3
MgO	0.9	2.3	Anorthite	1.2	0.7
SO_3	0.2	4.4	Portlandite	0.4	0.2
Cr_2O_3	0.1	0.1	Magnetite	0.2	-
Mn_3O_4	0.1	0.1	Cristobalite	0.1	0.1
P_2O_5	0.1	0.2	Gypsum	-	0.6
BaO	-	0.4	Graphite	-	2.0
Na_2O	-	0.1	Diopside	-	4.5
SrO	-	0.3	K_2CO_3	-	0.9
			Kaolinite	-	0.6
			Pyrrhotite	-	0.3
			Maghemite	0.5	-
			Periclase	0.3	-
			Portlandite	0.4	-

6.3.3.1 H_2O Leaching

The XRF and XRD results obtained after leaching the ash samples with H_2O (deionized water), at a temperature of 80°C, for 4 hours, using a 1:5 solid to liquid ratio (Section 6.2.4.1.1), are presented in Table 6-6 and Table 6-7 respectively. The XRF results seen for the SA1 ash sample after leaching, showed a leached ash residue with a chemical composition resembling that of the original ash sample. The difference in concentration values was <4% when comparing these two samples (Table 6-5; Table 6-6). The XRD results showed a decrease in quartz concentration from 44.3% to 35.3% after leaching of the coal ash. The decrease is attributed to an increase in amorphous material from 47.6% to 56.8%. The detection limit for accurate mineral phase determination is >5% mineral presence in the sample. For this reason, mineral phases <5% will be noted but not be discussed.

$$K_2CO_3 + 2H_2O \rightarrow 2KOH + H_2O + CO_2 \quad (6\text{-}5)$$

The XRF results obtained for the SA2 blend (mixture of K_2CO_3 and SA2) ash sample, showed an increase in CaO concentration from 8.9% to 12.3%. This increase may be due to the decrease seen for the K_2O concentration from 18.4% to 13.3%. Changes in the other elemental oxide percentages were <3%. The XRD results showed only small changes, < 4% in the concentrations of the mineral phases after water leaching, when compared with the original ash sample (Table 6-5).

Table 6-6: XRD (normalized) and XRD results (wt.%) after H_2O (deionized) leaching of ash samples

Sample	*SA1*	*SA2 Blend*	*Sample*	*SA1*	*SA2 Blend*
Lixiviant	*H_2O*	*H_2O*	*Lixiviant*	*H_2O*	*H_2O*
SiO_2	58.7	39.1	Amorphous	56.8	72.2
Al_2O_3	27.0	23.8	Quartz	35.3	3.0
K_2O	0.7	13.3	Calcite	1.1	8.7
CaO	2.7	12.3	Illite	0.4	6.6
Fe_2O_3	4.5	5.6	Hematite	1.7	4.1
TiO_2	1.6	1.8	Anorthite	1.2	2.3
SO_3	2.7	1.7	Anhydrite	0.1	0.7
MgO	1.1	1.2	Sodalite	-	0.5
BaO	0.5	0.6	Magnetite	0.4	0.4
SrO	0.0	0.3	Anatase	0.8	0.3
ZrO_2	0.1	0.1	Mullite	-	0.3
Cr_2O_3	0.2	0.0	Portlandite	0.3	0.3
Na_2O	0.0	0.0	Gypsum	0.4	-
			Muscovite	0.5	-
			Maghemite	0.2	-
			Diopside	0.2	-

6.3.3.2 Alkaline Leaching

The XRF and XRD results obtained after leaching of the ash samples with the 1 M NaOH and 8 M NaOH solutions, at a temperature of 80°C, for 4 hours, using a solid to liquid ratio of 1:5 (Section 6.2.4.1.2), are presented in Table 6-7 and Table 6-8 respectively. The XRF results found for the SA1 ash sample after being leached with the 1 M NaOH solution, showed a decrease of <4% for the SiO_2 concentration and <3% for the Al_2O_3 concentration. The decrease may be due to the increase of Na_2O concentration coupled with the dissolution of a small percentage of SiO_2 during the leaching experiments. The solubility of silica in NaOH is well known (Rattanasak & Chindaprasirt, 2009) (Equation 6-6). The XRD results showed a decrease in the quartz concentration from 44.3% to 30.3%, which resulted from the dissolution of the quartz phase during the leaching experiments. The increase in the amorphous material can be attributed to the formation of sodium aluminosilicate.

Possible reactions of quartz with sodium hydroxide are as follows as proposed by Rahman *et al.* (2017) (6-6) and Su *et al.* (2011) (6-7), respectively:

$$SiO_2 + 2NaOH \rightarrow Na_2SiO_3 + H_2O \text{ or } (Na_2SiO_2(OH)_2) \quad (6\text{-}6)$$

$$SiO_2 + OH^-(gls) \rightarrow H_2SiO^{2-}_4 \quad (6\text{-}7)$$

After leaching of the SA1 ash sample with the 8 M NaOH solution, XRF results showed a decrease in SiO_2 concentration from 62.1% to 50.5% and Al_2O_3 concentration from 28.3% to 23.1%. The decreases observed for these elemental oxides may be due to dissolution of the reactive silica and

alumina accompanied by the increase in the Na_2O concentration from 0% to 14.7%. Small changes (<2%) in the other elemental oxides was also seen in the XRF results. The XRD results showed a decrease in the quartz concentration from 44.3% to 21.6%. This decrease is partially due to dissolution of the metakaolinite in sodium hydroxide solution to amorphous precipitate and sodalite ($Na_8Al_6Si_6O_{24}$), which subsequently crystallised from this amorphous material (Equation 6-8). The sodium hydroxide leached ash samples contained 11% to 18% sodalite (Table 6-9 and Table 6-11).

Possible reactions in sodalite formation during alkaline leaching are as follows as reported by Rahman *et al.* (2017) (6-8), Yang *et al.* (2014) (6-9), and Su *et al.* (2011) (6-10 and 6-11) respectively:

$$3Al_2Si_2O_5(OH)_4 + 8NaOH \rightarrow 2Na_4Si_3Al_3O_{24}(OH) + 9H_2O \quad (6\text{-}8)$$

$$8NaOH + 6SiO_2 + 3Al_2O_3 + H_2O \rightarrow Na_8Al_6Si_6O_{24}(OH)_2(H_2O)_2 \quad (6\text{-}9)$$

$$OH^- + Al_2O_3 \rightarrow H_2O + Al(OH)^-_4 \quad (6\text{-}10)$$

$$6H_2SiO^{2-}_4 + 6Al(OH)^-_4 \rightarrow Na_6(AlSiO_4)_6 \cdot 4H_2O + 12OH^- + 8H_2O \quad (6\text{-}11)$$

Leaching of the SA2 blend (mixture of K_2CO_3 and SA2) ash samples with the 1 M NaOH solution, showed minor (<2%) changes in the Al_2O_3 and SiO_2 concentrations, compared to the original ash sample (Table 6-5; Table 6-7). An increase in the CaO concentration from 8.3% to 12.8% was seen due to the decrease of K_2O concentration from 18.4% to 12.6%. The XRD results showed a decrease in calcite concentration from 8.3% to 5.3%, as the anorthite concentration increased from 0.7% to 7.3%. Other changes observed in the mineral composition was a decrease in diopside concentration from 4.5% to 0% and an increase of illite from 0% to 4.6%. The presence of 1.5% mullite was also noted in the sample. These mineral phases present in the ash residue are insoluble in alkaline solution. The amorphous material and quartz concentrations showed minor changes (<3%) when compared with the original SA2 blend ash (Table 6-5). Leaching of the ash from the SA2 blend with the 8 M NaOH solution, showed dissolution of K_2O as the concentration decreased from 18.4% to 5.1%. An increase in Na_2O and CaO concentrations, from 0.1% to 15.7%, and 8.9% to 11% respectively, accompanied the decrease of potassium concentration. The increased sodium concentration was supported by the presence of sodalite (11%) (Equations 6-8, 6-9, and 6-11) observed in the ash residue as seen in the XRD results (Table 6-8). The calcite concentration decreased from 8.3% to 0.3% as the anorthite concentration increased from 0.7% to 5.8%. Minor changes were seen in the XRF and XRD results due to the dissolution of alkaline soluble compounds.

$$K_2CO_3 + 2NaOH \rightarrow Na_2CO_3 + 2KOH \quad (6\text{-}12)$$

The results obtained after leaching of the SA1 and SA2 blend ash samples with the 1 M NaOH solution, showed minor changes in the ash composition, according to XRF analysis, when compared to the original ash samples. Minimal changes to the mineral composition for the ash samples were also noted after XRD analysis of the ash residue samples. Leaching of the SA1 and SA2 blend ash

samples with the 8 M NaOH solution, not only removed alkaline soluble compounds, but also reacted with the metakaolinite in the ash samples to produce sodalite (zeolite).

Table 6-7: XRF (normalized) results (wt.%) for ash residues after leaching with 1 M and 8 M NaOH solutions

Sample	*SA1*		*SA2 Blend*	
NaOH Conc.	*1 M*	*8 M*	*1 M*	*8 M*
SiO_2	58.3	50.5	37.8	34.2
Al_2O_3	25.9	23.1	23.5	21.6
Na_2O	2.4	14.7	1.6	15.7
CaO	3.0	2.8	12.8	11.0
K_2O	0.7	0.3	12.6	5.1
Fe_2O_3	4.8	4.1	4.8	4.9
SO_3	1.1	1.1	1.6	2.6
MgO	1.2	1.0	2.4	2.0
TiO_2	1.6	1.5	1.9	1.8
BaO	0.5	0.6	0.5	0.6
SrO	-	-	0.3	0.3
ZrO_2	0.1	0.1	0.1	-
Cr_2O_3	0.1	0.1	-	-

Table 6-8: XRD results (wt.%) for ash residues after leaching with 1 M and 8 M NaOH solutions

Sample	*SA1*		*SA2 Blend*	
NaOH Conc.	*1 M*	*8 M*	*1 M*	*8 M*
Amorphous	63.6	57.1	76.8	71.4
Anorthite	1.7	1.6	7.3	5.8
Quartz	30.3	21.6	2.7	1.7
Sodalite	-	16.5	-	11
Calcite	1	0.4	5.3	0.3
Illite	-	-	4.6	-
Mullite	-	-	1.5	0.2
Magnetite	0.3	0.5	0.4	0.3
Portlandite	-	-	0.1	3.8
Hematite	1.4	0.7	-	-
Anatase	0.4	0.4	-	-
Periclase	0.2	0.3	0.5	-
Cristobalite	0.1	-	-	-
Diopside	0.1	-	-	-
Dolomite	0.3	-	-	-
Gypsum	0.3	0.4	-	0.5
Maghemite	0.2	0.3	-	-
Muscovite	0.1	-	-	0.6
Hatrurite	-	-	0.6	3
Rutile	-	-	-	1.3

6.3.3.3 Sequential Leaching

The XRF and XRD results obtained after implementation of the two sequential leaching procedures, as described in Section 6.2.4.1.3, are presented in Table 6-9 and Table 6-10 respectively. In the leaching of the SA1 ash sample with the H_2O and 8 M NaOH solutions, decreases in the SiO_2 concentration from 62.1% to 50.1%, Al_2O_3 from 28.3% to 22.6%, and K_2O from 0.8% to 0.3% were observed. This suggests dissolution of metakaolinite in the sodium hydroxide solution during the leaching steps. Also noted was the increase of Na_2O concentration from 0% to 15.8%. The presence of sodalite (17.6%) in the ash residue supports the increase in sodium concentration seen in the XRF results (Table 6-10). Dissolution of reactive silica occurs during alkaline leaching, which would account for the decrease in quartz concentration from 44.3% to 18.6% (Equations 6-6 and 6-7). This decrease will lead to the increase in amorphous material concentration from 47.6% to 58.6% as insoluble, non-crystalline phases are formed. The sodalite crystallized from the leached mixture leaving the potassium ions in the leach liquor. Small changes in the minor mineral phases were

seen after leaching of the ash samples. Leaching of the SA1 ash sample with the 1 M and 8 M NaOH solutions, showed a similar trend in XRF and XRD results, as described for the results obtained after the ash was leached with the H_2O and 8 M NaOH solutions. The XRF results yielded similar composition percentages as in the first sequential leaching process. The XRD results showed a decrease in quartz concentration from 44.3% to 17.3%; while an increase in amorphous material and sodalite concentrations from 47.6% to 66% and 0% to 15.5% was observed.

The XRF results obtained for the SA2 blend (mixture of K_2CO_3 and SA2) ash sample after leaching with the H_2O and 8 M NaOH solutions, showed a decrease in the K_2O concentration from 18.4% to 2.2%. This decrease showed that dissolution of potassium species occurred during both leaching steps (Equation 6-5 and 6-12). An increase in Na_2O concentration from 0.1% to 15.3% was also observed; which is due to the formation of zeolite phases, as the Na^+ bonds with the negatively charged aluminate in solution (Murayama *et al.*, 2002) (Equations 6-8 to 6-11). This formation is supported by the presence of sodalite (16.9%) in the ash residue after XRD analysis (Table 6-10). Also noted from the XRF result was an increase in the CaO concentration from 8.9% to 12.5%. This increase was due to the dissolution of soluble compounds/phases into the lixiviants. Other changes observed in the ash and mineral compositions for the ash residue, was <5%. Leaching of the SA2 blend ash with the 1 M and 8 M NaOH solutions yielded a trend in the XRF and XRD results similar to that observed for the ash leached with the H_2O and 8 M NaOH solutions. The XRF results showed a decrease in K_2O concentration from 18.4% to 2%, accompanied by an increase in Na_2O concentration from 0.1% to 14.7% and CaO from 8.9% to 14.4%. The increase of sodium in the ash residue was supported by the presence of sodalite (17.9%) in the ash residue sample.

The results obtained after sequential leaching of the coal ash samples, using different procedures, produced ash residues which yielded similar ash compositions through XRF analysis. When the XRF results for the ash residues samples, produced from the different procedures are compared, a difference of <1% is seen; while the XRD results differed with <3%.

Table 6-9: Normalized XRF results (wt.%) for the ash residues after sequential leaching (H_2O and 8 M NaOH solution; 1 M and 8 M NaOH solutions)

Sample	*SA1*		*SA2 Blend*	
Lixiviant Step1/ Step 2	*H_2O/8 M*	*1 M/8 M*	*H_2O/8 M*	*1 M/8 M*
SiO_2	50.1	50.5	35.8	35.1
Al_2O_3	22.6	21.9	22.5	21.6
Na_2O	15.8	15.1	15.3	14.7
CaO	2.3	2.8	12.5	14.4
Fe_2O_3	4.0	4.5	5.7	5.6
MgO	0.8	1.1	1.9	2.4
K_2O	0.3	0.3	2.2	2.0
TiO_2	1.4	1.5	2.0	1.9
SO_3	1.9	1.3	1.4	1.1
BaO	0.5	0.5	0.3	0.6
SrO	-	-	0.3	0.3
ZrO_2	0.1	0.1	-	0.1
Cr_2O_3	0.1	0.1	-	-

Table 6-10: XRD (wt.%) results for the ash residues after sequential leaching (H_2O and 8 M NaOH solution; 1 M and 8 M NaOH solutions)

Sample	*SA1*		*SA2 Blend*	
Lixiviant (Step1/ Step 2)	*H_2O/8 M*	*1 M/8 M*	*H_2O/8 M*	*1 M/8 M*
Amorphous	58.6	61	68.7	72.1
Sodalite	17.6	15.5	16.9	17.9
Quartz	18.6	17.3	2.8	2.8
Illite	-	-	3.3	1.2
Hematite	0.7	0.6	2.6	2.0
Anorthite	2.9	4.0	2.4	0.1
Portlandite	-	-	1.0	0.5
Calcite	0.3	0.3	0.7	0.8
Mullite	-	-	0.5	0.4
Magnetite	0.3	0.1	0.3	0.3
Anatase	0.2	0.2	0.2	0.1
Periclase	0.1	0.1	0.1	-
Maghemite	0.3	0.2	0.1	0.2
Rutile	-	-	0.1	0.1
Fluorapatite	0.3	0.4	-	-
Cristobalite	0.1	0.1	-	-
Diopside	-	-	-	0.2
Dolomite	-	0.1	-	-
Muscovite	-	-	-	0.6

6.3.4 ICP-OES Analysis

The results obtained after ICP-OES analysis of the leach liquor samples are presented in Table 6-11. Analysis of the leach liquor samples obtained after leaching of the SA1 ash sample with H_2O showed dissolution of <25 ppm for Al, K, Ti, and Si into solution. This is due to the insolubility of the stable mineral phases, in which these elements are found, in a water solution. Low dissolution of Al, Ti, and Si (<25 ppm) were also seen after leaching of the SA2 blend ash with H_2O. Higher dissolution values of 2218 ppm were determined for the potassium in the leach liquor. This is due to the solubility of K_2CO_3 in water (Equation 6-5).

The ICP-OES results after leaching the SA1 ash sample with 1 M and 8 M NaOH solutions, yielded similar dissolution efficiency values for Al, K, and Ti, even though the dissolution values were low. The dissolution of Si increased from 325 ppm to 1205 ppm as the NaOH concentration increased from 1 M to 8 M. This is due to more reactions taking place between the NaOH and quartz in the ash sample (Equations 6-6 and 6-7). The SA2 blend showed similar tendencies in the dissolution of Al, Ti, and Si when leached with the 1 M and 8 M NaOH solutions, as seen for the SA1 ash sample. During the leaching of the SA2 blend ash sample an increase in the K dissolution, from 2997 ppm to 6008 ppm, as the NaOH solution concentration increased from 1 M to 8 M was observed. This increase was due to reactions between the NaOH solution and the K_2CO_3 present in the ash (Equation 6-12).

Sequential leaching of the SA1 and the SA2 blend ash with H_2O followed by an 8 M NaOH solution yielded similar dissolution as seen when the ash samples were leached with the 8 M NaOH solution. This similarity was due to the limited sodium ions present in the solution for reactions with the mineral and amorphous phases in the ash. The sequential leaching process in which the SA1 and SA2 blend ash samples were first leached with the 1 M NaOH solution followed by the 8 M NaOH solution, showed an increase in dissolution values for Al, K, and Si. This increase in dissolution was due to the increase in sodium ions available for reactions.

Table 6-11: ICP-OES results (ppm) for Al, K, Ti, and Si in the leach liquors

	SA1 (ppm or mg/L)					*SA2 Blend (ppm or mg/L)*				
Lixiviant	*H_2O*	*1M*	*8M*	*H_2O/8M*	*1M/8M*	*H_2O*	*1M*	*8M*	*H_2O/8M*	*1M/8M*
Al	0.15	406	394	431.2	1010	22	260	139	302	648
K	2.16	25	136	160.2	144	2218	2997	6008	6971	7621
Ti	0.04	0.04	0.09	0.13	0.19	0.04	0.04	0.13	0.22	0.24
Si	6.18	325	1205	1169	1436	13	282	1225	1219	1226

6.3.5 Dissolution Efficiencies

6.3.5.1 Dissolution efficiencies for Al, K, and TI as determined from XRF results

The dissolution efficiencies for Al, K, and Ti, which were calculated from the XRF results obtained after the SA1 and SA2 blend ash had been subjected to the leaching experiments, are presented in Figure 6-2. The calculation of the dissolution efficiencies was determined by the equations presented in Section 6.2.4.2.1. After leaching the SA1 ash sample with H_2O, low dissolution efficiencies of 0.1% Al, 13.2% K, and 24.4% Ti, were obtained; while dissolution efficiencies of 3% Al, 33.4% K, and 2.5% Ti were observed for the SA2 blend ash sample. The 33.4% potassium dissolution efficiency seen for the SA2 blend ash was due to the dissolution of K_2CO_3 in water (Equation 6-5).

Leaching of the SA1 ash sample yielded dissolution efficiencies of 10.3% Al, 14.3% K, and 25.3% Ti when leached with the 1 M NaOH; and 7.8% Al, 57.6% K, and 19.3% Ti when leached with the 8 M NaOH. The increase in the dissolution efficiency of potassium from 14.3% to 57.6% as the NaOH solution concentration increases from 1 M to 8 M, is due to more reactions between the NaOH and the K_2CO_3. For the dissolution efficiencies of Al and Ti, a difference of ≤6% was observed when comparing the results after leaching the ash with 1 M and 8 M NaOH solutions. Leaching the SA2 blend ash sample yielded dissolution efficiencies of 4.9% Al, 37.3% K, and 0% Ti when leached with the 1 M NaOH solution; and 0% Al and Ti, and 70.5% K when leached with the 8 M NaOH solution. The negative values seen in Figure 6-2, indicates that no dissolution of the elements in the lixiviants took place during the leaching procedures.

The sequential leaching of the SA1 ash sample with H_2O followed by an 8 M NaOH solution, yielded dissolution efficiencies of 7.8% Al, 56.7% K, and 23% Ti; while dissolution efficiencies of 16.4% Al, 59.5% K, and 22.9% Ti were seen when leached with the 1 M NaOH solution followed by the 8 M NaOH solution. Dissolution efficiency of Al, K, and Ti from the SA1 ash sample through sequential leaching, showed similar results as found when the ash sample was leached with the 8 M NaOH solution. This suggests that the lixiviant concentrations were too low for dissolution of soluble minerals and metakaolinite. Sequential leaching of the SA2 blend ash sample yielded dissolution efficiencies of 0% Al, 88% K, and 0% Ti when leached with H_2O followed by an 8 M NaOH solution; with 8.7% Al, 89.6% K, and 0% Ti when the ash was leached with a 1 M NaOH solution followed by an 8 M NaOH solution. The high potassium dissolution efficiency values may be due to the solubility of the potassium species formed during heating of the SA2 coal and K_2CO_3 mixture under air. The potassium ions did not react with metakaolinite or crystallise together with the sodalite after leaching of the coal ash with sodium hydroxide solutions.

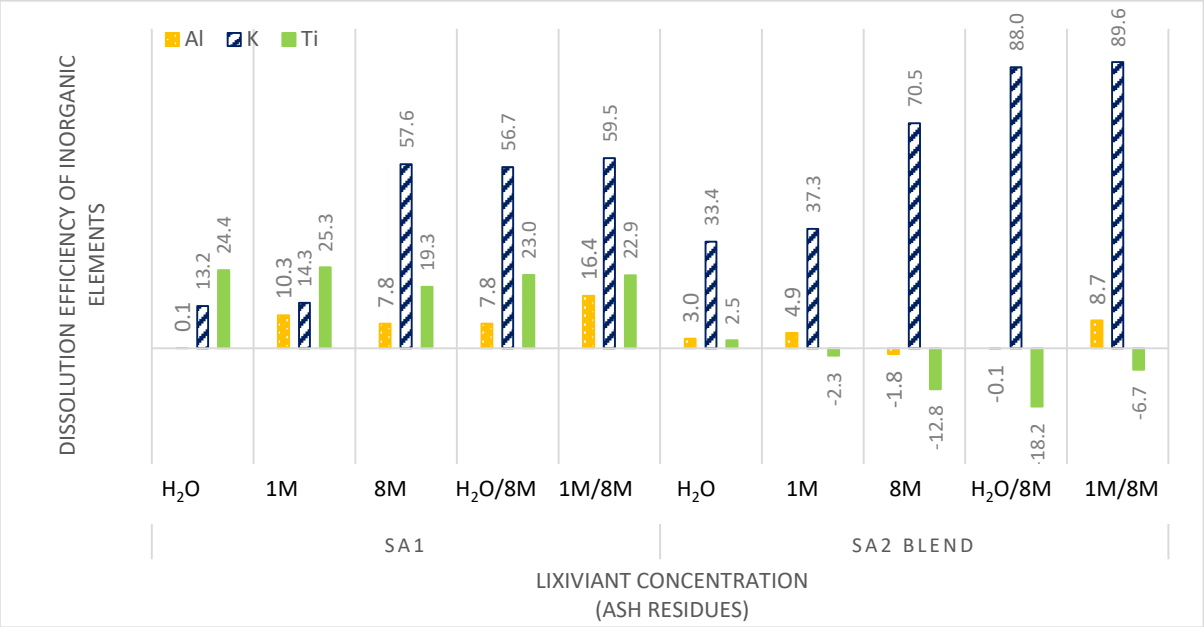

Figure 6-2: Dissolution efficiencies of Al, K, and Ti as determined from XRF analysis of the coal ash and leached ash residues

6.3.5.2 Dissolution efficiencies for Al, K, and Ti as determined from ICP-OES results

The dissolution efficiencies for Al, K, and Ti, which was calculated from the ICP-OES analysis results after SA1 and SA2 blend ash samples had been subjected to the leaching experiments, are presented in Figure 6-3. Subjecting the SA1 and SA2 blend ash samples to all the leaching procedures, produced low dissolution efficiencies when determined with ICP-OES analysis. The Al dissolution was <4% and Ti <0.1% for all the leach liquor samples obtained during experimentation.

The leaching of the SA1 ash sample with H_2O yielded K dissolution efficiency values <1%; while the SA2 blend (mixture of K_2CO_3 and SA2) ash sample yielded a 7.3% K dissolution efficiency. Leaching of the SA1 ash sample with the 1 M NaOH yielded a dissolution of <2% for K; and 10.2% K when leached with the 8 M NaOH solution. This increase in potassium dissolution with increasing NaOH concentration was also seen during the SA2 blend ash sample leaching. The SA2 blend ash showed a dissolution efficiency of 9.8% K when leached with the 1 M NaOH solution and 19.7% K when leached with the 8 M NaOH solution. This increase is due to more available reactants as the concentration of the lixiviant increases. The sequential leaching of the SA1 ash sample, when subjected to both sequential leaching procedures, showed a similar trend in potassium dissolution efficiency as seen when the ash was leached with the 8 M NaOH solution. This trend was also observed after sequential leaching of the SA2 blend ash sample. The difference in dissolution efficiency values for K was <5% when compared with the values calculated for the leach liquors obtained after leaching the ash with an 8 M NaOH solution.

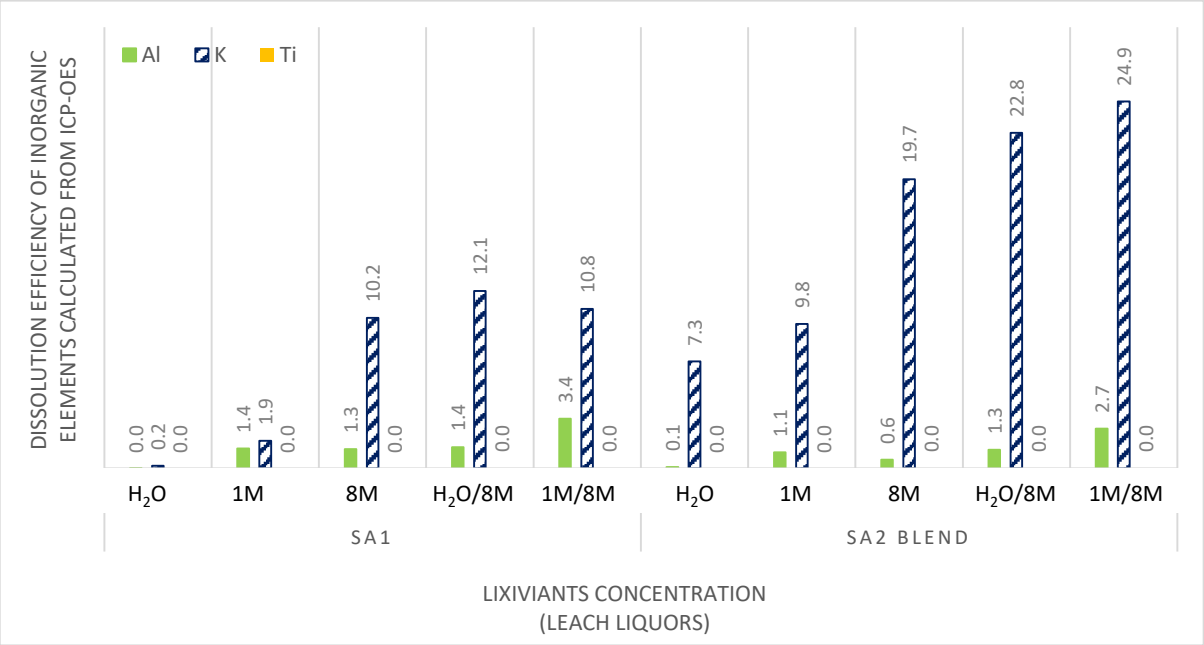

Figure 6-3: Dissolution efficiencies of Al, K, and Ti as determined from ICP-OES analysis of leach liquors

6.3.5.3 Dissolution efficiencies for Si as determined from XRF and ICP-OES results

The dissolution efficiencies for Si, as determined by the XRF analysis results obtained for the ash- and ash residue samples, and ICP-OES analysis results of the leach liquor samples are presented in Figure 6-4. From these results presented in Figure 6-4, it can be seen that low (<15%) dissolution efficiencies for Si was achieved after leaching of the SA1 and SA2 blend ash samples. This was true for all leaching procedures and analyses methods used in this investigation.

Dissolution efficiency of Si determined by XRF analysis results

The leaching of the SA1 and SA2 blend ash samples showed low dissolution efficiencies for Si when leached with H_2O; due to its crystalline nature (insolubility). A minor increase in Si dissolution efficiency was observed when the SA1 ash sample was leached with the 1 M and 8 M NaOH solutions. This may be due to limited reactions between Si-containing crystalline phases and the NaOH (Equation 6-6 and 6-7), or reactive silica found on the surface of the ash particles. Leaching the SA2 blend ash sample with the 1 M NaOH solution, showed a 2% increase in dissolution efficiency of inorganic elements, which may be due to dissolution. The low dissolution efficiency of Si seen after leaching of the SA2 blend ash sample with the 8 M NaOH may be attributed to the formation of sodalite (Equation 6-8, 6-9, and 6-11). Sequential leaching of the SA1 ash sample with the H_2O followed by an 8 M NaOH solution, showed negligible changes in the Si dissolution efficiency when compared to the results found after leaching the ash sample with 1 M and 8 M NaOH solutions. An increase in the dissolution efficiency of Si was seen when the SA1 ash sample was leached with a 1 M NaOH solution, followed by an 8 M NaOH solution. The same trend in silica dissolution

efficiency was also seen for the SA1 ash sample after sequential leaching and could be applied to the results obtained after leaching of the SA2 blend ash sample with the sodium hydroxide solutions.

Dissolution efficiency for Si determined by ICP-OES analysis results

The dissolution efficiencies determined for silica through ICP-OES analysis of the leach liquor samples are presented in Figure 6-4; along with the dissolution efficiency results determined with XRF analysis. The results in Figure 6-4 indicate low dissolution efficiency values for the SA1 and SA2 blend leach liquors; which do not follow the results calculated from the XRF results. This may be due to restrictions in the analytical technique when determining silica concentration in solution. The trend seen in the dissolution efficiency results is an increase in Si concentration in solution as the NaOH solution concentration increased.

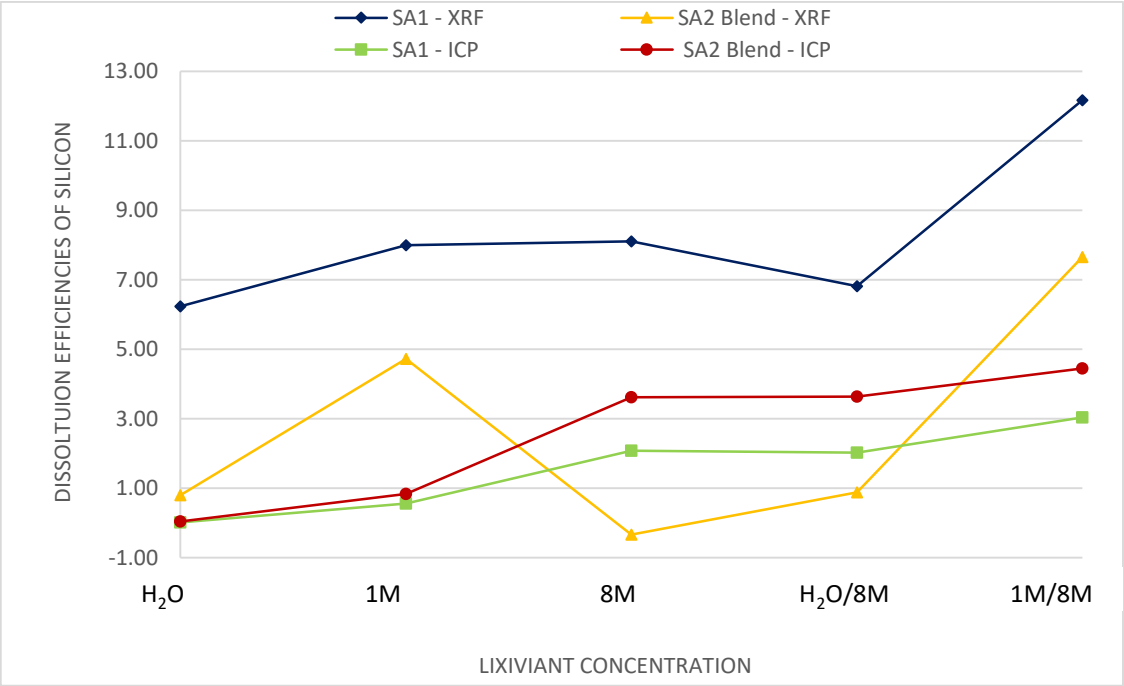

Figure 6-4: Dissolution efficiencies for Si as determined from XRF and ICP-OES analyses

6.3.6 Sodium and Sodalite

The percentages of sodium (XRF analysis) and percentages of sodalite (XRD analysis) in the ash and ash residue samples are presented in Figure 6-5. From the data in Figure 6-5, it is seen that the SA1 and SA2 blend ash samples, before leaching, contained no sodium or sodalite (zeolite phase); which is also seen after leaching the SA1 and SA2 blend ash sample with H_2O. As expected, a small increase in the sodium concentration was seen after leaching the SA1 and SA2 blend ash samples with the 1 M NaOH solution. Leaching of the SA1 ash sample with the 8 M NaOH solution yielded a concentration of 14.7% Na and 16.5% sodalite in the ash residue. This same trend was seen after leaching the SA2 blend ash sample; which resulted in a 15.7% Na concentration and 11% sodalite concentration in the ash residue. Since Murayama *et al.* (2002) found that zeolite

crystallization decreased in the presence of high potassium (K^+) concentration, the addition of K_2CO_3 to the sample may have influenced the sodalite formation. Sequential leaching of the SA1 ash sample did not significantly increase the sodium- or sodalite concentrations in the ash residue when the results were compared to the ash sample which had been leached with the 8 M NaOH solution. Sequential leaching of the SA2 blend ash sample leads to an increase in sodalite concentration (>15%) in the ash residue. Sequential leaching of ash removes soluble compounds during the first leaching step, leaving the reactants in the second leaching step-free for the formation of zeolites. Murayama *et al.* (2002) stated that OH^- promotes the reactions for zeolite formation (Equation 6-7 and 6-10). Jiang *et al.* (2015) explained that, after the initial dissolution of aluminosilicate and zeolite crystal formation, equilibrium is reached between the zeolite and soluble SiO_3^{2-} and $Al(OH)_4^-$ ions. Changing the leaching conditions will disrupt the equilibrium and formation of zeolite will again be initiated.

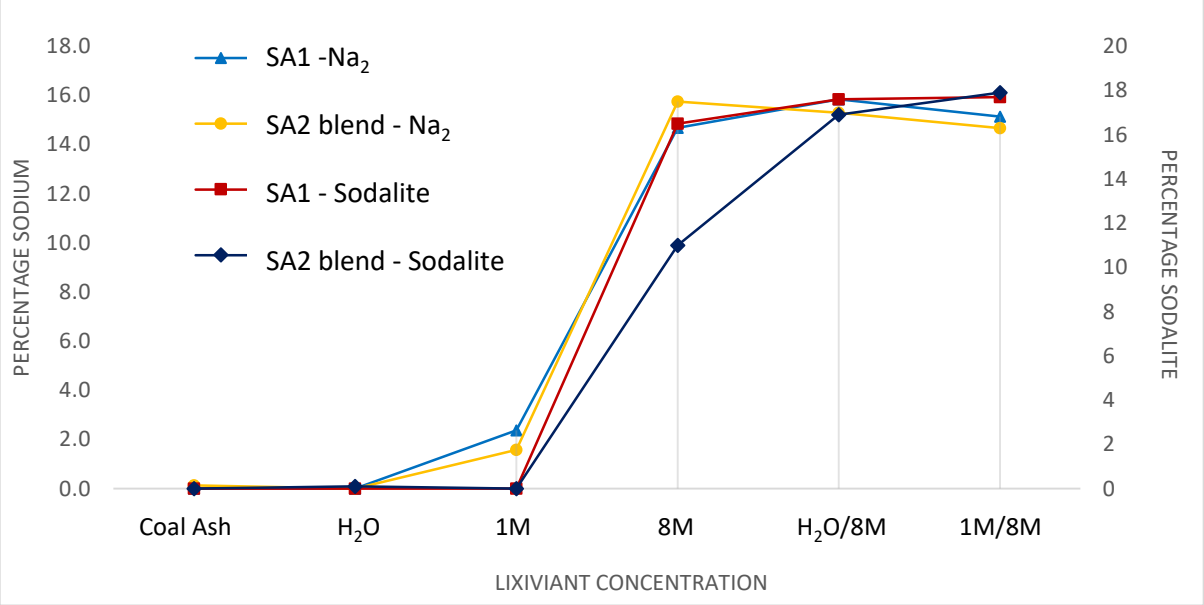

Figure 6-5: Sodium- and Sodalite percentages in coal ash and leached ash residues

6.4 Conclusions

Alkaline leaching of South African combustion ash produced at 700°C, in an attempt in recovering Al, K, and Ti using different leaching procedure was investigated. The leaching of the SA1 ash sample with H_2O and 1 M and 8 M NaOH solutions yielded dissolution efficiencies <10% of Al and <0% Ti. The dissolution efficiency values for potassium was approximately 14% when the ash sample was leached with H_2O and the 1 M NaOH solution. An increase in the potassium dissolution efficiency to 57%, was when the concentration of the NaOH solution increased to 8 M. This same trend in the dissolution of aluminium, potassium and titanium seen for the SA1 ash sample, could be applied to the results obtained for the SA2 blend ash sample. Dissolution efficiencies < 10% Al and

<3% Ti was seen for the SA2 blend ash when leached with H_2O, and 1 M and 8 M NaOH solutions. Potassium dissolution was 33% when leached with H_2O and a 1 M NaOH solution, but increased to 70% K when the NaOH concentration increased to 8 M.

Sequential leaching of the SA1 ash sample with H_2O followed by 8 M NaOH solution, yielded similar dissolution efficiency values for Al, K, and Ti, when compared to the results obtained after leaching the ash with the 8 M NaOH solution. The dissolution efficiencies determined after the second sequential leaching procedure, where the coal ash was leached with a 1 M NaOH solution followed by an 8 M NaOH solution, yielded dissolution efficiencies for Al, K, and Ti only slightly higher than those obtained in the first sequential leaching procedure. This small increase in the dissolution efficiency values suggests that the concentration of the NaOH solutions was still too low to effectively dissolve the inorganic components. The first sequential leaching procedure to which the SA2 blend ash sample was subjected, yielded 88% K with 0% Al and Ti; while the second sequential leaching yielded 89% K and 8.9% Al. This small percentage of aluminium leached may have occurred during the first step in the sequential leaching procedure, since increased NaOH concentration leads to the formation of sodium aluminium silicates.

Even though high silica dissolution efficiencies were expected after alkaline leaching; only small percentages were observed in the leach liquor. This is due to the formation of sodium aluminium silicates (sodalite known as Zeolite A) when high concentrations of NaOH solutions are used in the leaching process. The increase in NaOH concentration to 8 M NaOH, showed 16.5% sodalite in the SA1 ash residue and 11% sodalite in the SA2 blend ash residue. This plateau reached may be due to an equilibrium being reached between the sodalite and the aluminium and silica ions in solution.

Although the ICP-OES analysis of the leach liquor samples did not reflect the expected percentage of dissolution for the inorganic elements investigated, the trend in dissolution efficiency of inorganic elements determined through XRF analysis was observed. The discrepancies observed may be due to human error during the ICP-OES experimental work.

Through this investigation, it was concluded that alkaline leaching of the coal ash can be used for the recovery of potassium when coal fines are combusted at 700°C. The formation of zeolites during alkaline leaching of coal ash samples can be utilized in water purification industries or as molecule separators. Potassium containing leach liquor, obtained after filtering the leached ash could also be used in the fertiliser industry.

Chapter 7

Conclusions and Recommendations

This chapter contains the summarized conclusions made throughout this investigation, regarding the recovery of inorganic elements from coal ash. This chapter also includes recommendations to consider for future work.

7.1 Conclusions

"Ash produced during combustion/gasification of coal and coal fines is a good source material to be used for the recovery of aluminium- and other valuable inorganic metallic compounds, such as potassium and titanium. Instead of discarding the produced coal ash, recovery of inorganic elements can be achieved by submitting the coal ash to suitable recovery methods. The percentage of element recovered from the coal ash will depend on the recovery method, conditions, and the coal ash properties (composition/ mineral phases)."

– Hypothesis as stated in Section 1.1.2

7.1.1 FACTSAGE™ modelling

FACTSAGE™ modelling software and accompanying databases were utilized to predict the mineral transformations, slagging tendencies, and the influence of potassium on the slagging behaviour of four coal samples. The results from the simulation runs (reduction zone) showed that an increase in operating temperature leads to increased melt formation. This decrease in the ash fusion temperatures may be caused by the fluxing behaviour of the basic components' (Ca-, K-, and Fe-) present in the sample. It was also observed that the coal slagging tendencies depended on the mineral composition and transformations of these minerals. The addition of potassium to the SA1 and SA3 coal samples increased the melt formation with increasing potassium loading; while US1 and SA2 showed decreased melt formation with increased potassium loading.

Conclusion:

- The operating condition plays an important role in the extent of the melt formation, mineral transformation, and also the recoverability of these metallic compounds;

- Potassium addition to the coal, prior to thermal processing, had an influence on the extent of melt formation and on the ash fusion temperature;

- The basic components within the coal ash will influence the ash fusion temperatures depending on the ratios of these components present within the samples. This is due to the fluxing tendencies of basic components; and

- The simulation predictions on melt formation percentages obtained from theoretical (assumed) potassium addition to the coal, compared well to the simulation runs of the blended coal sample (coal sample with potassium). A temperature difference of ±200°C in the melt formation temperatures was seen when the simulation predictions with the theoretical potassium concentration were compared with the simulation predictions obtained

for the blended sample. This may due to complex reactions taking place between the potassium and mineral phases in the coal, which could not be predicted by the equilibrium model conditions.

7.1.2 Sulphuric Acid Leaching

Sulphuric acid leaching of the coal ash samples was done, to determine the dissolution of Al-, K-, and Ti-bearing compounds. Leaching the SA1 ash samples prepared at 700°C and 1050°C, with the 1.02 M and 4.08 M H_2SO_4 solutions, yielded dissolution efficiencies of <5% Al, ±17% K and <17% Ti respectively. Low dissolution efficiencies were caused by the formation of gelatinous calcium sulphate and silicic acid precipitates. The SA3 ash samples showed a similar trend in dissolution efficiencies of Al, K, and Ti as seen for the SA1 ash samples. Leaching the SA2 blend ash samples (prepared at 700°C and 1050°C) with the 1.02 M H_2SO_4 solution, resulted in the formation of gelatinous precipitates. Due to the high viscosity of these gelatinous materials, filtering was not possible. Leaching the SA2 blend ash samples prepared at 700°C and 1050°C, with the 4.08 M H_2SO_4 solution, yielded dissolution efficiencies up to 65% Al and 84% K.

Leaching the SA1 ash sample prepared at 700°C, with the 6.12 M H_2SO_4 solution using 1:5 and 1:10 solid to liquid ratios, yielded Al dissolution efficiencies of 59% and 56%; and K dissolution efficiencies were 54% and 43%, respectively. The increase in dissolution efficiency values was due to an increase in sulphuric acid concentration (low pH values). The dissolution efficiency of Ti through this leaching process was <20% for both solid to liquid ratios. Leaching the SA1 ash prepared at 1050°C with the 6.12 M H_2SO_4 solution using 1:5 and 1:10 solid to liquid ratios, yielded dissolution efficiencies <10% for Al, K, and Ti. This is due to the formation of more stable minerals (mullite, anorthite, Na/K-feldspar). This same trend in Al, K, and Ti dissolution efficiencies observed for the SA1 ash sample was found for the SA3 ash samples.

High dissolution efficiencies for Al and K were obtained when leaching the SA2 blend ash with the 6.12 M H_2SO_4 solution using the different solid to liquid ratios. The SA2 blend ash prepared at 700°C yielded 87% and 82% Al, and 89% and 91% K when it was leached with the 1:5 and 1:10 solid to liquid ratios, respectively. High dissolution efficiencies of these elements can be attributed to the metakaolinite, amorphous potassium species, potassium carbonate and potassium aluminium sulphate which are soluble in the sulphuric acid solutions. The titanium dissolution efficiency was determined to be <25% when leached under these conditions. This trend in the dissolution of Al, K, and Ti was also observed for the SA2 blend prepared at 1050°C, where high Al and K, and low Ti dissolution efficiency values were observed.

Conclusions:

- Leaching of coal ash with low concentration sulphuric acid solutions does not yield high dissolution values due to the formation of gelatinous precipitates;

- The addition of potassium carbonate prior to ash production, increased the dissolution propensity of Al and K from the ash, even when using low acid concentration solutions. This is due to the formation of soluble mineral phases;

- The increased acid concentration (6.12 M H_2SO_4) yielded the highest dissolution efficiencies for Al and K from the coal ash prepared at 700°C. This can be attributed to the presence of higher sulphate ions in solution, resulting in more reactions between the acid and mineral phases, and less stable phase minerals present in the ash produced at 700°C;

- Varying the solid to liquid ratio (1:5 and 1:10) when leaching the ash samples with the 6.12M H_2SO_4 solution, showed a difference of <15% in the dissolution efficiency values determined for the various coal ash samples;

- ICP-OES digestion results correlated well to the Al dissolution efficiencies determined from the XRF results. However, more discrepancies were found when the analysis method was used to determine the concentration of K and Ti in solution; and

- Complexometric titration of the leach liquor solutions supported the trend of Al dissolution from the ash samples, if not the exact percentages. This may be due to human error during any one of the different experimental steps.

7.1.3 Ammonium Sulphate Sintering

Recovery of Al from coal ash samples was attempted by using an ammonium sulphate sintering procedure; where the sintered ash residue was subjected to a dissolution procedure. Sintering the SA1 ash sample with ammonium sulphate showed dissolution efficiencies of 43% Al, 56% K, and 50% Ti. The dissolution efficiencies of K and Al observed for the SA2 blend ash sample were 30% Al and 59% K. No dissolution for Ti was determined for this ash sample. XRD results for SA2 blend, when sintered with $(NH_4)_2SO_4$, indicated the presence of potassium-alum in the leached residue. The formation of this mineral phase prevented the dissolution of Al into solution during the dissolution procedure.

Conclusions

- Ammonium aluminium sulphate and aluminium sulphate was formed during the sintering of ammonium sulphate with the coal ash samples. These mineral phases are soluble and were leached from the ash residue during the dissolution procedure;

- The added potassium reacted with the ammonium sulphate to form ammonium/potassium aluminium sulphate (soluble in water) and potassium-alum (insoluble), during the sintering procedure of the SA2 blend ash. This resulted in low dissolution efficiency values;

- The formed potassium-alum can be recovered from the coal ash via another dissolution (acidic) procedure, which will increase the overall Al dissolution efficiency; and

7.1.4 Sodium Hydroxide Leaching

The coal ash samples were subjected to direct- and sequential dissolution methods, with sodium hydroxide solutions as lixiviant. Alkaline leaching of the coal ash samples was done to determine the dissolution of Al, K, and Ti, and the formation of zeolite structures. The influence of added potassium compound on the dissolution and zeolite formation was also investigated. Dissolution efficiencies of <15% for Al and K were observed for the SA1 ash sample when leached with the 1 M NaOH solution. An increase in K (57%) was observed as the alkaline concentration increased to the 8 M NaOH solution. This same trend was observed for the SA2 blend ash sample; with a dissolution efficiency of <40% K when leached with the 1 M NaOH solution and 70% K when leached with the 8 M NaOH solution. This increase in K dissolution efficiency may be due to unreacted K_2CO_3, still present in the ash sample, reacting with the alkaline solution. Sequential leaching of the SA1 ash sample showed only minor changes in the dissolution efficiencies of Al and K when compared with direct leaching results. The SA2 blend ash sample, however, showed an increase in the potassium dissolution efficiency, reaching a value of 89%.

Conclusions

- The dissolution efficiencies obtained after direct- (8 M NaOH) and sequential leaching of the two coal ash samples, showed similar dissolution trends and values. This suggests that most, if not all, reactions between the mineral content and the alkaline solutions for these two coal samples took place;

- The formation of sodalite (zeolite A) crystals, when an 8 M NaOH solution was used during the leaching process, prevented the dissolution of Al from the ash into solution;

- Zeolite formation halted (at 16%) as an equilibrium between the alumina and silica ions in solution and zeolite growth was reached;

- The addition of potassium to the SA2 ash sample may have had an inhibiting influence on zeolite growth; and

- ICP-OES analysis of the leach liquor samples did not reflect the expected dissolution efficiencies as determined with XRF analysis.

7.1.5 Concluding Remarks

- FACTSAGE™ modelling software can be a useful tool for the prediction of coal behaviour during thermal processing, but simulations need to be done bearing in mind that coal processing does not occur at equilibrium. From the simulation results, SA1 and SA3 ash samples had similar ash compositions, and as a result, showed similar FACTSAGE™ simulation results. The mineral transformation for the coal sample with the added K_2CO_3 (SA2 blend) did not correspond with experimental data. This may be due to complex reactions taking place between the additive and mineral content of the coal sample. A complete understanding of these complex reactions is necessary for future prediction work. Even though the simulation runs did not accurately predict all mineral transformations that occurred, it is still a useful tool in determining possible mineral phases and slagging tendencies. These prediction results can be used to determine specific conditions needed for the extraction of inorganic compounds from ash samples.

- The SA1 and SA3 ash samples were submitted to sulphuric acid leaching procedures in the attempt to recover Al. From the dissolution efficiency results, similar values for the dissolution of Al, K, and Ti were obtained for these ash samples. This tendency for SA1 and SA3 to follow similar trends was also predicted by FACTSAGE™ simulations. For these reasons, the SA3 ash sample was excluded from further investigations.

- The coal ash samples, SA1, SA2 blend, and SA3, was subjected to three different extraction methods in which the dissolution efficiencies of Al, K, and Ti was determined. These methods have been utilized with varying degrees of success in previous studies on coal fly ash and clay samples. The first methods applied, was where the ash samples were subjected to sulphuric acid leaching, from which it could be seen that the higher concentration H_2SO_4 solution, higher leaching temperature, and longer leaching time, lead to an increase in dissolution efficiencies for Al and K. This was especially true for the ash samples prepared at 700°C, which might be due to more unstable mineral phases being present in the ash.

The effectiveness of the ammonium sulphate sintering process on the recovery of Al from coal ash (laboratory-produced), was the second recovery method used. The results showed that the sintering procedure increased the dissolution efficiency for the SA1 ash sample by almost 40%, due to the formation of soluble ammonium aluminium sulphate and aluminium sulphate. This substantial increase was not seen for the SA2 blend ash sample; which may be due to the formation of insoluble potassium-alum. Another dissolution procedure is needed for the dissolution of the potassium-alum. This will increase the overall dissolution of Al and K from the sample. The last method investigated was alkaline leaching of the coal ash samples. Low dissolution of Al was observed due to the formation of zeolites structures when leached with high NaOH concentration solutions. Soluble sodium silicate and sodium aluminate are formed when low NaOH concentration solutions are used.

- The addition of K_2CO_3 to the SA2 coal sample prior to ash preparation had the following influences on the dissolution of Al, K, and Ti:
  - The added potassium increased the dissolution efficiency of Al during sulphuric acid leaching, even when using low acid concentration solutions was used. The increase is due to the formation of soluble potassium aluminium sulphate. Unreacted potassium still present in the sample also leached from the coal ash during this procedure.
  - During the ammonium sulphate sintering process, added potassium reacted with the ammonium sulphate and mineral matter to form potassium aluminium sulphate (soluble) and potassium- alum (insoluble phases).
  - The high concentration of potassium in the coal ash sample inhibited zeolite growth.

After subjecting the coal ash samples to these recovery methods, it was found that sulphuric acid leaching was the more effective recovery method for Al and K from the coal ash. This may be due to the digestion of more stable mineral phases by the sulphuric acid. The addition of potassium promoted the dissolution of Al through the formation of soluble potassium aluminium sulphate. The ammonium sintering process needs an additional dissolution procedure to increase the overall dissolution of Al from the ash.

7.2 Recommendations for Future Studies

This investigation addressed the dissolution of inorganic compounds, specifically aluminium, potassium, and titanium from ash produce during low-temperature combustion of specific coal samples (pulverized fines). Based on the results observed throughout this investigation, an in-depth investigation is needed in certain areas. Suggestions for future work are stated for the individual investigation areas:

7.2.1 FACTSAGE™ Modelling

- Prediction of the percentage potassium not captured in the melt or lost through gas evolution. This may yield valuable insight during experimental work on the leachability and fate of K-containing compounds;

- Simulation work on the influence of specific compounds, their percentages and their composition on the slagging behaviour of coal during thermal processing;

- Further investigation into the complex reactions between the mineral phases with the potassium compound which was added to the coal. These predictions must then be confirmed with experimental data.

7.2.2 Sulphuric Acid Leaching

- Detailed investigation of K_2CO_3 reactions with the mineral matter in South African coal samples should be done. Knowledge of these reactions and their products may be used to determine optimum dissolution conditions for aluminium, potassium and titanium. The investigation of K_2CO_3 reactions with the mineral matter forms part of the FACTSAGE™ mineral reaction prediction work (described in Section 7.2.1).

- An economic pre-treatment method or washing step of the coal ash samples should be investigated before acid leaching is done - this is needed to remove all aqueous soluble compounds. Removal of these compounds will prevent a decrease in acid concentration (less interaction between non-essential mineral phases and the acid) and may also render low sulphuric acid concentration leaching to be beneficial.

- Dissolution experiments (after investigation of previously mentioned recommendations) on coal ash samples collected from a power plant, i.e. after coal combustion.

- The use of more analytical techniques which may give insight into the dissolution of the inorganic components from the coal ash.

7.2.3 Ammonium Sulphate Sintering

- Investigate the interactions and influences of K_2CO_3 on Al extraction during the sintering procedure (when the coal is spiked with K_2CO_3 before ash preparation). This would lead to a better understanding of the mineral phases formed during the sintering process; which could be used for determining the dissolution procedure conditions.

- Optimum dissolution procedure of all aluminium and potassium-containing compounds.

7.2.4 Sodium Hydroxide Leaching

- In-depth characterizing of the coal ash sample; coupled with morphology analysis of the ash sample, before and after alkaline dissolution experiments. This could give insight into the influence of mineral matter on zeolite growth; and subsequently the optimization of the zeolite growth process.

- In-depth investigation of the influence an added potassium compound has on the zeolite formation; and its leachability during the alkaline dissolution process.

- Optimization of the alkaline dissolution method in order to promote zeolite crystal formation.

- Use the optimized alkaline dissolution method to determine if simultaneous extraction of other valuable inorganic compounds (Ca, Fe) is possible.

- Subject coal ash samples collected from a power plant (i.e. after coal combustion) to the optimized alkaline dissolution method and determine zeolite crystal formation. This may give valuable insight into coal ash behaviour when compared to the results obtained from laboratory ash.

BIBLIOGRAPHY

Adrian, A. & McCulloch, H. 1966. Pressure leaching of ores with particular reference to the upgrading of aluminate solutions. II. *Alkaline pressure leaching of Sasol fly ash, Gov. Met. Lab (Repub. SA), No. C,* 13 (65):13.

Alguacil, F.J., Amer, S. & Luis, A. 1987. The application of Primene 81R for the purification of concentrated aluminium sulphate solutions from leaching of clay minerals. *Hydrometallurgy,* 18:75-92.

Audley, G.J. 1987. An evaluation of methods for enhancing the CO_2-reactivity of a caking bituminous coal. *Fuel,* 66 (12):1635-1641.

Bai, G., Qiao, Y., Shen, B. & Chen, S. 2011. Thermal decomposition of coal fly ash by concentrated sulfuric acid and alumina extraction process based on it. *Fuel Processing Technology,* 92 (6):1213-1219.

Bale, C.W., Belisle, E., Chartrand, P., Decterov, S.A., Eriksson, G., Gheribi, A.E., et al. 2016. FactSage thermochemical software and databases, 2010-2016. *CALPHAD: Computer Coupling of Phase Diagrams and Thermochemistry,* 54:35-53.

Bale, C.W., Belisle, E., Chartrand, P., Decterov, S.A., Eriksson, G., Hack, K., et al. 2009. FactSage thermochemical software and databases - recent developments. *CALPHAD: Computer Coupling of Phase Diagrams and Thermochemistry,* 33:295-311.

Bale, C.W., Chartrand, P., Decterov, S.A., Eriksson, G., Hack, K., Mahfoud, R.B., et al. 2002. FactSage Thermochemical Software and Databases. *CALPHAD: Computer Coupling of Phase Diagrams and Thermochemistry,* 26:189-228.

Barry, T.S., Uysal, T., Birinci, M. & Erdemoglu, M. 2018. Thermal and Mechanical Activation in Acid Leaching Processes of Non-bauxite Ores Available for Alumina Production—A Review. *The Society for Mining, Metallurgy & Exploration*.

Bayer, G., Kahr, G. & Mueller-Vonmoos, M. 1982. Reactions of ammonium sulphates with kaolinite and other silicate and oxide minerals. *Clay Minerals,* 17:271-283.

Behera, S.K., Chakraborty, S. & Meikap, B. 2017. Chemical demineralization of high ash Indian coal by using alkali and acid solutions. *Fuel,* 196:102-109.

Belviso, C. 2018. State-of-the-art applications of fly ash from coal and biomass: A focus on zeolite synthesis processes and issues. *Progress in Energy and Combustion Science,* 65:109-135.

Benson, S.A., Sondreal, E.A. & Hurley, J.P. 1995. Status of coal ash behaviour research. *Fuel Processing Technology,* 44 (1-3):1-12.

Bexley, K., Green, P.D. & Thomas, K.M. 1986. Interaction of mineral and inorganic compounds with coal: The effect on caking and swelling properties. *Fuel,* 65 (1):47-53.

Blissett, R.S. & Rowson, N.A. 2012. A review of the multi-component utilisation of coal fly ash. *Fuel,* 97:1-23.

Bruno, G., Buroni, M., Carvani, L., Del Piero, G. & Passoni, G. 1988. Water-insoluble compounds formed by reaction between potassium and mineral matter in catalytic coal gasification. *Fuel,* 67:67-72.

Bukhari, S.S., Behin, J., Kazemian, H. & Rohani, S. 2015. Conversion of coal fly ash to zeolite utilizing microwave and ultrasound energies: a review. *Fuel,* 140:250-266.

Bunt, J.R., van Nierop, P., Matjie, R.H., Ritter, B., Steynberg, E.C. & Katabua, M.J. 1998. South Africa Patent No. 98/583.

Burnet, G., Murtha, M.J. & Dunker, J.W. 1984. *Recovery of metals from coal ash*. DOE Iowas State University Ames: Ames Laboratory.

Canon, R.M., Kelemers, A.D., MC Kowell, W.J., Seeley, F.G. & Watson, J.S. (1979). *Metal removal from coal ashes and waste*. Unpublished manuscript, California San Diego.

Cheng-you, W., Hong-fa, Y. & Hui-fang, Z. 2012. Extraction of aluminium by pressure acid-leaching method from coal fly ash. *Trans. Nonferrous Met. Soc. China,* 22:2282-2288.

Cheung, O. & Hedin, N. 2014. Zeolites and related sorbents with narrow pores for CO_2 separation from flue gas. *RSC Advances,* 4 (28):14480-14494.

Comrie, D.C. & Kriven, W.M. 2004. Composite cold ceramic geopolymer in a refractory application. (*In* Advances in Ceramic Matrix Composites IX, Proceedings)

Doucet, F.J., Mohamed, S., Neyt, N., Castleman, B.A. & van der Merwe, E.M. 2016. Thermochemical processing of a South African ultrafine coal fly ash using ammonium sulphate as extracting agent for aluminium extraction. *Hydrometallurgy,* 166:174-184.

Dutta, B.K., Khanra, S. & Mallick, D. 2009. Leaching of elements from coal fly ash: Assessment of its potential for use in filling abandoned coal mines. *Fuel,* 88 (7):1314-1323.

Falcon, R. & Snyman, C. 1986. An introduction to coal petrography: atlas of petrographic constituents in the bituminous coals of Southern Africa. (*O*rganised by Geological Society of South Africa Johannesburg.

Fan, Y., Zhang, F.-S., Zhu, J. & Liu, Z. 2008. Effective utilization of waste ash from MSW and coal co-combustion power plant—Zeolite synthesis. *Journal of hazardous materials,* 153 (1-2):382-388.

Formella, K., Leonhardt, P., Sulimma, A., Van Heek, K.-H. & Jüntgen, H. 1986. Interaction of mineral matter in coal with potassium during gasification. *Fuel,* 65 (10):1470-1472.

Freeman, M.J. 1993. *The manufacture of alumina in South Africa* (No. M376 D). 200 Hans Strijdom Drive, Randburg, SA: Mintek Report.

Fukasawa, T., Karisma, A.D., Shibata, D., Huang, A.-N. & Fukui, K. 2017. Synthesis of zeolite from coal fly ash by microwave hydrothermal treatment with pulverization process. *Advanced Powder Technology,* 28 (3):798-804.

Ge, Z., Jin, H. & Guo, L. 2014. Hydrogen production by catalytic gasification of coal in supercritical water with alkaline catalysts: Explore the way to complete gasification of coal. *International Journal of Hydrogen Energy,* 39 (34):19583-19592.

Gheribi, A.E., Audet, C., Le Digabel, S., Belisle, E., Bale, C.W. & Pelton, A.D. 2012. Calculating optimal conditions for alloy and process design using thermodynamic and property databases, the FactSage software and the Mesh Adaptive Direct Search algorithm. *Computer Coupling of Phase Diagrams and Thermochemistry,* 36:135-143.

Grainger, L. & Gibson, J. 2012. Coal utilisation: technology, economics and policy. Springer Science & Business Media.

Green, P.D., Edwards, I.A.S., Marsh, H., Thomas, K.M. & Watson, R.F. 1988. Coal thermoplasticity and coke structure as related to gasification. *Fuel,* 67:389-395.

Guo, Q., Zhou, Z., Wang, F. & Yu, G. 2014. Slag properties of blending coal in an industrial OMB coal water slurry entrained-flow gasifier. *Energy Conversion and Management,* 86:683-688.

Hanxu, L.I., Ninomiya, Y., Zhongbing, D. & Mingxu, Z. 2006. Application of the FactSage to Predict the Ash Melting Behavior in Reducing Conditions. *Chinese J. Chem. Eng.,* 14 (6):784-789.

Hattingh, B.B., Everson, R.C., Neomagus, H.W.J.P. & Bunt, J.R. 2011. Assessing the catalytic effect of coal ash constituents on the CO_2 gasification rate of high ash, South African coal. *Fuel Processing Technology,* 92:2048-2054.

Highfield, J., Lim, H., Fagerlund, J. & Zevenhoven, R. 2012. Activation of serpentine for CO_2 mineralization by flux extraction of soluble magnesium salts using ammonium sulfate. *RSC Advances,* 2:6535-6541.

Ibrahim, K., Moumani, M.K. & Mohammad, S.K. 2018. Extraction of g-Alumina from Low-Cost Kaolin. *Resources,* 7 (4).

Iqbal, A., Sattar, H., Haider, R. & Munir, S. 2019. Synthesis and characterization of pure phase zeolite 4A from coal fly ash. *Journal of Cleaner Production,* 219:258-267.

Izquierdo, M. & Querol, X. 2012. Leaching behaviour of elements from coal combustion fly ash: An overview. *International Journal of Coal Geology,* 94:54-66.

Jak, E. 2002. Prediction of coal ash fusion temperatures with the F*A*C*T thermodynamic computer package. *Fuel,* 81:1655-1668.

Jak, E., Degterov, S., Hayes, P.C. & Pelton, A.D. 1998. Thermodynamic modelling of the system Al_2O_3-SiO_2-CaO-FeO-Fe_2O_3 to predict the flux requirements for coal ash slags. *Fuel,* 77:77-84.

Jiang, Z., Yang, J., Ma, H., Wang, L. & Ma, X. 2015. Reaction behaviour of Al_2O_3 and SiO_2 in high alumina coal fly ash during alkali hydrothermal process. *Trans. Nonferrous Met. Soc. China,* 25:2065-2072.

Jibril, B., Al-Maamari, R.S. & Al-Amri, I. 2009. Effects of potassium distributions in carbonizations of bituminous coal. *Journal of Analytical and Applied Pyrolysis,* 85 (1-2):529-533.

Kai, H., Inoue, K., Harada, H., Kawakita, H. & Ohto, K. 2011. Leaching behaviour of heavy metals with hydrochloric acid from fly ash generated in municipal waste incineration plants. *Trans. Nonferrous Met. Soc. China,* 21:1422-1427.

Kentucky, U.o. 2018, 2018/06/22. Kentucky Geological Survey. *Earth Resources - Our Common Wealth* www.uky.edu/KGS/coal/coal-macerals.php Date of access: 31/5/ 2019.

King, J.F., Taggart, R.K., Smith, R.C., Hower, J.C. & Hsu-Kim, H. 2018. Aqueous acid and alkaline extraction of rare earth elements from coal combustion ash. *International Journal of Coal Geology,* 195:75-83.

Kiyoura, R. & Urano, K. 1970. Mechanism, Kinetics, and Equilibrium of thermal decomposition of ammonium sulfate. *Ind. Eng. Chem. Process Ds. Develop,* 9:489-494.

Klopper, L., Strydom, C.A. & Bunt, J.R. 2012. Influence of added potassium and sodium carbonates on CO_2 reactivity of the char from a demineralized inertinite rich bituminous coal. *Journal of Analytical and Applied Pyrolysis,* 96:188-195.

Kong, L., Bai, J., Bai, Z., Guo, Q. & Li, W. 2014. Improvement of ash flow properties of low-rank coal for entrained flow gasifier. *Fuel,* 120:122-129.

Kong, L., Bai, J., Li, W., Bai, Z. & Guo, Z. 2011. Effect of lime addition on slag fluidity of coal ash. *Journal of Fuel Chemistry and Technology,* 39:407-411.

Li, H., Junbo, H., Wang, C., Bao, W. & Sun, Z. 2014. Extraction of alumina from coal fly ash by mixed-alkaline hydrothermal method. *Hydrometallurgy,* 147-148:183-187.

Li, L., Liao, X., Wu, Y. & Liu, Y. 2012. Extracting Alumina from Coal Fly Ash with Ammonium Sulfate Sintering Process. *The Minerals, Metals & Materials Society*:215-217.

Liu, B., He, Q., Jiang, Z., Xu, R. & Hu, B. 2013. Relationship between coal ash composition and ash fusion temperatures. *Fuel,* 105:293-300.

Liu, Q., Hu, H., Zhou, Q., Zhu, S. & Chen, G. 2004. Effect of inorganic matter on reactivity and kinetics of coal pyrolysis. *Fuel,* 83 (6):713-718.

Liu, Z.-l. & Zhu, H.-h. 1986. Steam gasification of coal char using alkali and alkaline-earth metal catalysts. *Fuel,* 65 (10):1334-1338.

Mark, U., Anyakwo, C.N., Onyemaobi, O. & Nwobodo, C.S. 2019. The Thermal Activation of Nsu Clay for Enhanced Alumina Leaching Response. *International Journal of Engineering and Technologies,* 16:34-46.

Matjie, R., Scurrell, M. & Bunt, J. 2005a. The selective dissolution of alumina, cobalt and platinum from a calcined spent catalyst using different lixiviants. *Minerals Engineering,* 18 (8):801-810.

Matjie, R.H. (1997). *The selective removal of iron and titanium from an aluminium containing aqueous phase*. Unpublished manuscript.

Matjie, R.H. 2008. Sintering and slagging of mineral matter in South African coals during the coal gasification process*.* The University of Pretoria) 77 p.

Matjie, R.H., Bunt, J.R. & van Heerden, J.H.P. 2005b. Extraction of alumina from coal fly ash generated from a selected low rank bituminous South African coal. *Minerals Engineering,* 18 (3):299-310.

Matjie, R.H., Li, Z., Ward, C.R. & French, D. 2008. Chemical composition of glass and crystalline phases in coarse coal gasification ash. *Fuel,* 87:857-869.

Matjie, R.H., Li, Z., Ward, C.R., Kosasi, J., Bunt, J.R. & Strydom, C.A. 2015. Mineralogy of Furnace Deposits Produced by South African Coals during Pulverized-Fuel Combustion Tests. *Energy & Fuels,* 29 (12):8226-8238.

Matjie, R.H., van Alphen, C. & Pistorius, P.C. 2006. Mineralogical characterisation of Secunda gasifier feedstock and coarse ash. *Minerals Engineering,* 19:256-261.

Medina, A., Gamero, P., Querol, X., Moreno, N. & De León, B. 2010. Fly ash from Mexican mineral coal I: Mineralogical and chemical characterization. *Journal of Hazardous Materials,* 181:82-90.

Murayama, N., Yamamoto, H. & Shibata, J. 2002. Mechanism of zeolite synthesis from coal fly ash by alkali hydrothermal reaction. *International Journal of Mineral Processing,* 64 (1):1-17.

Nahas, N.C. 1983. Exxon catalytic coal gasification process. *Fuel,* 62:239-241.

Nayak, N. & Panda, C.R. 2010. Aluminium extraction and leaching characteristics of Talcher Thermal Power Station fly ash with sulphuric acid. *Fuel,* 89:53-58.

Neupane, G. & Donahoe, R.J. 2013. Leachability of elements in alkaline and acidic coal fly ash samples during batch and column leaching tests. *Fuel,* 104:758-770.

Norris, P., Chen, C. & Pan, W. 2010. A technique for sequential leaching of coal and fly ash resulting in good recovery of trace elements. *Analytica Chimica Acta,* 663:39-42.

Norrish, K. & Hutton, J.T. 1969. An accurate X-ray spectrographic method for the analysis of a wide range of geological samples. *Geochimica et Cosmochimica Acta,* 33 (4):431-453.

Numluk, P. & Chaisena, A. 2012. Sulfuric Acid and Ammonium Sulfate Leaching of Alumina from Lampang Clay. *E-Journal of Chemistry,* 9 (3):1364-1372.

Oboirien, B.O., Engelbrecht, A.D., North, B.C., du Cann, V.M., Verryn, S. & Falcon, R. 2011. Study on the structure and gasification characteristics of selected South African bituminous coals in fluidised bed gasification. *Fuel Processing Technology,* 92 (4):735-742.

Patterson, J.H. & Hurst, H.J. 2000. Ash and slag qualities of Australian bituminous coals for use in slagging gasifiers. *Fuel,* 79:1671-1678.

Paul, M., Seferinoğlu, M., Ayçık, G.A., Sandström, Å., Smith, M.L. & Paul, J. 2006. Acid leaching of ash and coal: Time dependence and trace element occurrences. *International Journal of Mineral Processing,* 79 (1):27-41.

Phillips, C.V. & Wills, K.J. 1982. A laboratory study of the extraction of alumina of smelter grade from China clay micaceous residues by nitric acid route. *Hydrometallurgy,* 9:15-28.

Rahman, M., Pudasainee, D. & Gupta, R. 2017. Review on chemical upgrading of coal: Production processes, potential applications and recent developments. *Fuel Processing Technology,* 158:35-56.

Rattanasak, U. & Chindaprasirt, P. 2009. Influence of NaOH solution on the synthesis of fly ash geopolymer. *Minerals Engineering,* 22 (12):1073-1078.

Rietveld, H.M. 1969. A profile refinement method for nuclear and magnetic structures. *Journal of Applied Crystallography,* 2:65-71.

Robl, T., Oberlink, A. & Jones, R. 2017. Coal Combustion Products (CCPs): Characteristics, Utilization and Beneficiation. Woodhead Publishing.

Samaras, P., Diamadopoulos, E. & Sakellaropoulos, G.P. 1996. The effect of mineral matter and pyrolysis conditions on the gasification of Greek lignite by carbon dioxide. *Fuel,* 75 (9):1108-1114.

Sangita, S., Nayak, N. & Panda, C.R. 2017. Extraction of aluminium as aluminium sulphate from thermal power plant ashes. *Trans. Nonferrous Met. Soc. Shina,* 27:2082-2089.

Seferinoglu, M. 2003. Acid leaching of coal and coal-ashes. *Fuel,* 82 (14):1721-1734.

Seggiani, M. 1999. Empirical correlations of the ash fusion temperatures and temperature of critical viscosity for coal and biomass ashes. *Fuel,* 78 (9):1121-1125.

Seidel, A. 1999. Self inhibition of aluminum leaching from coal fly ash by sulfuric acid. *Chemical Engineering Journal,* 72 (3):195-207.

Settle, F. 1997. Handbook of instrumental techniques for analytical chemistry. 1997. *New Jersey: By prentice Hall PTR*.

Slaghuis, J. 1993. Coal gasification, study guide for the national diploma in fuel technology. 1993. *ISBN: 0-620-17788-8*:202.

Smoot, L.D. & Smith, P.J. 1985. Coal combustion and gasification. New York: Plenum Press.

Song, W., Tang, L., Zhu, X., Wu, Y., Rong, Y., Zhu, Z., et al. 2009. Fusibility and flow properties of coal ash and slag. *Fuel,* 88 (2):297-304.

Speukman, S.A. 2012, 2. Basics of X-Ray Powder Diffraction. http://prism.mit.edu/xray Date of access: 14/02/ 2019.

Stach, E., Murchison, D., Taylor, G.H. & Zierke, F. 1982. Stach's textbook of coal petrology. Vol. 535: Borntraeger Berlin.

Su, S.Q., Yang, J., Ma, H.W., Jiang, F., Liu, Y.Q. & Li, G. 2011. Preparation of ultrafine aluminum hydroxide from coal fly ash by alkali dissolution process. *Integrated Ferroelectrics,* 128 (1):155-162.

Tang, J. & Wang, J. 2016. Catalytic steam gasification of coal char with alkali carbonates: A study on their synergic effects with calcium hydroxide. *Fuel Processing Technology,* 142:34-41.

Tomeczek, J. & Palugniok, H. 2002. Kinetics of mineral matter transformation during coal combustion. *Fuel,* 81 (10):1251-1258.

Torma, A.E. 1983. Extraction of Aluminium from fly ash. *Metals,* 37:589-592.

van Alphen, C. 2005. Factors influencing fly ash formation and slag deposit formation (slagging) on combusting a South African pulverised fuel in a 200MWe boiler. Johannesburg: University of the Witwatersrand.

van der Merwe, E.M., Gray, C.L., Castleman, B.A., Mohamed, S., Kruger, R.A. & Doucet, F.J. 2017. Ammonium sulphate and/or ammonium bisulphate as extracting agents for the recovery of aluminium from ultrafine coal fly ash. *Hydrometallurgy,* 171:185-190.

Van der Merwe, E.M., Prinsloo, L.C., Mathebula, C.L., Swart, H., Coetsee, E. & Doucet, F. 2014. Surface and bulk characterization of an ultrafine South African coal fly ash with reference to polymer applications. *Applied Surface Science,* 317:73-83.

Van Dyk, J., Waanders, F. & Hack, K. 2008a. Behaviour of calcium-containing minerals in the mechanism towards in situ CO_2 capture during gasification. *Fuel,* 87 (12):2388-2393.

van Dyk, J.C. 2006. Understanding the influence of acidic components (Si, Al, and Ti) on ash flow temperature of South African coal sources. *Minerals Engineering,* 19:280-286.

van Dyk, J.C. & Keyser, M.J. 2014. Influence of discard mineral matter on slag-liquid formation and ash melting properties of coal - A FACTSAGE simulation study. *Fuel,* 116:834-840.

van Dyk, J.C., Melzer, S. & Sobiecki, A. 2006. Mineral matter transformation during Sasol-Lurgi fixed bed dry bottom gasification–utilization of HT-XRD and FactSage modelling. *Minerals Engineering,* 19 (10):1126-1135.

van Dyk, J.C. & Waanders, F.B. 2008. An improved thermodynamic FACTSAGE simulation to simulate mineral matter transformation during a fixed bed counter-current gasification process, validated with HT-XRD. *International Mineral Processing Congress XXIV*.

van Dyk, J.C., Waanders, F.B., Benson, S.A., Laumb, M.L. & Hack, K. 2009a. Viscosity predictions of the slag composition of gasified coal, utilizing FacSage equilibrium modelling. *Fuel,* 88:67-74.

van Dyk, J.C., Waanders, F.B. & Hack, K. 2008b. Behaviour of calcium-containing minerals in the mechanism towards in situ CO_2 capture during gasification. *Fuel,* 87:2388-2393.

van Dyk, J.C., Waanders, F.B., Melzer, S., Baran, A., Hack, K. & Bunt, J.R. 2008c. Validation of a thermodynamic equilibrium model developed on South-African coal sources in order to simulate mineral transformations of various coals during gasification. *25th International Annual Pittsburgh Coal Conference*.

van Dyk, J.C., Waanders, F.B. & van Heerden, J.H.P. 2008d. Quantification of oxygen capture in mineral matter during gasification. *Fuel,* 87:2735-2744.

van Dyk, J.R., Benson, S.A., Laumb, M.L. & Waanders, B. 2009b. Coal and coal ash characteristics to understand mineral transformations and slag formation. *Fuel,* 88:1057-1063.

van Jaarsveld, J. & Van Deventer, J. 1999. Effect of the alkali metal activator on the properties of fly ash-based geopolymers. *Industrial & engineering chemistry research,* 38 (10):3932-3941.

Vassilev, S.V., Kitano, K., Takeda, S. & Tsurue, T. 1995. Influence of mineral and chemical composition of coal ashes on their fusibility. *Fuel Processing Technology,* 45:27-51.

Vassilev, S.V. & Vassileva, C.G. 2007. A new approach for the classification of coal fly ashes based on their origin, composition, properties, and behaviour. *Fuel,* 86 (10-11):1490-1512.

Wang, R.-c., Zhai, Y.-c., Wu, X.-w., Ning, Z.-q. & Ma, P.-h. 2014a. Extraction of alumina from fly ash by ammonium hydrogen sulfate roasting technology. *Transactions of nonferrous metals society of China,* 24 (5):1596-1603.

Wang, R., Zhai, Y. & Ning, Z. 2014b. Thermodynamics and kinetics of alumina extraction from fly ash using an ammonium hydrogen sulfate roasting method. *International Journal of Mineral, Metallurgy and Materials,* 21:144-149.

Ward, C.R. 1984. Coal Geology and Coal Technology. Blackwell Scientific Publications.

Ward, C.R. 2002. Analysis and significance of mineral matter in coal seams. *International Journal of Coal Geology,* 50 (1-4):135-168.

Wu, C., Yu, H. & Zang, H. 2012. Extraction of aluminum by pressure acid-leaching method from coal fly ash. *Trans. Nonferrous Met. Soc. China,* 22:2282-2288.

Wu, Y., Xu, P., Chen, J., Li, L. & Li, M. 2014. Effect of Temperature on Phase and Alumina Extraction Efficiency of the Product from Sintering Coal Fly Ash with Ammonium Sulfate. *Chinese Journal of Chemical Engineering,* 22 (11-12):1363-1367.

Xu, D., Li, H., Bao, W. & Wang, C. 2016. A new process of extracting alumina from high-alumina coal fly ash in NH_4HSO_4+ H_2SO_4 mixed solution. *Hydrometallurgy,* 165:336-344.

Yang, Q.-c., ZHENG, S.-l. & ZHANG, R. 2014. Recovery of alumina from circulating fluidized bed combustion Al-rich fly ash using mild hydrochemical process. *Transactions of nonferrous metals society of China,* 24 (4):1187-1195.

Yu, J., Lucas, J.A. & Wall, T.F. 2007. Formation of the structure of chars during devolatilization of pulverized coal and its thermoproperties: A review. *Progress in Energy and Combustion Science,* 33 (2):135-170.

Yuh, S.J. & Wolf, E. 1983. FTIR studies of potassium catalyst-treated gasified coal chars and carbons. *Fuel,* 62 (2):252-255.

Zazzeri, G., Lowry, D., Fisher, R.E., France, J.L., Lanoisellé, M., Kelly, B.F., et al. 2016. Carbon isotopic signature of coal-derived methane emissions to the atmosphere: from coalification to alteration. *Atmospheric Chemistry and Physics,* 16 (21):13669-13680.

Zhao, Y., Zhang, Y., Bao, S., Chen, T. & Han, J. 2013. Calculation of mineral phase and liquid phase formation temperature during roasting of vanadium-bearing stone coal using FactSage software. *International Journal of Mineral Processing,* 124:150-153.

Zhong, L., Zhang, Y. & Zhang, Y. 2009. Extraction of alumina and sodium oxide from red mud by a mild hydro-chemical process. *J Hazard Mater,* 172 (2-3):1629-1634.

Zhou, C., Liu, G., Yan, H., Fang, T. & Wang, R. 2012. Transformation behaviour of mineral composition and trace elements during coal gangue combustion. *Fuel,* 97:644-650.